MYOSIN-X IS A MOLECULAR MOTOR CENTRAL TO FILOPODIA FORMATION, ADHESION, AND SIGNALING

APARNA BHASKAR BOHIL

A dissertation submitted to the faculty of the University of North Carolina at Chapel Hill in partial fulfillment of the requirements for the degree of Doctor of Philosophy in the Department of Cell and Molecular Physiology - School of Medicine

Chapel Hill

2006

Approved by:

Dr. Richard E. Cheney

Dr. Eva S. Anton

Dr. James M. Anderson

Dr. Keith Burridge

Dr. Leslie V. Parise

ABSTRACT

APARNA BHASKAR BOHIL:

Myosin-X is a molecular motor central to filopodia formation, adhesion and signaling

(Under the direction of Dr. Richard E. Cheney)

Understanding cellular and molecular components of cell migration is critical to the advancement of normal physiology and cancer biology. There is growing realization that finger-like cellular protrusions called filopodia play central roles in the cell biology underlying angiogenesis and inflammation (Anderson and Anderson, 1976; Gerhardt et al., 2003). Despite this knowledge, very little is known about the fundamental mechanisms governing filopodia formation, signaling, and adhesion. Unconventional myosins, particularly the MyTH4-FERM class of myosins, are implicated in precisely these types of filopodial functions (Tuxworth et al., 2001). Myosin-X (Myo10) is a vertebrate-specific member of the MyTH4-FERM class of myosins that is expressed in most cells and tissues. When expressed in cells, GFP-Myo10 displays a striking localization to tips of filopodia and undergoes intrafilopodial motility (Berg and Cheney, 2002). The experiments described in this dissertation demonstrate that Myo10 is a component of a putative filopodial tip complex, that it binds integrins (Zhang et al., 2004), and that it is a potent inducer of dorsal filopodia (Bohil et al., 2006).

DEDICATION

In keeping with my ancient tradition, I dedicate this thesis to...
MATA, PITA, GURU, and DEVA
(Mother, Father, Teacher, and God)

ACKNOWLEDGEMENTS

The work described here besides being a mental endeavor had me seesawing through a gamut of emotions. I experienced everything from exuberance and blithe to anger, frustration, and melancholy. Heartfelt thanks are due to people who saved me from insanity.

At the top of the list is my thesis advisor Dr. Richard E. Cheney. I could not have imagined having a better advisor and mentor for my PhD, and without his common sense, knowledge, perceptiveness and cracking-of-the-whip I would never have finished. I shall forever be indebted to him for his generosity with my time and for his unstinted confidence in me. I am thankful to my thesis committee for their insightful and thought provoking questions, for helping me stay focused, and for their kind words of encouragement. Heartfelt thanks are due to the entire department of Cell and Molecular Physiology, particularly to Jan McCormick, Adriana Tavernise, and Yvonne Cooper for their warmth and affection and for making life in graduate school so much easier. Special thanks to Drs. Ann Stuart, Robert Sealock, Alan Fanning and Michael Goy for many useful and stimulating discussions of science. I am indebted to my many colleagues for providing a stimulating and fun environment in which to learn and grow. I am especially grateful for the personal and scientific support extended by my lab mates and colleagues Jonathan Berg, Olga Rodriguez, Omar Quintero, Aurea DeSousa, Damon Jacobs, Melinda DiVito, Brian Robertson, and Taofei Yin. It has been a pleasure to work closely with Eric Vitriol and Mike Kerber. I would specially like to thank

Damon Jacobs, who I hold in high regard, for making my transition into the United States a pleasurable experience and for being such an awesome colleague and friend. I would also like to thank members of the Otey lab especially Dr. Carol Otey, Andrew Rachlin, Dan Arneman, and Silvia Goicoechea for sharing their expertise and reagents with me and for their friendship. Our common interests in the cytoskeleton and in life made our interaction quite enjoyable.

Grad school wouldn't have been as much fun without the support of my best friend and colleague Nicole Ramocki, who helped me get through the difficult times. I thank her for the emotional support, comraderie, entertainment and caring. I also cannot thank enough my friends Gokul Varadhan, Naga Govindaraju, and Sampath Vetsa for their continued support. I also feel incredibly lucky to have had Mariya Chhatriwala as a roommate and good friend.

I shall be forever indebted to my family, especially my grandfather Sundaram, my brother Ananth, my sister Anita, and my parents, Bhaskar and Jaya for their immutable support, understanding and love. I would like to specially thank my parents for creating an environment in which following this path seemed so natural. I would also like to thank my new family, Veena and Anil Bohil for their support and for giving me a place to call "home" in this country. Lastly, but not the least, I thank my husband Gorav Bohil, whose patience, love and understanding helped me joyfully get through four years of a long distance relationship while pursuing a PhD. His support of my career and life goals has been phenomenal and his companionship has been a blessing.

TABLE OF CONTENTS

LIST OF TABLES

TABLE

LIST OF FIGURES

FIGURE

ABBREVIATIONS

Abi 1	Abelson tyrosine kinase interacting protein 1
ALK6	Activin Like Kinase 6
Arp	Actin Related Protein
ATP	Adenosine Tri Phosphate
BMP	Bone Morphogenetic Protein
BMPR	Bone Morphogenetic Protein Receptor
CAD	Cath A Differentiated Mouse Neuronal Cell Line
CFP	Cyan Fluorescent Protein
CPAE	Cow Pulmonary Aortic Endothelial
DCC	Deleted in Colorectal Cancer
DNA	Deoxyribo Nucleic Acid
EM	Electron Microscopy
Ena	Enabled
EGF	Epidermal Growth Factor
ECM	Extra-Cellular Matrix
FAK	Focal Adhesion Kinase
FERM	Band 4.1/ezrin/radixin/moesin
GFP	Green Fluorescent protein
GTP	Guanosine Tri Phosphate
HMM	Heavy Mero Myosin
HEK	Human Embryonic Kidney

IFM	Intra-Filopodial Motility
IFT	Intra-Flagellar Transport
mDia	Mammalian diaphanous
Mena	Mammalian enabled
MARV	Marburg Virus Particles
MMP	Matrix Metallo Proteinase
Myo1	Myosin I
Myo3	Myosin III
Myo7	Myosin VII
Myo10	Myosin-X
Myo15	Myosin XV
MyTH4	Myosin Tail Homology 4
NGF	Nerve Growth Factor
PI3K	Phosphatidyl Inositol 3-Kinase
PTB	Phospho-Tyrosine Binding
PH	Pleckstrin Homology
RT-PCR	Reverse Transcriptase Polymerase Chain Reaction
Rif	Rho in filopodia
SEM	Scanning Electron Microscopy
sh RNA	short hairpin Ribo Nucleic Acid
SH	Slow Hydrolysis
siRNA	small interfering Ribo Nucleic Acid
TIRF	Total Internal Reflection Fluorescence microscopy

VEGF	Vascular Endothelial Growth Factor
VEGFR	Vascular Endothelial Growth Factor Receptor
VASP	Vasodilator Stimulated Phosphoprotein
VP40	Viral Matrix Protein 40
WB	Weak Binding
WASP	Wiskott Aldrich Syndrome Protein
YFP	Yellow Fluorescent Protein

CHAPTER 1

BACKGROUND AND SIGNIFICANCE

The leading edge of most motile cells is characterized by sheet-like lamellipodia and thin, long finger-like extensions called filopodia. Despite recent progress made in understanding lamellipodia extension, the molecular mechanisms regulating filopodia formation still remain largely unknown. Filopodia are long known to play important roles in both vertebrate and invertebrate biology. In many organisms, filopodia act as cellular sensors or antennae and orchestrate important developmental events such as gastrulation in sea-urchin, dorsal closure in fruit fly, and growth cone path finding in flies and mammals (Miller et al., 1995; Wood and Martin, 2002). In higher organisms, filopodia are also thought to play an important role in the formation of immunological synapses, and angiogenesis (Gerhardt et al., 2003; Onfelt et al., 2004). Perhaps the most recent and most exciting development in the field of filopodia biology is the implication that filopodia serve as conduits to receptor, growth factor, and virus trafficking in mammalian cells via a less understood, nevertheless interesting phenomenon termed as intrafilopodial motility (Lehmann et al., 2005; Lidke et al., 2005; Lidke et al., 2004). Despite these fundamental roles of filopodia in important biological functions, the mechanisms underlying extension, retraction and intrafilopodial dynamics of filopodia remain unclear. In this chapter, we will focus on highlighting some of the unanswered questions underlying mechanisms of filopodia

formation and discuss more recent developments since the discovery of a novel form of motility within filopodia- intrafilopodial motility (IFM).

What are filopodia?

Filopodia are typically 0.1-1 micron long (although some filopodia are reported to extend up to several hundred microns) and 0.1 micron thick and are generally thought to arise from the leading edge of cells. In some cell types such as in B16 mouse melanoma cells, filopodial actin bundles, which we term "rootlets" are embedded in the lamellipodial network and may or may not protrude beyond the leading edge. These structures are also referred to as microspikes. Although filopodia are generally thought to arise from the leading edge of cells recent studies demonstrate that filopodia can arise from the dorsal surface of many cells (Bohil et al., 2006). Dorsal filopodia are found on the surfaces of many cells such as lymphocytes. Each filopodium is composed of a dense core of parallel-bundled actin filaments, typically 10-15 filaments each with the barbed ends of actin filaments oriented towards the tip of the filopodium. The actin filaments within the filopodium are bundled together by bundling proteins and fascin is thought to be the major bundling protein within filopodia and this actin filament core is encased by plasma membrane (Svitkina et al., 2003). Actin polymerization is thought to occur at the tip of the filopodium and actin de-polymerization is thought to occur at the base of the filopodium (towards the cell body). The actin filaments within the filopodium undergo constant retrograde flow towards the cell body and polymerization at the tip opposes the retrograde flow of actin filaments towards the cell body. Thus filopodial length depends upon a balance between actin polymerization at the tip and retrograde actin flow (Figure 1.1). Given that retrograde flow is relatively constant in

most vertebrate cells, it is the regulation of polymerization at the filopodial tip that is critical for filopodia extension and retraction (Mallavarapu and Mitchison, 1999). Since the fast growing end of the actin filament is at the tip of the filopodium, it is clear that the tip is a key structure regulating filopodial actin dynamics. EM micrographs reveal the presence of an as yet uncharacterized structure at the tip of filopodium called the filopodial tip complex (Svitkina et al., 2003). Filopodia are highly dynamic structures that extend and retract to explore and interact with the environment and the half-life of a typical filopodium is approximately 5-10 seconds. Here, it is important to note that most studies on filopodia have focused on substrate-attached filopodia and dorsal (non-substrate attached) filopodia may have similar or distinct properties. Very little is known about dorsal filopodia and the information we have so far about dorsal filopodia is riddled with numerous questions. In this regard, the three outstanding questions are, (1) Do dorsal filopodia have a filopodial tip complex? (2) Do dorsal filopodia arise via convergent elongation? (3) Do proteins within dorsal filopodia undergo intrafilopodial motility (Figure 1.2)?

Filopodia are not to be confused with retraction fibers that in fixed cells might be confusingly similar to filopodia. Retraction fibers are membranous processes that remain adherent to the substrate following cell rounding or contact inhibition and retraction of the cells leading edge. Little is known about the formation or molecular components of retraction fibers, but that they are rich in f-actin and share structural similarities with filopodia. Since there are no known molecular markers to distinguish filopodia from retraction fibers, it is currently necessary, if not imperative to use time-lapse microscopy for such distinction.

To add to the confusion, a detailed study of current literature reveals that filopodia

come disguised under numerous aliases such as microvilli, microextensions, cytonemes, hairs, nanotubular highways, etc. To maintain simplicity in this dissertation we shall refer to most thin long cellular structures that fit the criteria mentioned above, including cytonemes and nanotubes, as filopodia, while strictly reserving the terms microvilli and stereocilia to actin-rich extensions of the brush border and inner-ear respectively.

How are filopodia formed?

One model that proposes an elegant mechanism for filopodia formation is termed the convergent elongation model. According to this model actin filaments that make up the lamellipodia at the leading edge of cells converge to initiate filopodia formation by giving rise to a structure known as the lamda (λ) precursor. Actin polymerization propels the growth of these converged filaments to give rise to long filopodia that are then bundled together by bundling proteins such as fascin (Svitkina et al., 2003). The core set of proteins required to form a filopodia is thought to thus include WASP (Wiskott Aldrich Syndrome Protein), which upon binding by small GTPase Cdc42 is relieved of its inhibition and can now bind Arp2/3, an actin nucleator. Arp2/3 then serves to nucleate actin polymerization and induce formation of short, branched network of actin filaments characteristic of the lamellipodium (Hufner et al., 2001; Hufner et al., 2002; Mullins et al., 1998). In cells, the protein that brings about convergence of actin filaments has not yet been identified. However, it is known that VASP (Vasodilator Stimulated Phosphoprotein) is present at the convergent zones. VASP is a protein that can compete with capping protein (a protein that caps the barbed ends of actin filaments thus preventing growth of the filament) and tip the balance from lamellipodia-like short, branched filaments to filopodia-like long, unbranched

filaments (Bear et al., 2002). Consistent with this model, star bundles similar to filopodia has been reconstituted *in vitro* using a basic set of pure proteins that include WASP coated beads, Arp2/3, actin, and fascin. Like filopodia, star bundles are enriched in fascin and lack Arp2/3 complex and capping protein and grow at the barbed end. Similar to cells, in this *in vitro* set up, the transition from a dendritic (lamellipodial) to a bundled (filopodial) organization is induced by depletion of capping protein, and addition of capping protein to the basic set restores the dendritic mode (Vignjevic et al., 2003). It must be noted that even though star bundles are similar to filopodia in core structure and composition, star bundles constituted *in vitro* lack the plasma membrane, myosins, and the filopodial tip complex, whose role in filopodia function is not yet known. Furthermore, the velocity of actin polymerization of star bundles is slower than normal filopodia.

Despite these advances in our knowledge of filopodia formation it is evident from recent research that the mechanism of filopodia formation is not likely to be as simple as postulated by the convergent elongation model. Proteins and conditions that are reported to induce filopodia are listed in Table 1.1. This growing list needs to be investigated and validated further before we begin to comprehend the mechanism underlying filopodia formation.

Figure 1.1 Model of filopodial actin dynamics.

The figure is a minimal model of a typical leading edge of a cell that has four thin, long, cellular structures from left to right. Parallel bundled actin filaments are shown in red. The filopodial tip complex is shown as a light blue star. Arrows depict movement in the direction of the arrow. The first extension is a retraction fiber that is generated from the retraction of the cell membrane. The second extension is a lambda precursor or an initiation complex that is thought to be a precursor to filopodia. The third extension is an extending filopodium. Actin polymerization is thought to occur at the tip of the filopodium and the filopodial actin filaments are thought to undergo retrograde flow towards the cell body. In an extending filopodium, the rate of actin polymerization at the tip is thought to exceed the rate of actin depolymerization at the base of the filopodium. The fourth extension is a retracting filopodium. Actin depolymerization is thought to occur at the base of the filopodium. In a retracting filopodium, the rate of actin depolymerization at the base of the filopodium is typically greater then the rate of actin polymerization at the tip.

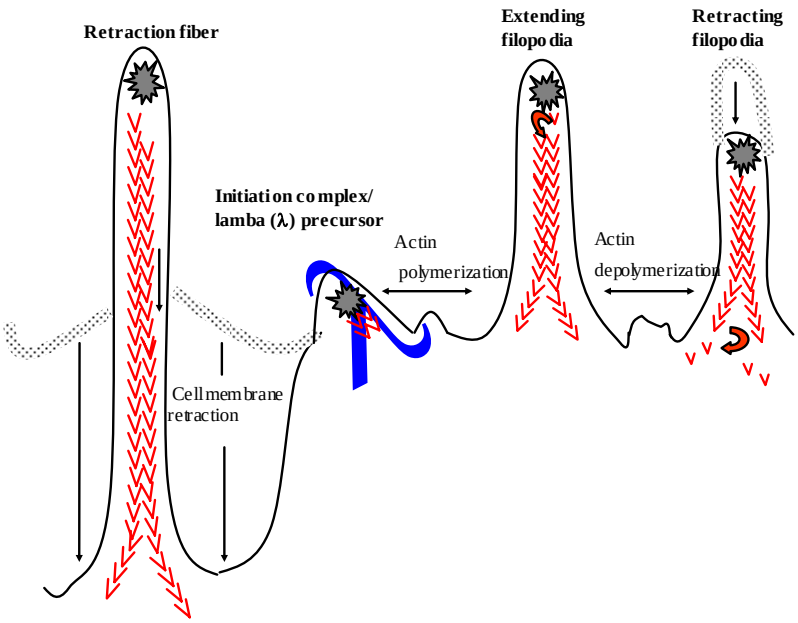
Retraction fiber
Extending filopodia
Retracting filopodia
Initiation complex/ lamba (λ) precursor
Actin polymerization
Actin depolymerization
Cell membrane retraction

Figure 1.2 Model of dorsal and substrate-attached filopodia.

A model showing substrate-attached and dorsal filopodia. This model outlines some of the key questions regarding substrate-attached and dorsal filopodia.

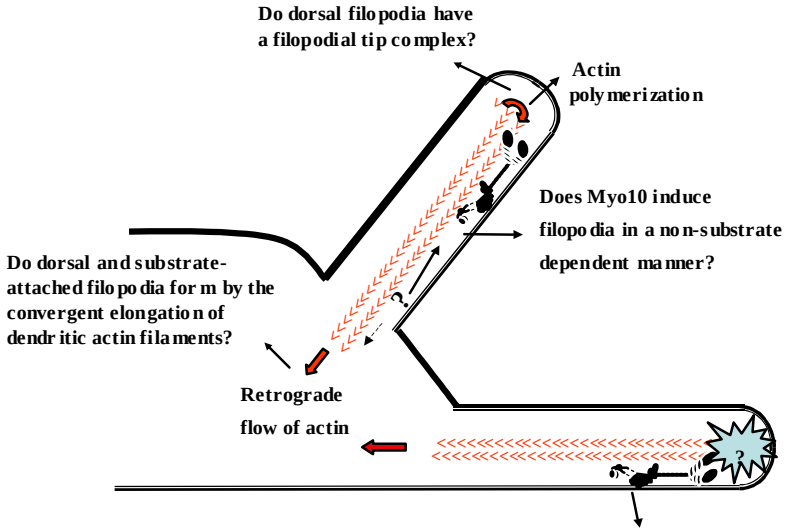
Do dorsal filopodia have a filopodial tip complex?
Actin polymerization
Does Myo10 induce filopodia in a non-substrate dependent manner?
Do dorsal and substrate-attached filopodia form by the convergent elongation of dendritic actin filaments?
Retrograde flow of actin
Does Myo10 act as a molecular clutch to induce substrate-attached filopodia

Table 1.1 Molecules involved in filopodia formation.

The table highlights some of the players that are thought to be involved in filopodia formation pathways.

Molecules	Treatment	Cell Type	Reference
Ena/VASP	Overexpression, dominant negative, knockout	Mammalian cells, Dictyostelium	Lebrand et al., Neuron 2004; Han et al., JBC 2002
dDia2 / mDia2	Overexpression, knock-down	Dictyostelium, mammalian cells	Schirenbeck et al., Nat. Cell Biol. 2005; Wallar et al., JBC 2006
IRSp53	Overexpression	Mammalian cells	Millard et al., EMBO J 2005
Myosin-X	Overexpression, knock-down, dominant negative	Mammalian cells	Berg et al., Nat. Cell Biol. 2002 Bohil et al., PNAS 2006
Rif/ Cdc42 / Vav/ TC10	Overexpression, dominant negative	Mammalian cells	Pellegrin and Mellor., Curr Biol. 2005 Nobes and Hall., Cell 2005 Kranewitter et al., Cell Motil Cytoskeleton 2001 Murphy et al., Oncogene 1999
PI3Kinase	Inhibition by wortmannin,LY	Mammalian cells	Tornieri et al., Cell Motil. Cytoskeleton 2006
Increased Calcium	Intracellular release from caged compounds	Mammalian cells (neurons)	Cheng et al., J Neurobiol 2002
Delta, Netrin receptor DCC	Dose treatment, drug inhibition	Mammalian cells (neurons)	De Joussineau et al., Nature 2003 Shekarabi and Kennedy., Mol Cell neurosci 2002

Unresolved questions and opportunities for future research

Although the convergent elongation model proposes an elegant mechanism for filopodia formation, it remains to be identified how cells form filopodia in the absence of Cdc42 and N-WASP or in the presence of functionally inhibited Arp2/3 (key players in the convergent elongation model) (Czuchra et al., 2005; Falet et al., 2002; Steffen et al., 2006). Since each filopodial actin filament is oriented with its barbed end towards the tip, nucleation of new filaments may not even be necessary during filopodial extension. However, Arp2/3 and WASP may still be important for filopodial initiation. (Higgs and Pollard, 2000a; Svitkina et al., 2003). Interestingly, interfering with Arp2/3 or N-WASP function in cells does not interfere with the cells ability to make filopodia indicating that other proteins are likely to regulate actin polymerization at the tips of filopodia. Actin nucleators called formins, which do localize to filopodial tips, have recently emerged as excellent candidates to regulate filopodial actin polymerization (Higashida et al., 2004). Additionally, the formation of dorsal filopodia, which does not arise from the leading edge, remains a complete mystery and it remains to be established whether in these structures actin filaments arising from “actin patches” converge and elongate.

VASP proteins participate in the actin polymerization process and localize to filopodial tips (Dent and Gertler, 2003). In addition to their localization to filopodial tips. VASP proteins also localize to focal adhesions, and puncta along stress fibers (Reinhard et al., 1992). More importantly, VASP is thought to act as a competitive inhibitor of capping. (Bear et al., 2000). The anti-capping property of VASP has recently come under some scrutiny raising important questions. *In vitro* data from biochemical analysis demonstrate that while VASP can aid in actin polymerization, it does not inhibit capping (Schirenbeck et

al., 2006). It must be noted here that while this recent data suggests that VASP cannot un-cap capped actin filaments, it however does not rule out the possibility that VASP can compete with capping protein for barbed ends of actin filaments as is also demonstrated by similar biochemical assays (Barzik et al., 2005). Additionally the role of VASP is somewhat unclear given the data that mena (mammalian enabled, a VASP family member) /VASP null cells when supplemented with myosin-X, an unconventional myosin that is implicated in filopodia formation, can induce filopodia formation in these cells indicating that VASP is not necessary for filopodia formation (Bohil et al., 2006). To establish whether VASP is necessary for filopodia formation, it remains to be tested whether expression of proteins like formins, WASP and Cdc42 in Mena/VASP null cells yield similar results.

In addition to proteins that aid in actin polymerization, small GTPases like Cdc42 appear to function as master regulators of filopodia formation (Nobes and Hall, 1995). However a recent discovery suggests that Cdc42 knockout fibroblasts can still retain their ability to form filopodia indicating that Cdc42 is also not necessary for filopodia formation (Czuchra et al., 2005). It must be noted that in Cdc42 null cells it is possible that other GTPases of the Cdc42 family like TC10 (Murphy et al., 1999), which have also been implicated in filopodia formation might compensate for the lack of Cdc42 or that Cdc42 independent pathways such as the Rif (Rho in filopodia- a small GTPase that belongs to the Rho family of GTPases that induces dorsal filopodia in a Cdc42 independent but mDia2 dependent manner) pathway for filopodia formation might be able to provide an explanation as to how Cdc42 null cells still form filopodia (Ellis and Mellor, 2000; Pellegrin and Mellor, 2005). In this regard, a most recent study reveals that Cdc42 null primary embryonic mouse fibroblasts do not have filopodia and lack the ability to make new filopodia (Yang et al.,

2006). These conflicting reports indicate that further research is required before we draw conclusions regarding the role of Cdc42 in filopodia formation.

The filopodial tip complex - a specialized site of adhesion, a polymerization machine, or a signaling complex?

The tip of the filopodium is central to filopodial actin dynamics and a growing number of proteins are reported to localize to the tip. These include proteins that play a role in adhesion, actin polymerization and signaling. Adhesion receptors such as integrins (a3b1 and avb6), some tetraspanins (CD81 and CD151), matrix metalloproteinases (MMP9), abl tyrosine kinase interacting protein (Abi1), and lamellipodin are all reported to localize to the tip (Krause et al., 2004; Penas et al., 2000; Stradal et al., 2001; Thomas et al., 2001; Wu et al., 1996). Since the filopodial tip has long been recognized as a site of contact and adhesion and since adhesion receptors such as integrins and talin localize to the tip, we hypothesize that the filopodial tip serves as a specialized adhesion complex distinct from the focal adhesion (Figure 1.3 and Table 1.2). Since several tip proteins such as VASP, formins, and Abi1, are involved in actin polymerization and signaling, it is also intriguing to think of the filopodial tip complex as a polymerization machine or a signaling center. Given that the filopodial tip is 100 nm wide and the core of the filopodium is composed of parallel-bundled actin filaments (important factors that might limit diffusion), it is not yet clear how receptors and other proteins localize to the tips.

Figure 1.3 Model of the filopodial tip complex.

A model of a filopodium where the parallel-bundled actin filaments are shown in red, the filopodial tip complex is shown in light blue. Some of the proteins that have been shown to be present at the tip of the filopodium are listed.

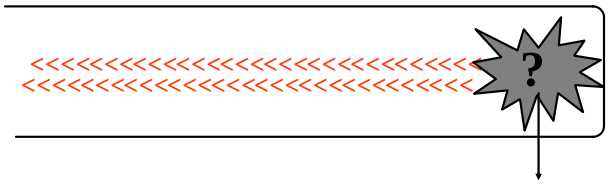

VASP

Integrins

Myosin-10

Formins

Abi1

X?

Table 1.2 The filopodial tip complex-a specialized site of adhesion.

Table outlines some of the basic differences between a focal adhesion, a focal complex and a tip complex.

Trait	Filopodial tip complex	Focal complex	Focal adhesion
Size and shape	<1 um, Punctate (Svitkina et al., JCB 2003)	1 um, Punctate?	2-10 um, Elongated?
Upstream GTPase	Cdc42, RIF (Nobes and Hall., Cell 2005; Pellegrin et al., Curr Biol. 2005)	Rac1 (Allen et al., JCS 1997)	RhoA (Barry and Critchley., JCS 1994)
Time scale of assembly/disassembly	Minutes?	Seconds (Rottner et al., Curr Biol. 1999)	Minutes (Ronen Zaidel-Bar et al., JCS 2003)
Connection with actin	Tips of filopodial actin filaments (Svitkina et al., JCB 2003)	In a loose mesh?	At termini of stress fibers (Ridley and Hall; Cell 1992)
Force dependence	Dependent on substrate attachment?	May depend on retrograde flow of actin at the lamellipodium?	Dependent on acto-myosin contractility phosphorylation and focal complexes (Bershadsky et al., Eur J of Cell Biol. 2006)
Tyrosine phosphorylation	Tyrosine phosphorylated (Robles et al., J Neurosci 2005)	Highly tyrosine phosphorylated (Kirchner et al., JCS 2003)	Tyrosine phosphorylation diminishes with maturation (Kirchner et al., JCS 2003)
Prominent proteins	B1, B3, & B6 integrins, talin, VASP, VEGFR2, mDia2, paxillin?	B3 integrin, talin, paxillin, vinculin, FAK (Zaidel-Bar et al., Biochem Soc Trans. 2004)	Same as focal complex plus alpha-actinin, VASP, tensin, and zyxin (Zaidel-Bar et al., Biochem Soc Trans. 2004)

Myo10 is an unconventional myosin that localizes to tips of filopodia

Myo10 is a MyTH4-FERM myosins that is unique in that it contains multiple PH (Pleckstrin Homology) domains. The 237 KDa Myo10 heavy chain contains a head/motor domain, 3 IQ motifs, a predicted stalk of coiled coil, and a unique tail (Berg et al., 2000). The tail includes 3 PH domains, which have been implicated in PI3K signaling, a FERM domain of unknown function, and a MyTH4 domain that binds microtubules (Weber et al., 2004) (Figure 1.4).

When expressed in cells, both endogenous and exogenous Myo10 exhibit a striking localization to tips of filopodia. Myo10 was the first myosin to be described to exhibit this unusual localization pattern. In this regard, GFP-Myo10 is one of the strongest and most specific markers of filopodial tips yet discovered. In addition to localizing at filopodial tips, GFP-Myo10 also undergoes striking forward and rearward movements within filopodia, which we term intrafilopodial motility (Berg and Cheney, 2002). These studies also indicate that Myo10 uses its motor domain to localize to filopodial tips. Myo10 also has functional effects on filopodia since over-expressing full length Myo10 (but not "tail-less" or "tail-alone" constructs) led to a four-fold increase in length and number of substrate-attached filopodia (Berg and Cheney, 2002). This is particularly interesting as it raises a number of important questions regarding the mechanism of filopodia induction by Myo10. Despite these recent advances in our understanding of properties and functions of Myo10, identification of its cargoes, binding partners and mechanism of action is required to comprehend Myo10's role in filopodial dynamics and function.

Figure 1.4 Model of the domain structure of Myo10.

A working model of the structure of myosin-X (Myo10). The different domains of Myo10 are shown here in this model. Myo10 is thought to function as a dimer.

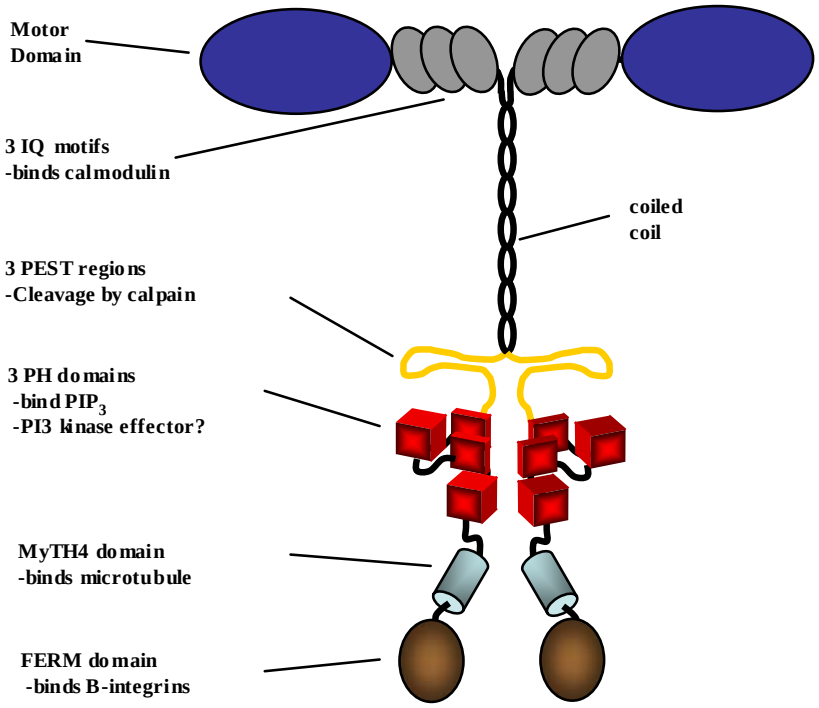
Motor
Domain
3 IQ motifs
-binds calmodulin
coiled
coil
3 PEST regions
-Cleavage by calpain
3 PH domains
-bind PIP3
-PI3 kinase effector?
MyTH4 domain
-binds microtubule
FERM domain
-binds B-integrins

Intrafilopodial motility as a novel mode of trafficking

The use of time-lapse microscopy as a tool to study cell behavior has provided the field of filopodia research with new and exciting data that not only are filopodia highly dynamic structures, but also that particles move within it. The discovery of forward movements of cytoplasmic aggregates or phase dense granules in filopodia that moved outward at 1.8 μm/sec in filopodia, that was blocked by ATP depletion and cytochalasin but not by nocodazole (a microtubule depolymerizing agent) favored the possibility that the forward movements might be powered by a myosin (Sheetz et al., 1990) (Figure 1.5). These aggregates might very well include EGF receptors, integrins, and formins. Recent advances in imaging technology have made this technically challenging phenomenon easier to study giving rise to some very exciting and promising new discoveries in the field of neurobiology, blood vessel physiology, and microbiology. Berg et al in 2002 had shown that an unconventional myosin called Myosin-X (Myo10) moved anterograde at about 0.1 μm/sec and retrograde at 0.01 μm/sec (corresponding to the retrograde flow rate of actin) and termed this novel form of motility within filopodia as intrafilopodial motility (IFM). Since this discovery a wide repertoire of particles has recently been reported to move within filopodia. These include, phase dense granules, EGF coated beads, integrins, and even extra-cellular particles like viruses. While the rates of anterograde and retrograde movements of these particles fall within a range of 0.1-0.3 μm/sec, some particles such as the formin mDia1 are reported to move at rates of a 1 μm/sec (Grabham et al., 2000; Higashida et al., 2004; Lehmann et al., 2005; Lidke et al., 2005; Lidke et al., 2004; Sheetz et al., 1990). Table 1.3 summarizes the actin-based movements observed in filopodia.

Figure 1.5 Model of intrafilopodial motility of Myo10.

A model a hypothetical mechanism for intrafilopodial motility powered by myosin molecules. According to our hypothesis, forward motility of proteins such as integrins, VASP, is powered by the motor activity of myosin proteins, while rearward motility is thought to occur due to clutch like coupling to retrograde flowing actin.

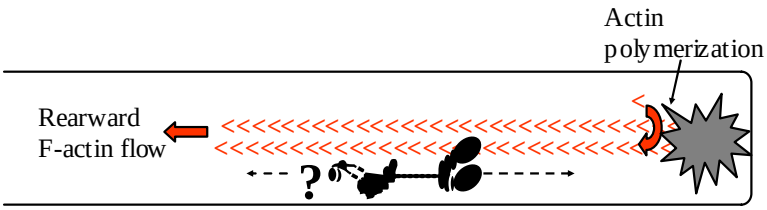

Rearward motility due to coupling to rearward F-actin flow?

Rearward moving partides:
Integrins, EGF coated beads, ErbB1 receptors, and viruses

Forward motility powered by myosins (Myo10/Myo15)?

Forward moving particles:
Integrins, formins, X?

Table 1.3 Summary of intrafilopodial movements.

Table lists some of the recorded events of intrafilopodial motility found in literature.

Cell Type	Retrograde Actin flow rate	Rearward Particle	Forward Particle	References
Mouse cortical neuron growth Cone	N/d	0.1-0.5 μm/sec (2A1 bead)	1-2 μm/sec (2A1 bead)	Sheetz et. al., Cell 1990
Mouse 3T3 fibroblast	N/d	0.05-0.15 μm/sec (FNIII bead)	N/d	Felsenfeld et al., Nature 1996
Chicken sympathetic neuron growth cone	N/d	0.05-0.15 μm/sec (β1 integrin mAb)	0.5-2 μm/sec (β1 integrin mAb)	Grabham et al., JCS 2000
Human cervical cancer fibroblast	15 um/sec	0.015 μm/sec (GFP-Myo10)	0.075-0.2 μm/sec (GFP-Myo10)	Berg and Cheney., NCB 2002
Xenopus XTC fibroblast	N/d	N/d	2 μm/sec (GFP-mDia1ΔN3)	Higashida et al., Science 2004
Human epithelial carcinoma A431 cells	N/d	0.01 μm/sec (Quantum dot-EGF coated beads)	N/d	Lidke et al., Nat. Biotechnol.□ 2004
Human epithelial carcinoma A431 cells	N/d	0.055 μm/sec (Quantum dot-ErbB1 receptor)	N/d	Lidke et al., JCB 2005
African Green Monkey kidney epithelial COS-7 cells	N/d	0.02 μm/sec (GFP-Myo15)	N/d	Belyantseva et al., Nat. Cell Biol. 2005
Human Embryonic Kidney HEK 293 cells expressing receptor mCAT-1	N/d	0.1-0.16 μm/sec (Murine Leukemia Virus particles)	N/d	Lehmann et al., JCB 2005

N/d = Not defined; FN = Fibronectin

Viruses hijack IFM to establish and spread infection in cells

Microorganisms like *Eischeria coli* and *Listeria monocytogenes* have been previously shown to cleverly hijack the host cell cytoskeleton in order to establish and spread infection (Cameron et al., 2000; Sanger et al., 1996). Recent reports have now shown that virus binding to filopodia induces a rapid and highly ordered lateral movement, termed "surfing" toward the cell body before cell entry. This virus cell surfing along filopodia is mediated by the underlying actin cytoskeleton and depends on functional myosin II, which is thought to control retrograde flow of actin towards the cell body. Any disruption of viral cell surfing significantly reduces viral infection (Lehmann et al., 2005). These results shape the future of the field of viral infection by demonstrating that viruses possess an innate talent to hijack host machineries for establishing infection by using IFM. It should be noted that the nature of these movements could only be truly appreciated by viewing the movies of IFM.

The availability of more sophisticated and new technology such as TIRF, and single photon microscopy clearly demonstrate that the field of filopodia research is slowly encompassing broader areas of research as is evident by the stimulating discoveries discussed here. What we see here is only the beginning of novel things to be learnt and suggests that filopodia, albeit seemingly simple, are probably involved in a myriad of complex biological phenomena.

DISCUSSION

Filopodia and other actin-rich cellular extensions

Cells have a dynamic actin cytoskeleton characterized by protrusive structures such

as lamellipodia, phagocytic cups and filopodia. Differences in signaling pathways and effector molecules are probably account for such diverse and unique morphologies. However, through the use of actin as a versatile building material, specialized sub cellular compartments consisting of bundles of filamentous actin have evolved. The simplest of these structures are filopodia. Others include microvilli, stereocilia, and dendritic spines; it has been hypothesized that filopodia serve as precursors to some or all of these structures.

The parallel bundles of actin in filopodia, microvilli, and stereocilia are packed in regular arrays by actin cross linkers such as fimbrin (Drenckhahn et al., 1991; Heintzelman and Mooseker, 1992), espin (Zheng et al., 2000), and other cross linkers such as fascin (Otto et al., 1979) for filopodia and villin for microvilli (Bartles, 2000; Bretscher and Weber, 1979). Although these structures are morphologically similar, there are significant differences between the highly dynamic filopodia and the more stable microvilli or stereocilia. The actin bundles of filopodia are embedded within the lamellipodia and undergo continuous retrograde flow (Mallavarapu and Mitchison, 1999). Actin bundles of microvilli are anchored in the terminal web, an actin rich cortical domain enriched with numerous other components of the membrane cytoskeleton (Hirokawa et al., 1982). Actin bundles of stereocilia taper towards the base of the process and the remaining rootlets anchor into the cuticular plate (Tilney et al., 1980). Mature microvilli and stereocilia have a more stable configuration than filopodia, which can extend and retract within minutes (Rzadzinska et al., 2005). However, labeling of intestinal epithelial cells suggests that microvillar structural proteins undergo constant turnover and additional evidence suggests that microvilli can exhibit dynamic changes. It is thus possible that very slow retrograde flow of actin bundles, offset by slow actin polymerization at the microvillar tips accounts for the turnover of

structural components and that these rates can change following various stimuli, such as diet and disease (Loomis et al., 2003). It should be noted here that actin-based structures similar to filopodia cover the surfaces of cells such as lymphocytes. Although these structures are referred to as microvilli, it is probably more similar in organization and structure to filopodia and thus referring to these structures, as filopodia rather than microvilli is probably more appropriate and less confounding.

Intrafilopodial motility shares striking similarities with intraflagellar transport

There are remarkable parallels between IFM and intraflagellar transport (IFT). Intraflagellar transport (IFT), which is characterized by cargo-carrying kinesin and dyenin-mictrotubule based motors is thought to play a role in the assembly and maintenance of microtubule-rich cilia and flagella. The process of IFT is an elegant demonstration of the construction of cellular structures by the delivery of, assembly, and recycling of components (Rosenbaum and Witman, 2002). It appears that the forward and rearward movements of myosins in filopodia represent an analogous mechanism for transport of cargo, adhesion molecules, structural components or signaling molecules to tips of actin-based structures. A major difference between these systems is that retrograde flow of actin filaments could provide a mechanism for transporting receptors or other particles such as viruses to the cell body without requiring a retrograde motor protein as in the case of dyenin in IFT.

Unconventional myosins and intrafilopodial motility

The myosin super-family of actin-based motor proteins is known to power many forms of movement such as vesicle transport, phagocytosis, and muscle contraction. Of the

known myosins, particularly interesting are the MyTH4-FERM myosins, a "super class" whose tail domains are characterized by the presence of MyTH4 and FERM domains. In *Dictyostelium discoideum*, Myo7 (a MyTH4-FERM myosin) localizes to the tips of filopodia and its deletion leads to loss of filopodia, inhibition of phagocytosis, and defects in adhesion (Han et al., 2002; Titus, 1999; Tuxworth et al., 2001). There are four MyTH4-FERM myosins in humans, Myo7a, Myo7b, Myo10 and Myo15a (Berg et al., 2001). Myo7a expression is limited largely to hair cells of the inner ear, to retinal pigmental epithelial cells, testis, and kidney (Weil et al., 1995). Reports on Myo7b indicate that this myosin is expressed in microvilli of epithelial cells (Chen et al., 2001). Myo15a is expressed almost exclusively in sensory epithelia of the inner ear and in the pituitary gland. Recent studies indicate that Myo15a localizes to the tips of filopodia when expressed in cells. Both Myo7 and Myo10 play a role in phagocytosis, adhesion, and filopodia. Myo15 and Myo10 also share some similarities; both proteins localize to tips of filopodia (Belyantseva et al., 2003) and undergo intrafilopodial motility (IFM) when expressed in cultured cells. Myosins are thus very likely candidates to transport receptors, and other molecules to tips of filopodia.

The discoveries described here only mark the commencement of promising discoveries yet to be made on these intriguing cellular fingers-filopodia.

CHAPTER TWO

Myosin-X (Myo10), a core component of the filopodial tip complex, binds to β-integrins at tips of filopodia

The filopodial tip is characterized by the presence of an amorphous dense material called the filopodial tip complex. While the filopodial tip complex has been hypothesized to play a central role in filopodia extension or retraction and cargo loading and unloading, its structure and components are still unknown. Myosin-X (Myo10) is an unconventional myosin that is hypothesized to be a component of a putative filopodial tip complex. In this regard, Myo10 is one of the strongest tip markers we have encountered. Despite recent progress that Myo10 localizes to filopodial tips and undergoes intrafilopodial motility within filopodia (Berg and Cheney, 2002), the mechanism of action, identity of cargoes, and cellular functions of Myo10 are largely unknown. Interestingly, β-integrins and tyrosine-phosphorylated proteins have previously been observed to localize to and undergo movements within neuronal filopodia, but the mechanism of these directed movements towards filopodial tips is largely unknown. While it has been speculated that a myosin might mediate the transport of integrins and tyrosine-phosphorylated proteins to filopodial tips, the identity of this myosin remains a mystery (Grabham et al., 2000; Grabham and Goldberg, 1997; Robles et al., 2005). We hypothesize that Myo10 can bind to, activate,

and transport integrins to filopodial tips. Here, we show that (1) Myo10 is a core component of the filopodial tip complex, (2) Myo10 can bind to and colocalize with integrins at filopodial tips and (3) Myo10 may activate β-integrins and undergo cotransport within filopodia.

INTRODUCTION

The slender actin-based protrusions known as filopodia play a key role in biological processes ranging from growth cone guidance to angiogenesis (Gerhardt et al., 2003; O'Connor et al., 1990). Filopodia are composed of a core of parallel-bundled actin filaments and the tips of these actin-rich structures are characterized by the presence of an amorphous dense material when visualized by electron microscopy (Mooseker and Tilney, 1975). The tip of the filopodium is central to filopodial actin dynamics (Mallavarapu and Mitchison, 1999) and a growing number of proteins are reported to localize to the tip. These include proteins that play a role in adhesion, actin polymerization and signaling. Adhesion receptors such as integrins (α3β1 and αvβ6), some tetraspanins (CD81 and CD151), unconventional myosins (Myo10, Myo15, and Myo3A) matrix metalloproteinases (MMP9), mena/VASP, formins, abl tyrosine kinase interacting protein (Abi1), and lamellipodin are all reported to localize to the tip (Belyantseva et al., 2005; Berg and Cheney, 2002; Higashida et al., 2004; Krause et al., 2004; Les Erickson et al., 2003; Penas et al., 2000; Stradal et al., 2001; Thomas et al., 2001; Wu et al., 1996).

Since the filopodial tip has long been recognized as a site of contact and adhesion and since adhesion receptors such as integrins localize to the tip, we hypothesize that the filopodial tip serves as a specialized adhesion complex distinct from the focal adhesion.

Since several tip proteins are involved in actin polymerization and signaling, the filopodial tip complex may also act as a polymerization machine or a signaling center. It is important to understand the filopodial tip complex in greater detail because it is at the filopodial tip complex that filopodia extension and retraction is thought to occur.

In this regard the localization of β1-integrins and tyrosine phosphorylated proteins that are usually found in focal adhesions at the tips of filopodia (Grabham and Goldberg, 1997; Wu et al., 1996) is particularly interesting because of the observations that demonstrate that β1 -integrins (Grabham et al., 2000) and a reporter of phospho-tyrosine (Robles et al., 2005) undergo rapid forward movements and slower rearward movements within filopodia in a manner that is strikingly similar to Myo10.

Integrins are hetero-dimeric, integral membrane proteins composed of α and β subunits that couple the extra cellular matrix (ECM) outside a cell to the actin cytoskeleton inside the cell. The connection between the cell and the ECM enables the cell to exert pulling forces during cell migration and induces integrin-mediated inside-out and outside-in signaling. The integrin-based connections between ligands in the ECM and the microfilaments inside the cell are indirect: they are linked via scaffolding proteins like talin, Mena (Mammalian enabled)/ VASP (Vasodilator Stimulated Phosphoprotein), paxillin, and vinculin. These scaffolding proteins act by regulating kinases like FAK (Focal Adhesion Kinase) and together with signals arising from receptors for soluble growth factors like VEGF (Vascular Endothelial Growth Factor), EGF (Epidermal Growth Factor), and NGF (Nerve Growth Factor) (Bokel and Brown, 2002; Martin et al., 2002). These signals also regulate cell motility. In this regard, one of the critical questions in this area has been how integrins and tyrosine- phosphorylated proteins undergo directed transport to filopodial tips.

While it is speculated that integrins might be transported by myosins, this has not yet been demonstrated. Owing to its cellular localization at filopodial tips the unconventional myosin, Myo10 is well suited to play this role.

When expressed in cells, both endogenous and exogenous Myo10 exhibit a striking localization to the tips of filopodia. In addition to localizing at filopodial tips, GFP-Myo10 also undergoes striking forward and rearward movements within filopodia, which we term intrafilopodial motility. Myo10 also has functional effects on filopodia since over-expressing full-length Myo10 (but not "tail-less" or "tail-alone" constructs) led to a four- fold increase in number of substrate-attached filopodia (Berg and Cheney, 2002). Despite these recent advances in our understanding of Myo10's properties and functions, Myo10's cargoes and mechanism of action is unknown.

Myo10 is a MyTH4-FERM myosin that contains multiple PH (Pleckstrin Homology) domains. The Myo10 heavy chain contains a head/motor domain, 3 IQ motifs, a predicted stalk of coiled coil, and a unique tail (Berg et al., 2000). The tail includes 3 PH domains, which have been implicated in PI3K signaling, a MyTH4 domain that binds microtubules (Weber et al., 2004), and a FERM domain of unknown function. Here, it is interesting to note that the FERM domain of talin, a key protein of focal adhesions, can bind to and activate integrins at focal adhesions (Calderwood et al., 2002).

Based on the crystal structure of the FERM domains of ERM proteins, moesin, radixin, and band 4.1, the FERM domain of talin was predicted to contain three subdomains F1, F2, and F3. The F3 subdomain of talin is particularly interesting because it is the domain can bind to and activate integrins. The binding of the F3 domain of talin to β-integrins resembles the binding of PTB (Phospho-Tyrosine Binding) domains to sequences containing

the NPXY motif. The NPXY-dependent integrin binding to the PTB-like FERM subdomain F3 of talin suggests conserved mechanisms for integrin binding and activation. Note that contrary to what the naming suggests, the binding of PTB-like talin F3 subdomain (Calderwood et al., 2002) to integrin β tails is independent of tyrosine phosphorylation. Regulation of integrin binding by talin is instead thought to occur as a result of conformational changes that take place in the talin molecule itself. For instance, the integrin binding site in the FERM domain of talin head domain thought is to be masked by interactions with the COOH-terminal tail domain. The interaction of talin with phosphoinositides is thought to unmask the integrin binding site in the FERM domain of talin (Martel et al., 2001). Interestingly, integrin activation by the F3 subdomain of talin is thought to involve large changes in tertiary and quaternary structures of integrins that in turn is thought to lead to changes in integrin affinity for its ligand (Liddington and Ginsberg, 2002). Although the FERM domains of Myo10 and talin are not highly conserved, the critical role of integrin activation in cell function makes it important to test if the FERM domains of the two proteins share similar functions. Binding of Myo10 to integrins is also interesting because of the molecular clutch hypothesis, which proposes that a myosin may function as a link between filopodial actin filaments and cell-adhesion molecules bound to the extra - cellular matrix (Mitchison and Kirschner, 1988). However, the identity of these putative myosins has remained a complete mystery.

Myo10 emerged as a novel integrin binding protein in an attempt to identify novel binding partners for integrins. Staffan Stromblad's laboratory (Karolinska Institute, Sweden) screened a mouse embryo yeast -two-hybrid cDNA library using the cytoplasmic tail of human integrin β5 as bait. One of the positive clones they identified from this screen was

Myo10. This discovery is particularly interesting because similar to talin, (1) The F3 subdomain of Myo10 binds to NPXY motif of β-integrins, (2) The binding of the FERM domain to the NPXY motif of β-integrins is independent of tyrosine phosphorylation (Zhang et al., 2004), and (3) Myo10 can bind to phosphoinositides (Isakoff et al., 1998), which in talin is thought to regulate the talin's interaction with β-integrins. To verify the validity of this interaction, our laboratories established collaboration and performed several biochemical and cell biological tests. While our collaborators used immunoprecipitation experiments to show that the GFP-Myo10-Tail coprecipitated with β1, β3 and β5 integrins and β1 integrins coprecipitated with the GFP-Myo10 FERM domain, I performed experiments to test the validity of the interaction *in vivo*. Briefly, my experiments showed that filopodial tips of cells can be adhesive structures, that endogenous Myo10 and αvβ3 integrins colocalize in CPAE cells, that overexpression of GFP-Myo10 enhances β1 integrin localization at filopodial tips (Zhang et al., 2004) and that the FERM domain of Myo10 appears to activate β1 integrin. Furthermore, I also performed dual-color live cell video microscopy to demonstrate that GFP-β3 integrins and CFP-Myo10 undergo co transport within filopodia. Similarly, a reporter for phosphotyrosine (YFP-dSH2) and CFP-Myo10 also undergoes cotransport within filopodia. I also performed preliminary experiments using siRNA to show the movement of β3 integrins within filopodia is inhibited in Myo10 knock-down cells.

MATERIALS AND METHODS

Constructs

GFP-β3-integrin was a gift from Dr. Jonathan C. Jones (Tsuruta et al., 2002). The bovine GFP-Myo10 construct has been described previously (Berg and Cheney, 2002). The bovine CFP-Myo10 construct was generated by replacing GFP with CFP. The bovine GFP-Myo10-FERM construct was generated by digesting the bovine GFP-Myo10 construct with Kpn1 and ligating it into PEGFP-C2.

Transfection

Cells were transfected using Polyfect (Qiagen) according to the manufacturer's recommendations.

Immuno-electron microscopy

Immuno-electron microcopy and platinum replica electron microscopy was performed as described previously (Svitkina and Borisy, 1998; Svitkina and Borisy, 1999). Briefly, cells were washed in PBS and extracted with 1% Triton X-100 in PEM buffer (100 mM Pipes, pH 6.9, 1 mM EGTA, and 1 mM $MgCl_2$) containing 4% polyethylene glycol (PEG) and 2 μM phalloidin. Following extraction, cells were fixed with 2% glutaraldehyde in 0.1 M sodium cacodylate buffer, pH 7.3. Cells were incubated with anti-Myo10 #117 at 100 μg/ml for 1 hour. Following a brief wash, the cells were incubated overnight with goat anti-rabbit secondary conjugated to 10 nm colloidal gold (Sigma) diluted 1:5. Omar A.

Quintero performed these experiments in collaboration with Tanya M. Svitkina.

Antibodies

The following primary antibodies were used for immunostaining or immunoprecipitation: affinity-purified rabbit anti-Myo10 #117 (Berg et al., 2000), affinity purified chicken anti-Myo10 #3568 (Sousa et al., 2006), mouse anti-VASP (1μg/ml, Transduction labs), rabbit anti-VASP (1:1000 dilution, Becton-Dickinson), mouse anti-fascin (1:100, Dako-cytomation), and rabbit anti-pArc3 of the Arp2/3 complex (1:500 dilution), αvβ3 integrins (LM609 Chemicon 5mg/ml), β1 integrin (LM534 Chemicon at 1:1000 dilution from ascites fluid) Myo10 (117 polyclonal antibody at 1 μg/ml), Mena (1:500 dilution from Frank B. Gertler), talin (Sigma B6059, clone 8d4 2 μg/ml), paxillin (BD Transduction Laboratories, Clone 165, 0.5 μg/ml), vinculin (Sigma-Aldrich, hVIN1 used at a dilution of 1:400 from ascites fluid) FAK (BD Transduction Laboratories, 2.5 μg/ml), and phosphotyrosine (PY20, BD Transduction Laboratories, 1 μg/ml). Secondary antibodies conjugated to Alexa 488 or Alexa 568 were purchased from Molecular Probes and secondary antibodies conjugated to HRP were purchased from Jackson Laboratories and used at 1:1000 dilution.

Immunofluorescence microscopy

Cells were trypsinized ~18 hours after transfection and then replated onto 12 mm coverslips overnight. For immunostaining experiments, cells were then fixed with 3.7% paraformaldehyde at 37^{o}C for 10 minutes, permeabilized with 0.2% triton-X-100 for 5 minutes, and blocked at room temperature with goat serum for 30 minutes. Cells were

incubated for 1 hour with primary antibodies, rinsed 3x in PBS for 10 minutes each, and incubated for 45 minutes with 1 μg/ml Texas Red goat-anti mouse secondary antibody (Molecular Probes). Following incubation with secondary antibody, cells were rinsed 3x with PBS for 10 minutes each, mounted on glass slides, and imaged using a Nikon TE2000 fluorescence microscope equipped with a 60x 1.4NA objective. Images were collected using an Orca ER cooled CCD camera (Hamamatsu) and Metamorph software (Universal Imaging). Brightness and contrast were adjusted using Adobe Photoshop.

Knock-down of Myo10 using siRNA

A double stranded synthetic siRNA targeting Myo10 (5'-AAGTGCGAACGGCAAAAGAGA-3') and a control siRNA (5'-AATTCTCCGAACGTGTCACGT-3') were obtained from Qiagen tagged with fluorescein. A day before siRNA treatment, ~100,000 cells/well were plated onto 6-well plates at 50-60% confluence and incubated at 37^{o}C for 12 hours. Cells were then treated with a final concentration of 110-150 nM siRNA using RNAifect (Qiagen) following the manufacturer's instructions. The media was replaced ~16 hours after transfection and fluorescence microscopy was used to verify that ~100% of the cells had taken up the siRNA. At ~48 hours the cells from each well were replated, typically into 3 wells of a 6-well plate containing 22 mm square coverslips. At ~60-72 hours cells were processed for light microscopy and parallel samples were assayed by immunoblotting to verify knock-down. For siRNA experiments that also involved transfection with an expression plasmid, siRNA treated cells were transfected with GFP-β3-integrin construct at ~48 hours. Cells were allowed to grow an additional ~12 hours following transfection and were then used for time-

lapse video microscopy.

Imaging and analysis

Cells were imaged using an Orca ER CCD camera (Hamamatsu, Bridgewater, NJ) with Metamorph software (Universal Imaging, West Chester, PA) to control illumination shutters and camera exposure. Time-lapse images were obtained by sequential epifluorescent and phase illumination with a 60X phase 3 lens (Nikon, TE2000, Melville, NY). Time-lapse intervals were 5−10 s and exposure times were 100−300 ms, depending on the time-lapse interval and level of fluorescence. Cells were imaged over periods of 3−10 min at room temperature (25−30^{o}C). Movie files were created using QuickTime (Apple).

Blow-off experiments

HeLa cells were transfected with GFP-Myo10 and 18 hrs after transfection cells were trypsinized and replated onto glass bottom dishes. 18hrs after replating the dishes were placed on the stage of an inverted microscope and transfected cells were identified using a 63X phase 3 lens (Zeiss axiovert). A 5cc syringe fitted with a 21-gauge needle was filled with 37^{o}C buffer (Gibco Optimem without phenol red) and a short puff of buffer was released to blow the cell away. For fixed cell experiments, transfected cells were fixed with 4% paraformaldehyde and stained with rhodamine phalloidin (Molecular probes) to visualize actin and the cells were sucked into a flask using a vacuum line.

Integrin activation

For these experiments we followed the protocol for integrin activation described

previously (Tzima et al., 2002) with minor modifications. As described below, HeLa cells were transfected with GFP-Myo10-FERM, GFP-talin-FERM, or GFP construct. 12-18 hrs after transfection cells were trypsinized (in the absence of EDTA) and replated onto 18mm round coverslips. 12 hrs after replating, coverslips were washed briefly with PBS (phosphate buffer saline), lightly fixed with 1% paraformaldehyde and incubated with 9EG7 antibody (BD Pharmingen, 1 μg/ml) for 20 minutes. Cells were then washed three times with PBS to remove unbound antibody and incubated with secondary antibody Alexa Fluor 594 donkey anti-rat IgG (Invitrogen, 1μg/ml). Cells were washed three times with PBS, coverslips were mounted onto glass slides, and imaged using a 60X lens Nikon TE2000 (Nikon, Melville, NY) and an Orca ER cooled CCD camera (Hamamatsu, Bridgewater, NJ). The fluorescence intensity of cells was measured using the outline tool in Metamorph (Universal Imaging, West Chester, PA) and these values were subtracted from background values and used a measure of fluorescence intensity/integrin activation. Graphs were plotted and integrin activation is reported as Average pixel intensity +/- SEM (Standard Error of Means). The calculated p value as measured by a Tukey test was $p<0.01$.

RESULTS

Filopodial tips are adhesive structures

To test if filopodial tips were attached to substrate, we first transfected cells with GFP-Myo10 to label filopodial tips and replated transfected cells 18 hrs after transfection onto glass-bottom dishes. Transfected cells were either fixed with 4% paraformaldehyde or used live. We used two different methods to blow-off the cell body from the dish using either a

vacuum line or a puff of buffer. These blow-off experiments with either fixed (Figure 2.1A) or live cells (Figure 2.1B,C) transfected with GFP-Myo10 or GFP-Myo10-HMM (a construct that lacks most of the tail including the integrin binding domain) showed that most filopodial tips are adhesive structures. Note that some filopodial actin bundles also remained attached to the coverslip, raising the possibility that the motor domain of Myo10 remains attached to actin filaments as most of the cell body is blown off. A closer look at images before and after blow-off of cells transfected with GFP-Myo10 HMM showed that most filopodial tips remained attached to the substrate (Figure 2.1B,C) indicating that filopodial tips marked by GFP-Myo10 HMM remained adhesive perhaps due to the presence of endogenous Myo10.

Figure 2.1 Filopodial tips are adhesive structures.

A, HeLa cells transfected with GFP-Myo10 (green) were fixed and stained for actin using rhodamine phalloidin (red). The cell on the left is intact and unaffected by the vacuum line. The cell body of the transfected cell in the right was torn away with aspiration using a p200 pipette tip attached to vacuum line. This image shows that filopodial tips marked by green puncta of GFP-Myo10 remain attached to the coverslip. In some filopodia, filopodial actin bundles also remained attached to the coverslip. B, C: Similar experiments of live HeLa cells expressing GFP-Myo10 Left panel shows live HeLa cells transfected with GFP-Myo10 prior to blow-off. Right panel shows remnants of the same HeLa cell after blow-off. Note that the cell body is blown away leaving behind remnants of adhesive filopodial tips, which are marked by green puncta of GFP-Myo10. Also note that most substrate attached filopodial tips remain attached to the coverslip even though the cell body was blown away. Here, I focused on filopodia attached to substrate.

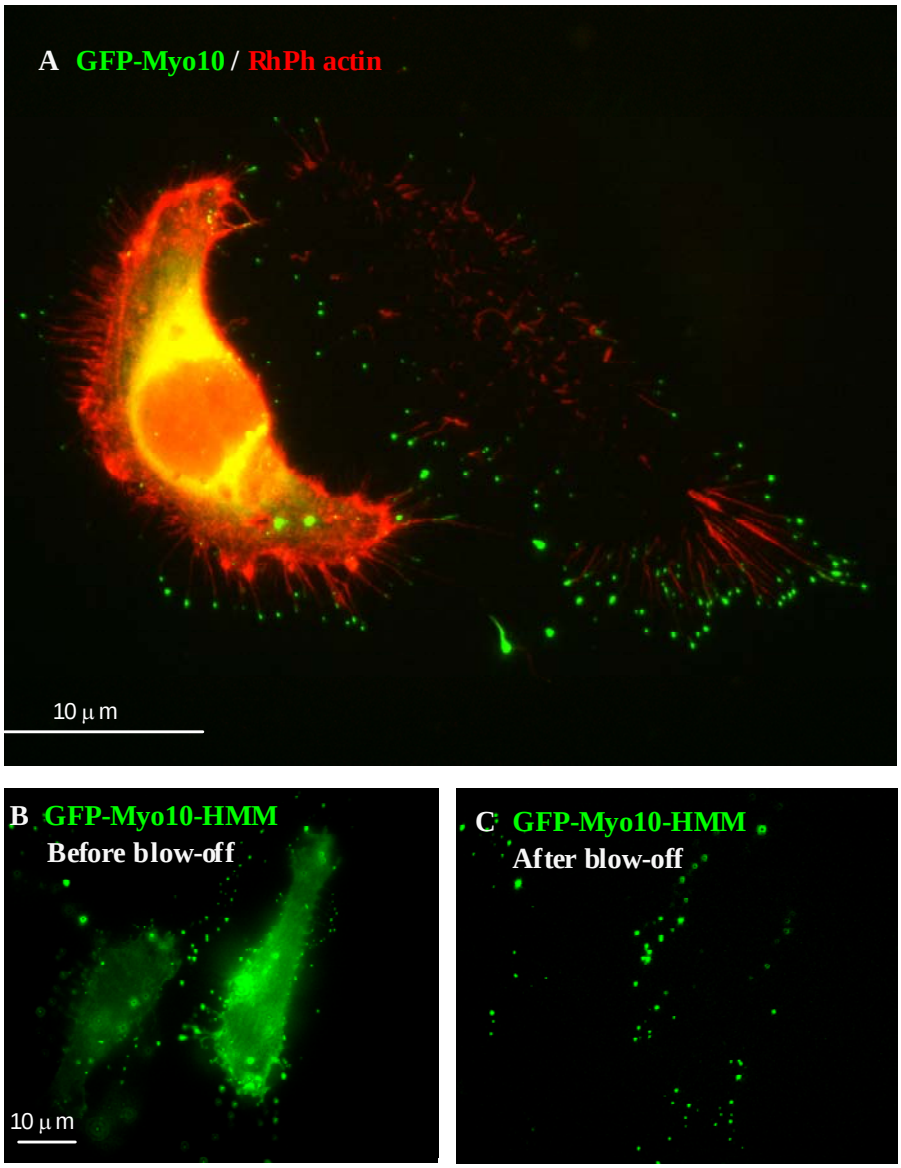
A GFP-Myo10 / RhPh actin
10 μm
B GFP-Myo10-HMM
Before blow-off
10 μm
C GFP-Myo10-HMM
After blow-off

GFP-Myo10 is a relatively stable component of the filopodial tip complex

Previous experiments by Svitkina et al. with cells permeabilized in the presence of a f-actin stabilizing buffer showed that VASP, but not fascin, remained attached at filopodial tips after overnight incubation. This observation led to the conclusion that VASP is a candidate to cause filament ends to associate (Svitkina et al., 2003). Since Myo10 is also present at tips of filopodia, we performed the same experiment under similar conditions to test if Myo10, like VASP is a component of the filopodial tip complex similar to VASP. For these experiments, we transfected HeLa cells with GFP-Myo10 and plated the cells onto glass-bottom dishes. The cells were then incubated in the presence of extraction buffer containing rhodamine phalloidin (which removes plasma membrane and proteins associated with membrane, but leaves the cytoskeleton intact) for various time points. Data from these experiments demonstrate that Myo10 also remains associated to filament barbed ends at filopodial tips (Figure 2.2) suggesting that Myo10 might also serve as a candidate protein that causes filaments to associate. Note that if Myo10 is a dimer containing it could potentially cross-link actin and mediate the association of actin filaments that are predestined to become filopodia. In this regard, both Myo10 and VASP both localize to structures called lambda precursors, which are sites where predestined filopodial actin filaments associate and then elongate to give rise to mature filopodia.

Immuno-EM demonstrates that Myo10 is a component of the filopodial tip complex.

In order to test whether endogenous Myo10 localizes to filopodial tips and lamda precursors similar to VASP we used platinum replica immuno EM technique as described by Svitkina et al. (Svitkina and Borisy, 1999). Please note that Omar Quintero did these

experiments in collaboration with Tanya Svitkina and Gary Borisy. Substrate-attached filopodia were visualized by platinum replica EM and data from these experiments showed that (1) each filopodium had approximately ten filaments and extended up to several microns in length, (2) the tip of the filopodium was characterized by the presence of an amorphous dense material called the filopodial tip complex, and (3) consistent with previous light microscopy data, immunogold labeling of Myo10 was most heavily concentrated at the tips of filopodia (Figure 2.3). The heavy labeling of the filopodial tip observed here with anti-Myo10 was strikingly different from the lamellipodial labeling patterns observed with anti-cofilin and anti-Arp2/3 (Svitkina and Borisy, 1999) indicating that Myo10 is a core component of the filopodial tip complex.

Endogenous Myo10 and αvβ3 integrins co-localize at filopodial tips

Given the observation that filopodial tips are adhesive structures, that Myo10 is a core component of the filopodial tip complex, that β1 integrins have been previously shown to localize to filopodial tips (Grabham and Goldberg, 1997), and that our collaborators had demonstrated that Myo10 and β-integrins could interact *in vitro*, we next asked whether endogenous Myo10 and β-integrins co-localized at filopodial tips in cells. For this experiment, CPAE (Cow Pulmonary Aortic Endothelial) cells were fixed and stained for Myo10 and αvβ3 integrin. Data from this experiment showed that endogenous Myo10 and αvβ3 integrins colocalized at tips of filopodia. Note that Myo10 is absent from most focal adhesions that stained positively for αvβ3 integrins strongly suggesting that filopodial tips and focal adhesions might be fundamentally distinct structures (Figure 2.4). Figures 2.4 and 2.5 were published in the journal Nature Cell Biology (Zhang et al., 2004 Jun; 6 (6): 523-31).

Figure 2.2 Myo10 is a stable component of the filopodial tip complex.

HeLa cell transfected with GFP-Myo10 (green) and incubated with extraction buffer containing rhodamine phalloidin (red) for 24 hrs showing that GFP-Myo10 is stable at filopodial tips when filopodial actin is stabilized by phalloidin and the plasma membrane is extracted using detergent.

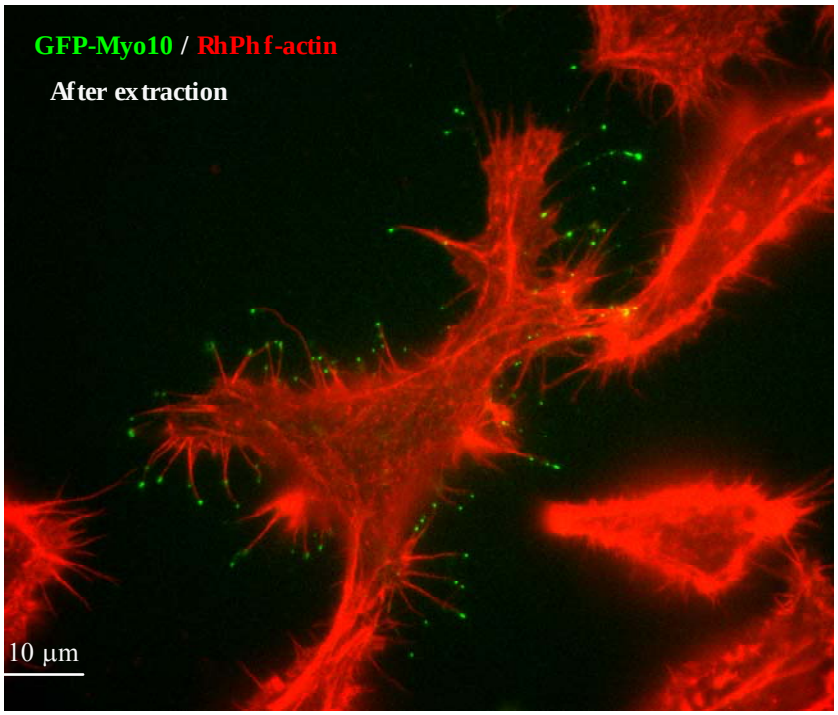
GFP-Myo10 / RhPh f-actin
After extraction
10 µm

Figure 2.3 Localization of Myo10 to the filopodial tip complex by immuno-EM.

High magnification view of a substrate-attached filopodium from a HeLa cell labeled with anti-Myo10 and 10 nm gold showing localization of endogenous Myo10 at the filopodia tip complex. Note that the gold particles have been pseudocolored light yellow.

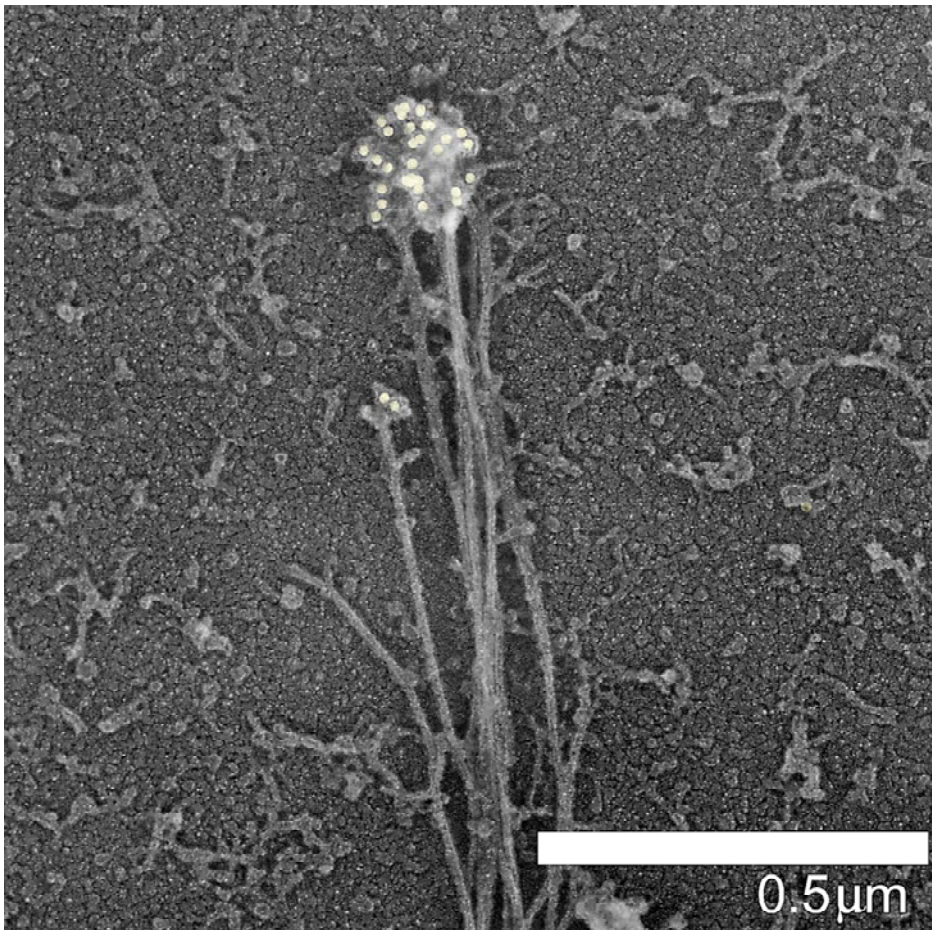
0.5µm

Figure 2.4 Endogenous Myo10 and αvβ3 integrins colocalize at filopodial tips.

Image shows an edge of a CPAE cell fixed and stained for Myo10 (green) and αvβ3 integrin (red). Note that endogenous Myo10 and αvβ3 integrin colocalize at tips of filopodia. In some filopodia, Myo10 signal also appears along the filopodia. Myo10 is absent from most focal adhesions that stain positively for αvβ3 integrin. Scale bar equals 5 μm. This figure was published in Nature Cell Biology (Zhang et al., 2004 Jun; 6 (6): 523-31)

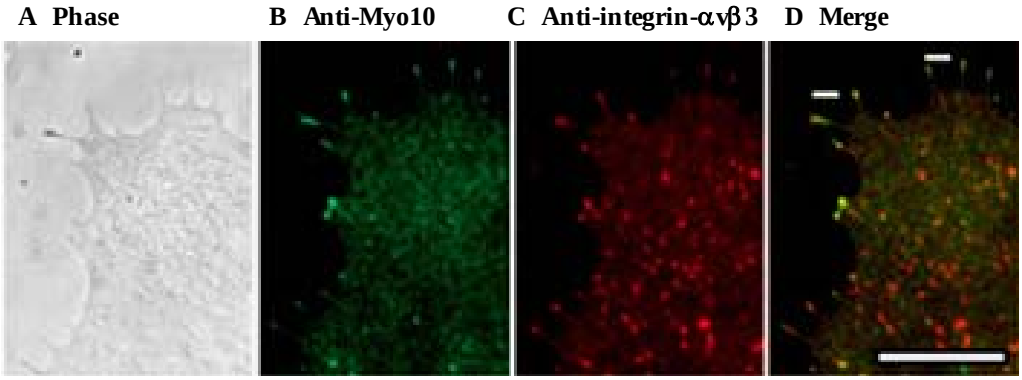
A Phase
B Anti-Myo10
C Anti-integrin-αvβ3
D Merge

Overexpression of Myo10 enhances integrin localization at filopodial tips

Since Myo10 can bind to β1, β3, and β5 integrins we next tested if Myo10 can colocalize with β1 integrins in cells. HeLa cells transfected with full length GFP-Myo10 and stained for β1 integrins showed clear colocalization of GFP-Myo10 and β1 integrins at tips of filopodia. In some cases, GFP-Myo10 appeared to extend further along as if in transit within filopodia. In HeLa cells transfected with GFP-Myo10 HMM (Heavy Mero Myosin), which does not contain the PH, MyTH4 and FERM domains of Myo10 but can localize to filopodial tips, β1 localization at filopodial tips was not detected. Similarly, in HeLa cells transfected with GFP-Myo10 tail, which contains the PH, MyTH4, and FERM domains of Myo10 and does not localize to filopodial tips, β1 integrin localization at filopodial tips was also undetectable**.** In these experiments we also observed that overexpression of GFP-Myo10 (but not GFP-Myo10 HMM, GFP-Myo10 Tail, or GFP alone) in HeLa cells appeared to enhance β1 integrin staining at filopodial tips (Figure 2.5) indicating that Myo10 might transport β1 integrins to filopodial tips.

β-integrins are candidate cargoes for Myo10

Several laboratories have made numerous unsuccessful attempts to GFP-tag β1 integrins. N or C-terminal tagged β1 integrins appear to either not fold properly, or display the characteristic focal adhesion staining pattern for integrins. Given this information we used a GFP- β3 integrin construct to test if β3 integrins serve as a cargo for Myo10. Note that this GFP- β3 integrin construct has previously been shown to localize to focal adhesions and in our hands also behaves in a manner characteristic of integrins thus indicating that it retains its ability to localize to focal adhesions. Although the primary localization of GFP-β3

Figure 2.5 Overexpression of GFP-Myo10 in HeLa cells enhances localization of β1 integrin at tips of filopodia.

HeLa cells were transfected with GFP, GFP-Myo10, GFP-Myo10 HMM, or GFP-Myo10 Tail (green) replated onto fibronectin (FN) coated coverslips for 3 hrs and fixed and stained for β1 integrin (red). In contrast to COS-7 cells tested, HeLa cells have numerous filopodia even in the absence of exogenous Myo10. GFP-Myo10 appears to enhance β1 integrin staining at filopodial tips, while GFP, GFP-Myo10 HMM, and GFP-Myo10 Tail do not. These results indicate that the motor domain is required for Myo10 to localize correctly to filopodial tips and to enhance β1 integrin localization at filopodial tips. Scale bar equals 5 μm. This figure was published in Nature Cell Biology (Zhang et al., 2004 Jun; 6 (6): 523-31)

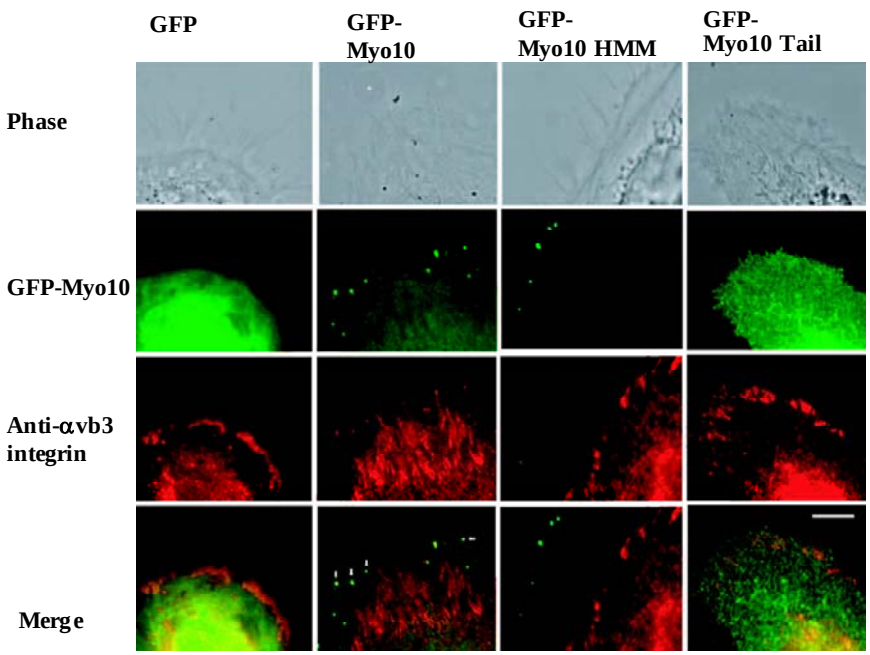
GFP
GFP-Myo10
GFP-Myo10 HMM
GFP-Myo10 Tail
Phase
GFP-Myo10
Anti-αvb3 integrin
Merge

integrin is at focal adhesions, puncta of GFP-β3 integrin was also observed at the tips of filopodia. Occasional puncta are also visualized along the filopodia, as though in transit to or from the tip (Figure 2.6). We next used HeLa cells transfected with either GFP-β3 integrin or CFP-Myo10 and GFP–β3 integrin to test if GFP-β3 integrin undergoes intrafilopodial motility and if CFP-Myo10 and GFP-β3 integrin undergo cotransport. We first used time-lapse imaging to investigate if GFP-β3 integrin undergoes intrafilopodial motility in the absence of exogenous Myo10. In these experiments, GFP-β3 integrin was detected at the tips of newly forming filopodia from the earliest observable time-point, and remained at the tips of filopodia that underwent extension or retraction. Virtually all substrate-attached filopodia had detectable levels of GFP-β3 integrin at their tips. These experiments also revealed that puncta of GFP-β3 integrin undergo intrafilopodial movements, with obvious rearward movements (towards the cell body) and subtler but faster forward movements (towards the tip) similar to the movements observed of GFP-Myo10. These movements are seen most clearly in the time-lapse movies presented as supplementary information. Forward movements corresponded to approximately 0.15 μm/sec and rearward movement corresponded to 0.01 μm/sec (Movie 2.1). These experiments demonstrate that the GFP- β3 integrin probe exhibited intrafilopodial motility similar to GFP-Myo10. The rearward movements correspond to the recordings of retrograde flow of actin reported for HeLa cells.

Once we confirmed that our GFP-β3 integrin probe underwent intrafilopodial motility in our assay, we next transfected cells with GFP-β3 integrin and CFP-Myo10 and used dual color time-lapse microscopy to study intrafilopodial motility. Data from these experiments revealed that GFP-β3-integrin and CFP-Myo10 can undergo co transport within filopodia (Figure 2.7 and Movie 2.2). As with Myo10, most of the movements within filopodia that we

observe with GFP-β3 integrins were slower rearward movements. This observation raises three important questions:

(1) Does Myo10 transport β3 integrins to filopodial tips?

(2) Does Myo10 anchor β3 integrins at filopodial tips?

(3) Does Myo10 and retrograde flow of actin within filopodia play a role in β integrin recycling from filopodial tips to the cell body?

In order to ensure that the intrafilopodial movements that we observed were specific for GFP-β3 integrin and are not due to bulk flow of cytoplasm within filopodia, we used GFP transfected cells as a negative control. Importantly, we did not observe any intrafilopodial movements of GFP in these cells indicating that the movements we observe with GFP-β3 integrin and Myo10 are probably not due to the bulk flow of cytoplasm (Movie 2.3).

Myo10 is essential for the transport of β3-integrin to tips of filopodia

To test whether Myo10 is necessary for the transport of GFP-β3 integrin to filopodial tips we first treated HeLa cells with a siRNA against endogenous Myo10 (as described in Chapter 3). We then transfected the siRNA treated cells with GFP-β3 integrin. As described in Chapter 3, Myo10 siRNA treated cells displayed a dramatic loss of dorsal filopodia, but still retained retraction fibers/ substrate-attached filopodia. Since retraction fibers are virtually indistinguishable from filopodia with respect to intrafilopodial motility, we used time-lapse microscopy to study whether GFP-β3 integrin can undergo intrafilopodial motility to filopodial tips in the absence of endogenous Myo10. Data from these preliminary experiments show that, GFP- β3 integrin localized to focal adhesions in both control cells and Myo10 siRNA treated cells (Movie 2.4). However, unlike control cells GFP- β3 integrins

was not detected at tips of retraction fibers (Figure 2.8 and Movie 2.5). These data indicate that Myo10 might play an important role in transport of β-integrins to filopodial tips.

Figure 2.6 GFP-β3 integrin appears to undergo movements within retraction fibers.

Figure shows phase and fluorescence images one frame of a movie of HeLa cells transfected with GFP-β3 integrin. Upper panel shows a phase image if a HeLa cells transfected with GFP-β3 integrin showing numerous retraction fibers and filopodia. Lower panel is a fluorescence image of a HeLa cell transfected with GFP-β3 integrin, where GFP-β3 integrins appears to be stretched all (arrows) along the retraction fiber/ filopodia indicative of movements within filopodia. Note that the GFP-β3 integrin construct localizes to focal adhesions validating its use as a probe for our experiments.

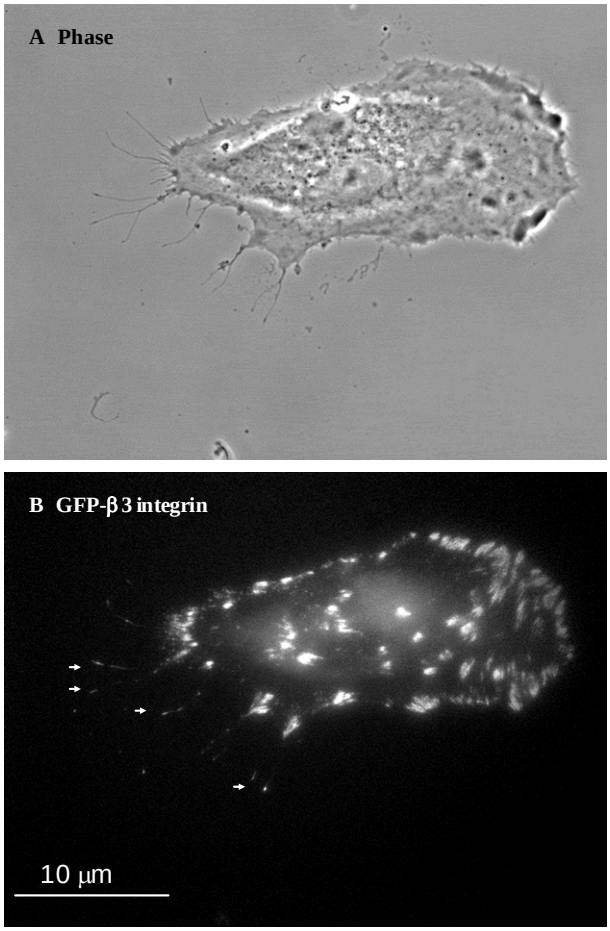
A Phase
B GFP-β3 integrin
10 μm

Figure 2.7 β3 integrin undergoes cotransport with Myo10.

In HeLa cells expressing CFP-Myo10 (green) and GFP-β3 integrin (red), both labels localize to puncta undergoing intrafilopodial motility. Note that both red and green puncta move relative to the white -dashed reference bar that marks the tip of the filopodium. Arrows indicate movement of puncta within the filopodium Scale bar, 10 μm. Timestamp denotes minutes: seconds.

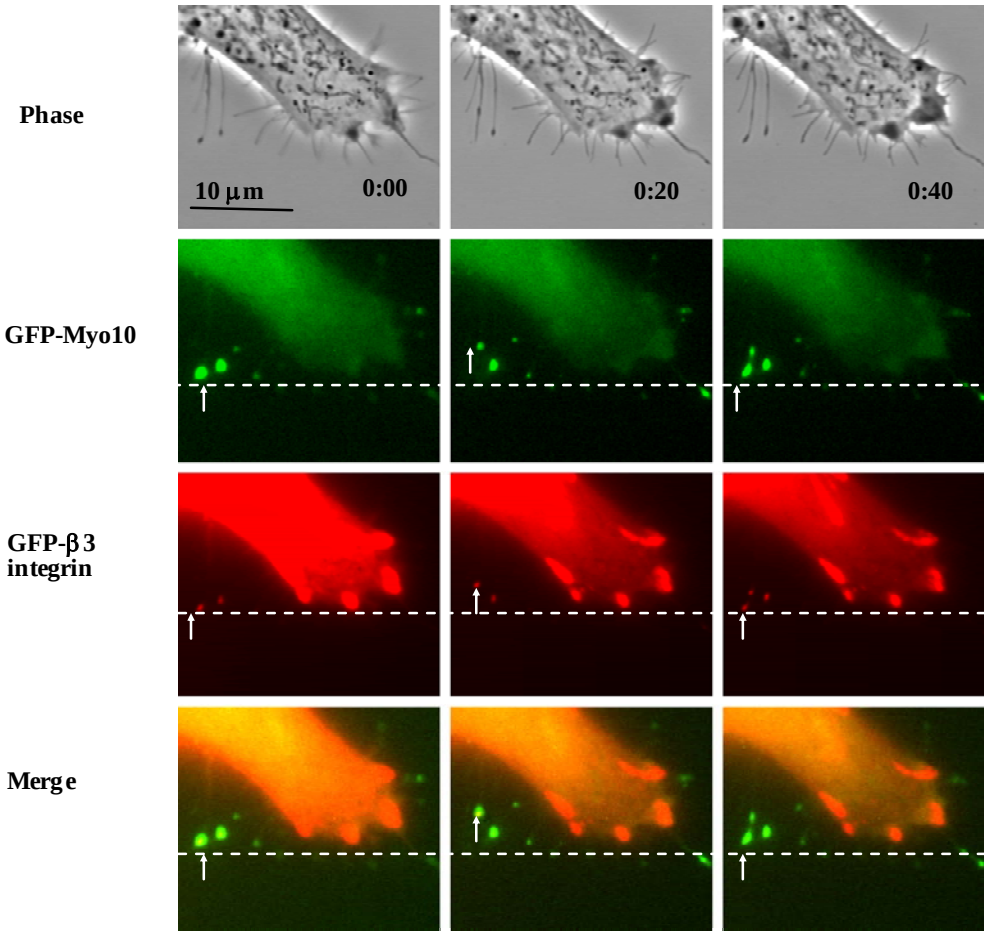
Phase
GFP-Myo10
GFP-β3 integrin
Merge
10 μm
0:00
0:20
0:40

Figure 2.8 siRNA mediated knock-down of Myo10 appears to inhibit integrin localization to filopodial tips.

HeLa cells treated with siRNA against Myo10 and transfected with GFP-β3 integrin are marked by the absence of intrafilopodial motility and integrin localization at the tips of filopodia. Arrows point to retraction fibers and the asterisk marks new filopodia. Scale bar, 10 μm. Timestamp denoted minutes: seconds.

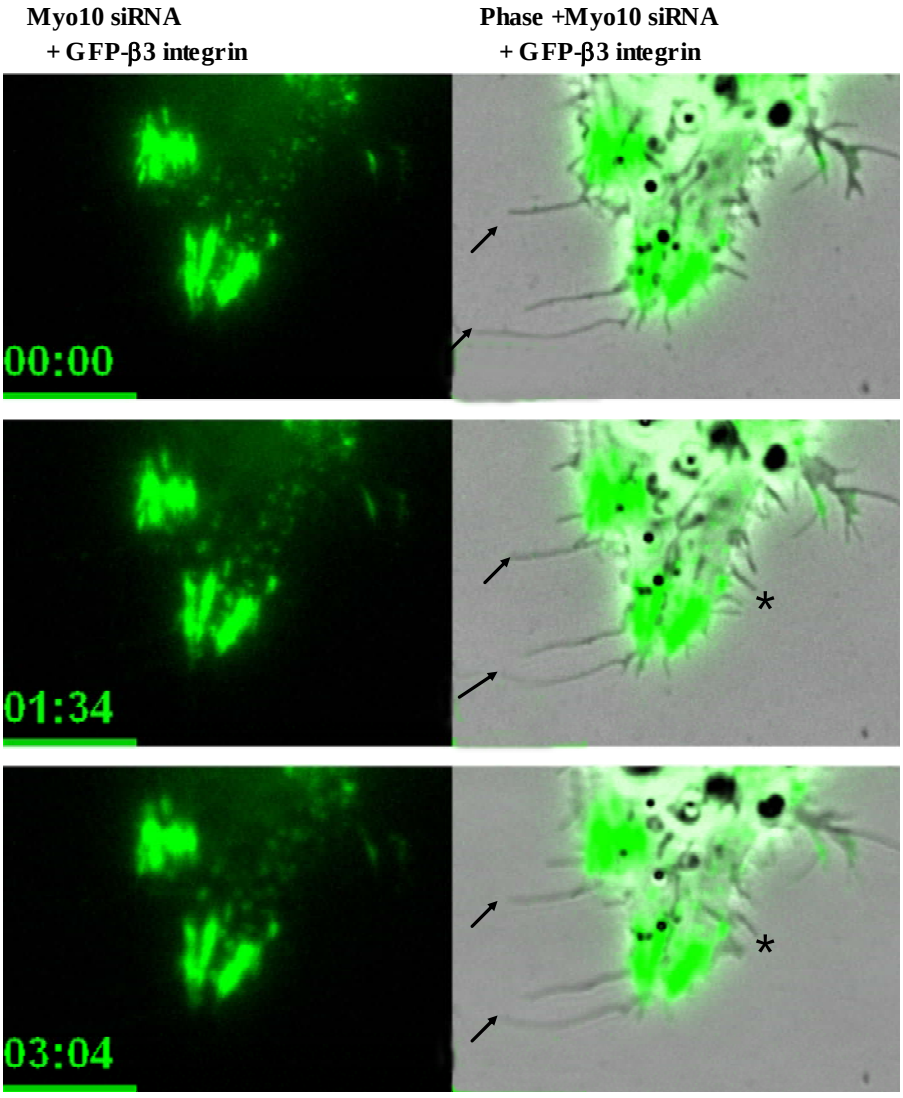
Myo10 siRNA
+ GFP-β3 integrin
Phase +Myo10 siRNA
+ GFP-β3 integrin
00:00
01:34
03:04
*
*

Phospho-tyrosine containing proteins can also undergo cotransport with Myo10

Since filopodial tips can be regulated by tyrosine phosphorylation and since phospho-tyrosine proteins have been previously reported to undergo intrafilopodial movements similar to Myo10, we next asked whether phospho-tyrosine proteins undergo cotransport with Myo10. HeLa cells co-transfected with YFP-dSH2 (a reporter of phospho-tyrosine) and CFP-Myo10 showed that phospho-tyrosine proteins and Myo10 undergo cotransport. The rates of forward movements were 0.16 μm/sec and rates of rearward movement were ~0.02 μm/sec (Figure 2.9 and Movie 2.6). Data from these experiments suggest two possibilities: (1) My10 is tyrosine phosphorylated and (2) Myo10 transports tyrosine-phosphorylated proteins such as integrins to filopodial tips.

The FERM domain of Myo10 can activate β1-integrins

Since integrin activation is critical to cell function and since talin, a key focal adhesion protein, can activate integrins at focal adhesions we next asked if the FERM domain of Myo10 could also activate β-integrins. To test this hypothesis, we first transfected HeLa cells, which express β1-integrins, with a GFP-Myo10 FERM domain construct. Using the 9EG7 antibody that reports ligand-bound, activated β1-integrins and immunofluorescence microscopy we found that GFP-Myo10 FERM domain can activate β1-integrins similar to the GFP-Talin FERM domain. In contrast, a GFP control construct was unable to activate β1-integrins. Note that the expression levels of GFP-talin FERM and GFP-Myo10 FERM were similar as assessed by fluorescence intensity measurements. This provides striking initial data that the FERM domain of Myo10 is as potent as the FERM domain of talin in activating integrins. Interestingly, similar experiments to test if FERM domain of Myo10 can activate

β3 integrins showed that while the FERM domain of talin could activate β3 integrins, Myo10 and GFP did not appear to activate β3 integrins (Figure 2.10).

The filopodial tip is a specialized site of adhesion that stains positively for Myo10, mena/VASP, talin, and FAK.

Since VASP, integrins and phosphotyrosine are also found in focal adhesions we asked if the filopodial tip was a specialized site of adhesion. In order to ask this question we stained HeLa cells with antibodies against known focal adhesion proteins such as VASP, mena, FAK, vinculin, talin, and paxillin. Immunostaining experiments revealed that while VASP, mena, and talin were present in all filopodial tips FAK and phospho-tyrosine was present in some but not all filopodia. Paxillin and vinculin on the other hand, were not present at filopodial tips. Interestingly, Myo10 was present at virtually all filopodial tips, but was undetectable at focal adhesions (Figure 2.11). Taken together these data suggest that the filopodial tip differs from focal adhesions by the presence of Myo10 and thus might serve as a specialized site of adhesion.

Figure 2.9 A probe for phospho-tyrosine containing proteins undergo co-transport with Myo10.

In HeLa cells expressing CFP-Myo10 (green) and YFP-dSH2 (red), both labels localize to puncta undergoing intrafilopodial motility. Note that both red and green puncta move relative to the white -dashed reference bar that marks the initial location of the filopodial puncta. Arrows indicate movement of puncta within the filopodium Scale bar, 10 μm. Timestamp denotes minutes: seconds.

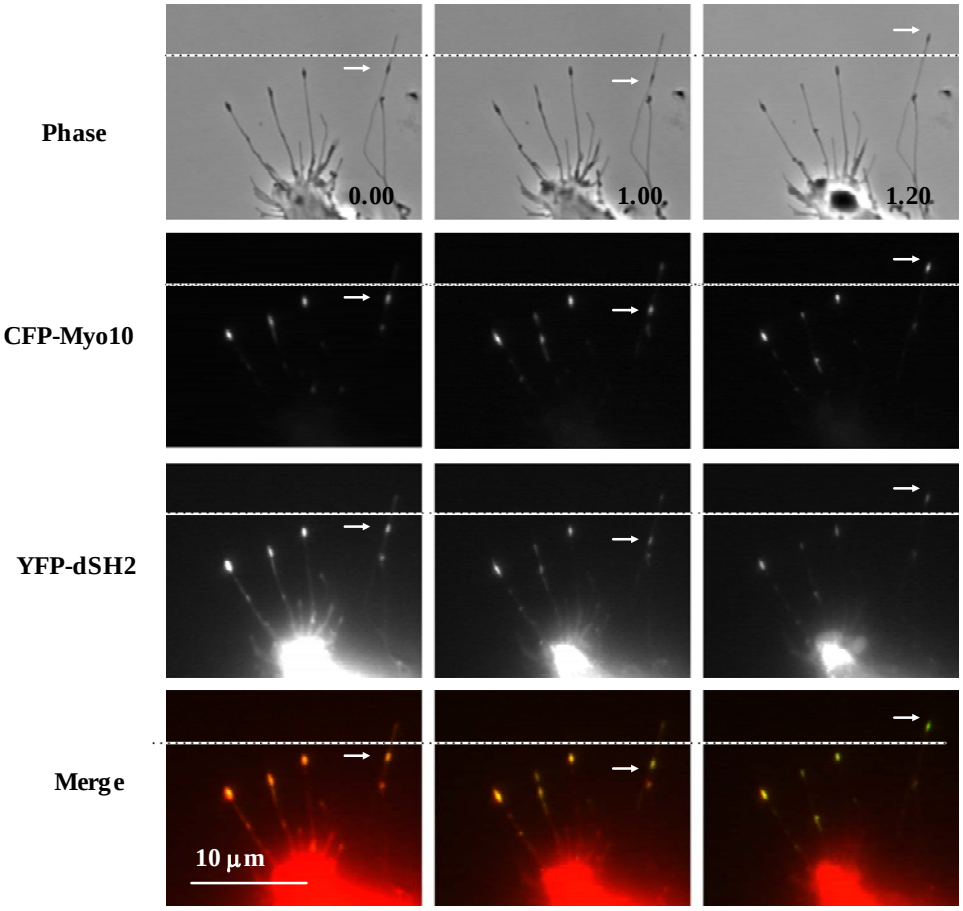
Phase
CFP-Myo10
YFP-dSH2
Merge
0.00
1.00
1.20
10 µm

Figure 2.10 The FERM domain of Myo10 activated β1-integrins.

Graphical representation of the average intensities +/- SEM of B16 melanoma cells transfected with either GFP-Myo10 FERM or GFP-talin FERM or GFP construct and incubated with an antibody that recognizes activated β1 integrins. Reported values are an indirect measure of integrin activation. Data shows that GFP-Myo10 FERM domain activates β1-integrins similar to GFP-talin FERM domain. Integrin activation of GFP-Myo10 FERM and GFP-Talin FERM was ~30% greater than control GFP transfected cells. p values were measured by using a Tukey test and $p<0.01$.

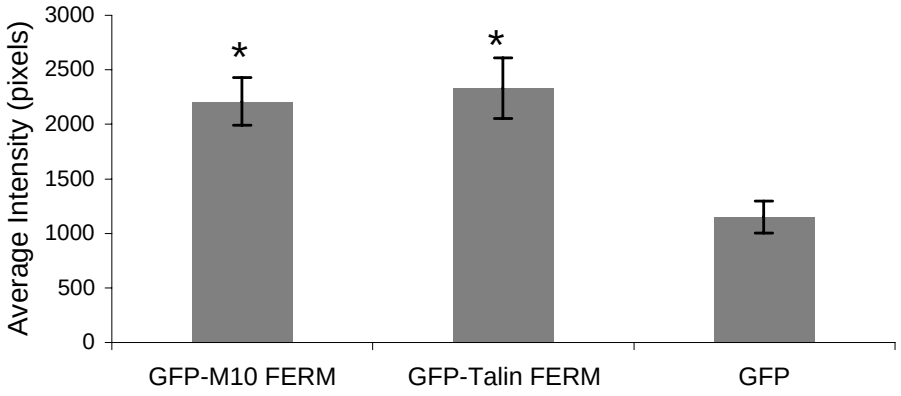
Average Intensity (pixels)
3000
2500
2000
1500
1000
500
0
*
*
GFP-M10 FERM
GFP-Talin FERM
GFP

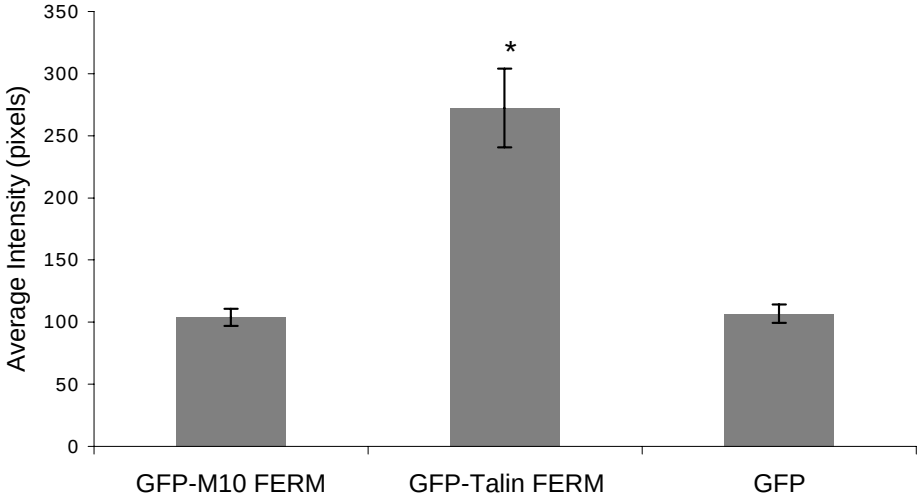
Average Intensity (pixels)
350
300
250
200
150
100
50
0
*
GFP-M10 FERM
GFP-Talin FERM
GFP

Figure 2.11 The filopodial tip stains positively for known focal adhesion proteins VASP, mena, and talin.

Immunofluorescence micrographs of HeLa cells expressing GFP-Myo10 and stained for focal adhesion proteins. GFP-Myo10 serves as a marker for filopodial tips. VASP, mena, and talin are present at virtually all filopodial tips. FAK and phosphotyrosine are present at some filopodial tips. Vinculin and paxillin were not detected at tips of filopodia.

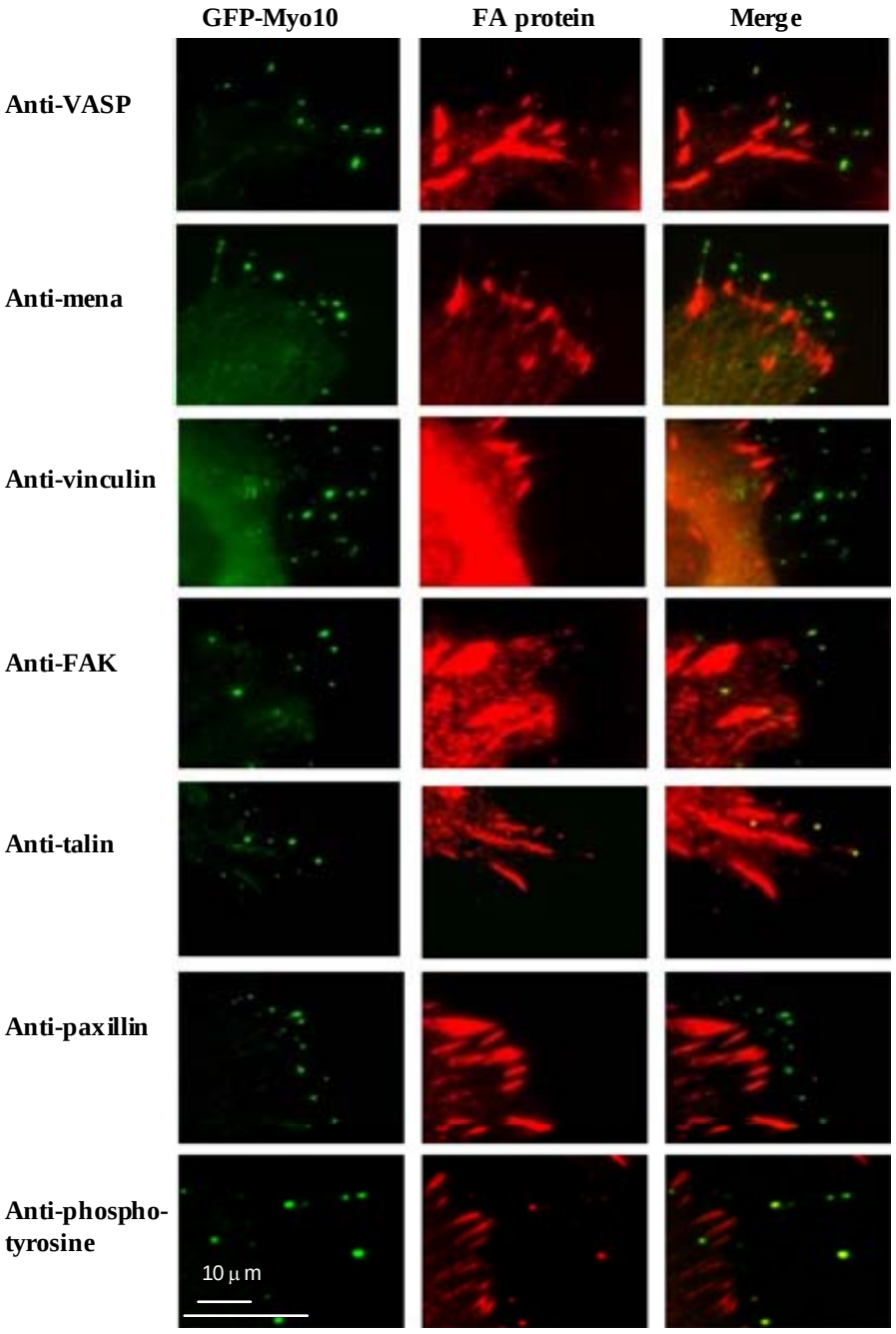
GFP-Myo10
FA protein
Merge
Anti-VASP
Anti-mena
Anti-vinculin
Anti-FAK
Anti-talin
Anti-paxillin
Anti-phospho-tyrosine
10 μm

DISCUSSION

Is Myo10 a motor that transports integrins in filopodia?

β1-integrins were first reported to move to filopodia tips of neuronal growth cones. The reported forward movements of β1-integrins were about 0.5-2 μm/sec and rearward movements were in the range of 0.05-0.15 μm/sec (Grabham et al., 2000). The previously measured forward movements are approximately twelve times faster than the movements we observe here with Myo10 and β1-integrins. Furthermore, the rearward movements, which are thought to correspond to retrograde flow of actin in filopodia, are approximately 2-6 fold faster than the rearward movements we observe here with Myo10 and β1-integrins. These discrepancies in rates could be attributed to differences in cell type and imaging or due to the presence of NGF, which was reported to stimulate forward transport. Different cells exhibit different retrograde flow rates. In *Aplysia* growth cone filopodia retrograde flow rates are significantly faster than HeLa cells and corresponds to approximately 0.05-0.1 μm/sec (Forscher and Smith, 1988)**.** Taken together, it is interesting to speculate that cell type and growth factors might influence intrafilopodial motility by regulating signaling proteins at the tips of filopodia. In this regard, it has been demonstrated that filopodia detect EGF (Epidermal Growth Factor) signals in the extra-cellular environment and respond by mediating directed retrograde transport of activated receptors within filopodia (Lidke et al., 2005).

MyTH4-FERM myosins and intrafilopodial motility

Out of the 40 known myosin genes in humans only a few myosins have been reported

to undergo intrafilopodial motility. Some of other unconventional myosins that do not belong to the MyTH4-FERM class of myosins can also localize to filopodial tips and undergo intrafilopodial motility such as Myo3A (Les Erickson et al., 2003). In particular, Myosin-X (Myo10) and Myosin-XV (Myo15) are most well characterized (Belyantseva et al., 2003; Berg and Cheney, 2002). Of these two myosins, Myo10 is ubiquitously expressed in most cells and tissues (Berg et al., 2000), while expression of Myo15 is restricted to stereocilia (actin-based structures related to filopodia) of the inner-ear and to the pituitary (Belyantseva et al., 2003; Lloyd et al., 2001). Interestingly, both the unconventional myosins that undergo intrafilopodial motility belong to the MyTH4-FERM class of unconventional myosins. MyTH4-FERM myosins also appear to share similar functions. For example, over-expression of Myo10 results in approximately 500 filopodia per cell and knocking-down of Myo10 results in a 60% reduction of filopodia (Bohil et al., 2006). Similarly, over-expression of Myo15 in stereocilia results in an increase in length of stereocilia and knock-out of Myo15 results in shorter stereocilia (Lin et al., 2005). Furthermore, recent data demonstrates that Myo15 transports protein whirlin to tips of stereocilia (Belyantseva et al., 2005) and here, we show that Myo10 transports integrins to tips of filopodia. These parallels suggest that intrafilopodial motility is a conserved function of the MyTH4-FERM class of myosins that might serve to transport cargo to tips of parallel-bundled actin based structures such as filopodia or stereocilia.

Retraction fibers and cell-cell contacts

Filopodia and retraction fibers share several common features. Both structures are thin, long cellular protrusions filled with parallel-bundled actin filaments. Both structures are

indistinguishable in fixed cells. Both structures support the bi-directional movement of particles as well as of GFP-Myo10. The main difference between retraction fibers and filopodia is the formation of these structures. One possibility is that retraction fibers may arise due to the retraction of the plasma membrane of cells while filopodia are thought to arise due to convergent elongation of actin filaments at the leading edge of the cell. Another possibility is that retraction fibers initiate from filopodia that are attached to the substrate (Svitkina et al., 2003). Retraction fibers may also arise after a filopodium makes contact with another cell and once a contact is made retraction fibers might serve to maintain the contact between the cells. In this regard, recent reports have implicated filopodia in mediating cell-cell contact between epithelial cells (Vasioukhin et al., 2000) and immune cells (Onfelt et al., 2004). While these advances arm us with some information, the exact role and mechanism of formation of retraction fibers is still unknown.

Myosins and adhesions

The role of myosins in mediating cell-cell adhesion is unexplored. Rat class I myosin, myr3, an ortholog of human MYO1E, was shown to localize to cell-cell adhesions in cultured cells (Stoffler et al., 1995). Furthermore, in HeLa cells overexpressing constitutively active Cdc42, myr3 colocalized with cell junction proteins, N-cadherin and β-catenin at sites of cell-cell contacts (Stoffler et al., 1998). Additionally, nonmuscle myosin-II, which is a key motor protein that drives cell shape change and cell movement, co localizes with PS2 integrin in developing muscle termini in *Drosophila melanogaster* and PS2 integrin appears to be required for the maintenance of nonmuscle myosin-II localization (Bloor and Keihart, 2001). Another unconventional myosin, Myo7A was also shown to interact with a

transmembrane protein vezatin. Vezatin localizes to cell-cell contacts and interacts with E-cadherin/ a-catenin complex, suggesting that it may link cell adhesion molecules to the actin cytoskeleton (Kussel-Andermann et al., 2000). Since Myo10 and Myo7a belong to the same family of MyTH4-FERM myosins, these data along with our data shown here that Myo10 binds to and activates integrins, raises the interesting possibility that myosins might link adhesion complexes to the underlying actin cytoskeleton and thereby anchor them.

The filopodial tip complex as specialized site of cell adhesion

The tip of the filopodium is clearly the business end of the structure and is the first site that comes in contact with the extra cellular matrix. Interestingly, a closer look at the filopodial tip reveals the presence of an amorphous dense material called the filopodial tip complex, whose identity and function is virtually unknown. The presence of vinculin, FAK and phosphotyrosine at tips of retraction fibers and in some but not all filopodia raises an interesting question as to whether the filopodial tip adhesion gradually evolves into a focal adhesion. In this regard, recent studies have shown that integrin-containing filopodial tips first form a primary adhesion, which then accumulates other focal adhesion proteins in a specific order to give rise to a mature focal adhesion (Partridge and Marcantonio, 2006). Since the differences in molecular components between focal adhesions and focal contacts is not exactly clear we were unable to draw conclusions from these experiments as to whether the tip adhesion resembles a focal contact. Since the presence of adhesion molecules such as integrins, focal adhesion proteins like FAK, paxillin, talin, mena, and signaling components like tyrosine phosphorylation is a characteristic of focal adhesions and since Myo10 is only present in filopodial tips and is absent in focal adhesions, it is interesting to speculate the

filopodial tip might serve as a specialized site of adhesion and signaling. Since Myo10 localizes to filopodial tips, but not to focal adhesions, it provides a clear molecular distinction between these two forms of integrin-containing adhesions. It will thus be important to compare the molecular composition of filopodial tip complexes and focal adhesions. In addition, it will be important to determine if there are molecular differences between the tip complexes of substrate-attached filopodia and those of actively extending filopodia.

CHAPTER THREE

MYOSIN-X (MYO10) IS A MOLECULAR MOTOR THAT FUNCTIONS IN FILOPODIA FORMATION

Despite recent progress in understanding lamellipodia extension, the molecular mechanisms regulating filopodia formation remain largely unknown. Myo10 is a MyTH4-FERM myosin that localizes to the tips of filopodia and is hypothesized to function in filopodia formation. To determine if endogenous Myo10 is required for filopodia formation, we have used scanning EM to assay the numerous filopodia normally present on the dorsal surfaces of HeLa cells. We show here that siRNA mediated knock-down of Myo10 in HeLa cells leads to a dramatic loss of dorsal filopodia. Overexpressing the coiled coil region from Myo10 as a dominant negative also leads to a loss of dorsal filopodia, thus providing independent evidence that Myo10 functions in filopodia formation. We also show that expressing Myo10 in COS-7 cells, a cell line that normally lacks dorsal filopodia, leads to a massive induction of dorsal filopodia. Since the dorsal filopodia induced by Myo10 are not attached to the substrate, Myo10 can promote filopodia by a mechanism that is independent of substrate attachment. Consistent with this, a Myo10 construct that lacks the FERM domain, the region that binds to integrin, retains the ability to induce dorsal filopodia. Deletion of the MyTH4-FERM region, however, completely abolishes Myo10's filopodia

promoting activity, as does deletion of the motor domain. Additional experiments on the mechanism of Myo10 action indicate that it acts downstream of Cdc42 and can promote filopodia in the absence of VASP proteins. Together these data demonstrate that Myo10 is a molecular motor that functions in filopodia formation. Please note that this chapter was published in the Proceedings of the National Academy of Sciences (Bohil AB et al., 2006 Aug 15; 103 (33): 12411-6)

INTRODUCTION

The finger-like cellular extensions known as filopodia play important roles in numerous biological processes including growth cone guidance (O'Connor et al., 1990), wound-healing (Wood et al., 2002), angiogenesis (Gerhardt et al., 2003), and cell-cell signaling (Ramirez-Weber and Kornberg, 2000). Despite these important roles, the molecular mechanisms underlying the formation of filopodia and related structures such as intestinal microvilli and inner ear stereocilia are not yet understood (Faix and Rottner, 2005; Pollard and Borisy, 2003). Filopodia are known to contain a core of parallel-bundled actin filaments whose barbed ends are located at the filopodial tip, and filopodial growth requires actin polymerization at these barbed ends. The GTPase Cdc42 is a master regulator of filopodia formation (Nobes and Hall, 1995) and can interact with proteins such as N-WASP (Wiskott-Aldrich Syndrome Protein) to activate Arp2/3 and nucleate new actin filaments (Pollard and Borisy, 2003). Although the branched actin array generated by activated Arp2/3 may be important for initiating filopodia (Svitkina et al., 2003), Arp2/3 is not present on mature filopodial actin bundles (Svitkina and Borisy, 1999). Thus other proteins such as

VASP and formins are likely to regulate actin polymerization at the tips of filopodia. VASP family proteins, for example, are present at the tips of filopodia and can stimulate filopodia formation, presumably due to their anticapping activity (Bear et al., 2000; Lebrand et al., 2004). Filopodia formation also involves actin bundling, and fascin appears to serve as a major actin bundling protein in filopodia (Svitkina et al., 2003).

Myo10 is a vertebrate specific MyTH4-FERM myosin that is expressed in most tissues, exhibits a striking localization at the tips of filopodia, and can undergo movements known as intrafilopodial motility within filopodia (Sousa and Cheney, 2005). The Myo10 heavy chain contains a myosin head domain responsible for motor activity (Homma and Ikebe, 2005; Kovacs et al., 2005), a neck domain consisting of 3 IQ motifs that bind to calmodulin light chains, and a unique tail (Berg et al., 2000). The tail includes a region predicted to form a coiled coil which can form dimers (Knight et al., 2005), 3 PH domains implicated in PI3-kinase signaling, a MyTH4 domain that can bind microtubules (Weber et al., 2004), and a FERM domain that can bind β-integrins (Zhang et al., 2004). Overexpressing full-length Myo10 increased substrate-attached filopodia 4-fold (Berg and Cheney, 2002), which suggests that Myo10 plays an important role in filopodia formation. Myo10 could promote filopodia indirectly by transporting or anchoring integrins at the filopodial tip (Zhang et al., 2004), therefore stabilizing filopodia by enhancing substrate attachment. Myo10 could also induce filopodia more directly, e.g., by functioning as part of a filopodial tip complex or by transporting molecules required for filopodia formation. We show here that Myo10 is a potent inducer of dorsal filopodia and can thus induce filopodia independently of effects on substrate attachment. Furthermore, we show that endogenous Myo10 is required for formation of normal levels of dorsal filopodia and acts downstream of

Cdc42, thus demonstrating for the first time that this MyTH4-FERM myosin functions in filopodia formation.

MATERIALS AND METHODS

Constructs

Human GFP-fascin in pEGFP-C1 (Adams and Schwartz, 2000), human GFP-VASP in pEGFP-N1 (Svitkina et al., 2003), untagged bovine Myo10 in pcDNA3.1, and the bovine GFP-Myo10, GFP-Myo10-HMM, GFP-Myo10 tail, and GFP-Myo10 headless constructs in pEGFP-C2 have been described previously (Berg and Cheney, 2002). The bovine GFP-Myo10 construct was converted to CFP-Myo10 by replacing GFP with CFP. The bovine GFP-Myo10 ΔFERM construct in pEGFP-C2 includes aa 1-1916 and the GFP-Myo10 ΔMyTH4-FERM construct in pEGFP-C2 includes aa 1-1523. The GFP-Myo10 coiled coil construct in pEGFP-C2 includes aa 812-946 and was generated by PCR from human Myo10 (Rogers and Strehler, 2001) and the control GFP-Myo5a coiled coil construct includes aa 913-1116 of chicken Myo5a. The dominant negative human GFP-Cdc42(15A) (Reuther et al., 2001) and the constitutively active GFP-Cdc42(61L) in pEGFP-C3 were generous gifts of Dr. Keith Burridge. Since the GFP-Cdc42(15A) construct appeared to be more effective than a Myc-Cdc42(N17) construct in suppressing dorsal filopodia in HeLa cells, the 15A construct was used here.

The bovine GFP-Myo10 ΔFERM construct was generated by truncating GFP-Myo10 at the KpnI site (nucleotide 5749-5745 of bovine Myo10, accession # NM_174394) and includes amino acids 1-1916. The bovine GFP-Myo10 ΔMyTH4-FERM construct was

generated by truncating GFP-Myo10 at the BglII site (nucleotides 4571-4575) and includes amino acids 1-1523. The human GFP-Myo10 coiled coil construct was generated by PCR (forward primer, 5`tcagatctccaattgctggcaga3`; reverse primer 5`tcgaagcttttgagggactcgaggaa3`) using human Myo10 as a template and cloned into the BglII and HindIII sites of pEGFP-C2. The GFP-Myo10 coiled coil construct thus includes nucleotides 2436-2838 and amino acids 812-946 of human Myo10 (accession #9910110). The chicken GFP-Myo5a coiled-coil construct used as a control was cloned into the EcoR1 and BamH1 sites of pEGFP-C2 using PCR (forward primer 5'atgaattcaagaagctgaagatagaggct3' and reverse primer 5'atggatcctccaggcttggggatgctcac3') and includes nucleotides 2820-3431 and amino acids 940-1143 of chicken myosin-V (NM 205300).

Cell culture

COS-7, HeLa, HEK-293, and CAD cells were all maintained at 37C and 5% CO_2 in DMEM supplemented with 10% FBS and 100 U/ml PenStrep. MV^{D7} cells were grown in DMEM supplemented with 15% FBS, 100 U/ml PenStrep, 4 mM L-glutamine, and 50 U/ml of interferon gamma.

Transfection

All cells were transfected with cDNA constructs using Polyfect (Qiagen) except for MV^{D7} cells, which were transfected using the Amaxa nucleoporation protocol for mouse embryonic fibroblasts. Following the overnight transfections, cells were trypsinized and replated onto glass coverslips for 12 hours in the presence of serum prior to fixation. For

fluorescence-correlative SEM the cells were plated onto 12 mm gridded round glass coverslips (Eppendorf) whereas cells sorted by FACS were plated onto 12 mm round glass coverslips. Although COS-7 cells normally lack dorsal filopodia, during mitosis they round up and elaborate numerous dorsal filopodia, so mitotic cells were excluded from our analysis (~3% of cells). Quantitative immunoblotting with anti-Myo10 indicated that COS-7 cells express approximately 65% as much endogenous Myo10 as HeLa cells and that the average level of overexpression with GFP-Myo10 in COS-7 cells was ~100-fold. Similar blots indicated that the GFP-Myo10 coiled coil was overexpressed at least ~30 fold and blots with anti-GFP indicated that the GFP-Myo5a coiled coil was expressed at approximately the same level.

Fluorescence microscopy

Cells were trypsinized ~18 hours after transfection and then replated onto 12 mm coverslips overnight. For immunostaining experiments, cells were then fixed with 3.7% paraformaldehyde at 37C for 10 minutes, permeabilized with 0.2% triton-X-100 for 5 minutes, and blocked at room temperature with goat serum for 30 minutes. Cells were incubated for 1 hour with primary antibodies to VASP (2 μg/ml; Transduction Labs) or fascin (1:50; Dako Cytomation) followed by staining with rhodamine phalloidin to label F-actin (Molecular Probes). Cells were then rinsed 3x in PBS for 10 minutes each and then incubated for 45 minutes with 1 μg/ml Texas Red goat-anti mouse secondary antibody (Molecular Probes). Cells were rinsed 3x with PBS for 10 minutes each, mounted on glass slides, and imaged using a Nikon TE2000 fluorescence microscope equipped with a 60x 1.4NA objective. Images were collected using an Orca II cooled CCD camera (Hamamatsu)

and Metamorph software (Universal Imaging). Brightness and contrast were adjusted using Adobe Photoshop.

Knock-down of Myo10 using siRNA

A synthetic siRNA targeting human Myo10 (5'AAGTGCGAACGGCAAAAGAGA3') that differs at 7 positions from bovine Myo10 and a control siRNA (5'AATTCTCCGAACGTGTCACGT3') were obtained from Qiagen with fluorescein tags at their 3' ends. A day before siRNA treatment, ~100,000 cells/well were plated onto 6-well plates at 50-60% confluency and incubated at 37C for 12 hours. Cells were then treated with a final concentration of 110-150 nM siRNA using RNAifect (Qiagen) following the manufacturer's instructions. The media was replaced ~16 hours after transfection and fluorescence microscopy was used to verify that ~100% of the cells had taken up the siRNA. At ~48 hours the cells from each well were replated, typically into 18 wells of a 24-well plate containing 12 mm glass coverslips. At ~60-72 hours cells were processed for scanning EM or light microscopy and parallel samples were assayed by immunoblotting to verify knock-down. For siRNA experiments that also involved transfection with an expression plasmid, siRNA treated cells were transfected with GFP-Myo10 or constitutively active GFP-Cdc42 constructs at ~48 hours. Cells were allowed to grow overnight following transfection, replated onto glass coverslips for ~12 hours, and then fixed and processed for fluorescence-correlative SEM.

SEM experiments

Cells on 12 mm round coverslips were rinsed briefly with PBS and then mixed with

room temperature 2.5% glutaraldehyde in 0.1 M sodium cacodylate buffer, pH 7.4 at room temperature. Coverslips were fixed for 1 hour at 4 C and then washed 3x for 5 minutes each with cacodylate buffer alone. All subsequent steps were performed at room temperature. Coverslips were treated with 1% osmium tetroxide in cacodylate buffer for 20 minutes and washed 3x with cacodylate buffer alone. Cells were then dehydrated in a graded series of 3 washes of 5 minutes each in 50, 60, 70, 80, 90, 95, and 100% (molecular sieve dried) ethanol. Dehydrated cells were critical point dried (Balzers Union) and coated with 7 nm of gold-palladium using a Hummer X sputter coater (Anatech Ltd). All coverslips from a given experiment were critical point dried together in the same chamber and sputter coated together. Images were generally collected at a tilt angle of 42 degrees and magnifications of 2470x for HeLa cells and 4270x for COS-7 cells using a Cambridge S200 scanning electron microscope attached to a digital camera (4 Pi Imaging digital system).

SEM experiments to test the filopodia promoting activity of GFP-Myo10 and other constructs were performed using three different approaches. (1) For preliminary comparative experiments, cells were transfected overnight with Polyfect and then replated ~12 hours onto 12 mm coverslips. The transfection efficiency for each construct was assessed by fluorescence microscopy of one coverslip and compared with the fraction of cells exhibiting dorsal filopodia on a duplicate coverslip prepared for SEM. Since control COS-7 cells normally lack dorsal filopodia, this approach provided a simple and rapid screen for filopodia induction, especially when the transfection efficiency exceeded ~30%. This method also allowed us to determine that the untagged bovine construct is a potent inducer of dorsal filopodia. (2) For the FACS approach, cells in 6-well dishes were transfected overnight using Polyfect, trypsinized, and subjected to FACS. The transfected cells were replated onto

12 mm coverslips for ~12 hours and then prepared for SEM. This approach provided the advantage for scanning EM that 100% of the cells on a given coverslip were transfected. (3) For the fluorescence-correlative SEM approach, cells were transfected overnight and then replated ~12 hours on gridded coverslips. Coverslips were rinsed briefly with PBS, pre-fixed 5 minutes with room temperature 3.7% paraformaldehyde, and then rinsed 3x with PBS. To identify and record the positions of individual transfected cells, the coverslips were then placed cell side up in a glass bottom dish (Willco) and imaged with fluorescence using an inverted microscope and a 20x 0.75 NA dry lens (Nikon). Coverslips were then prepared for SEM using standard procedures and SEM images of the transfected cells were collected. Since this correlative approach worked well even when transfection efficiencies were low and it provided the additional internal control of untransfected cells on each coverslip, it was used for most experiments.

RESULTS

Expressing Myo10 induces a massive increase in dorsal filopodia.

To test if Myo10 can directly induce filopodia, we used scanning electron microscopy (SEM) as a high-resolution assay to image the filopodia on the dorsal surfaces of cultured cells (Figure 3.1A-D). Control COS-7 cells transfected with GFP had virtually no filopodia (1 +/-0.4 dorsal filopodia per cell), whereas COS-7 cells transfected with GFP-Myo10 exhibited a massive increase in dorsal filopodia (553 +/-88) (Figure 3.6C). COS-7 cells that expressed higher levels of GFP-Myo10 elaborated more dorsal filopodia (Figure 3.2). These

data also show that the substrate-attached filopodia visible along the edges of cells that we (Berg and Cheney, 2002) and most other researchers have focused on previously using light microscopy sometimes constitute only a tiny subset of the total filopodia (Figure 3.1 C,D). Since dorsal filopodia are not attached to the substrate, analyzing them also simplifies interpretation and avoids the difficulties that arise if substrate-attached filopodia are confounded with retraction fibers.

Figure 3.1 Over-expression of Myo10 leads to a massive increase in dorsal filopodia.

(A-G) The expression levels of GFP-Myo10 in COS-7 cells as assessed by fluorescence microscopy correlates with the number of dorsal filopodia visualized by SEM. COS-7 cells were transfected overnight with the indicated constructs, replated on coverslips for ~12 hours, stained for F-actin (red) and imaged for GFP (green) or prepared for correlative SEM.

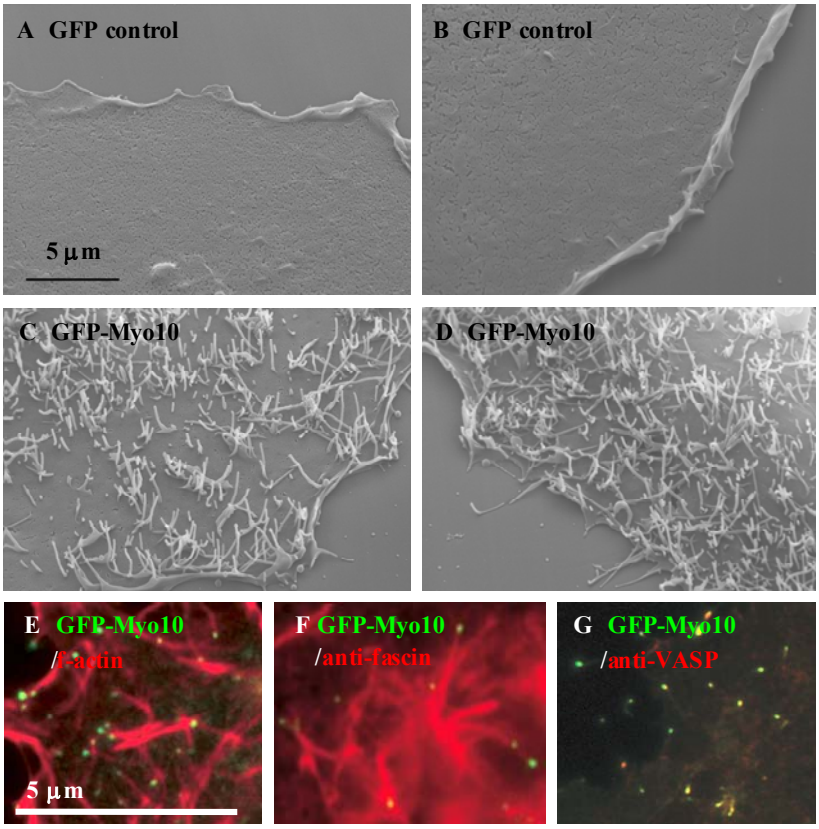
A GFP control
5 µm
B GFP control
C GFP-Myo10
D GFP-Myo10
E GFP-Myo10
/F-actin
5 µm
F GFP-Myo10
/anti-fascin
G GFP-Myo10
/anti-VASP

Figure 3.2 Myo10 expression level correlates with number of dorsal filopodia.

(A-C) The expression levels of GFP-Myo10 in COS-7 cells as assessed by fluorescence microscopy correlates with the number of dorsal filopodia visualized by SEM. COS-7 cells were transfected overnight with the indicated constructs, replated on coverslips for ~12 hours and processed for correlative SEM.

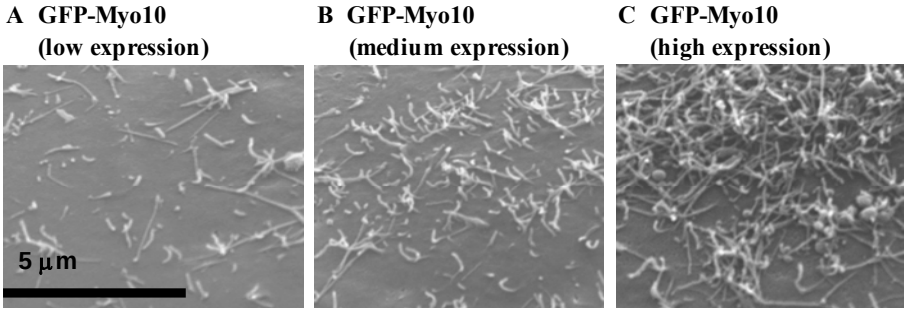
A GFP-Myo10
(low expression)
B GFP-Myo10
(medium expression)
C GFP-Myo10
(high expression)
5 μm

To verify that the Myo10-induced extensions are indeed filopodia, COS-7 cells expressing GFP-Myo10 were stained for filopodial marker proteins. As expected for filopodia, the extensions induced by GFP-Myo10 contain F-actin and fascin along their length and have VASP at their tips (Figure 3.1E-G). To further verify our assay, COS-7 cells were transfected with proteins previously reported to induce filopodia and imaged by SEM. GFP-VASP, GFP-fascin, and constitutively active Cdc42 each induced the formation of numerous dorsal filopodia morphologically similar to those induced by GFP-Myo10 (Figure 3.3A-C). Similar experiments showed that GFP-Myo10 also induces dorsal filopodia in many other cell types (not shown) including HEK-293 (Human embryonic kidney), HUVEC (Human umbilical vein endothelial cells), and CAD cells (a mouse neuronal cell line). Myo10 therefore promotes formation of dorsal filopodia in many different cell types and appears to be as effective as known filopodia inducers such as Cdc42 and fascin.

To determine which domains of Myo10 are required to induce filopodia, we tested a series of Myo10 deletion constructs for their ability to induce filopodia in COS-7 cells. Importantly, a construct lacking the FERM domain, the region that binds to integrins, was able to induce dorsal filopodia (Figure 3.4A-C). Constructs lacking both the MyTH4 and FERM domains, however, were unable to induce dorsal filopodia (Figure 3.4B). Consistent with this, a heavy meromyosin (HMM)-like Myo10 construct that consists of only the head, neck, and coiled coil region (ΔPH-MyTH4-FERM), also failed to induce dorsal filopodia (Figure 3.4C). Since all three deletion constructs localize to the tips of substrate-attached filopodia (Figure 3.4D-F), the failure of the ΔMyTH4-

Figure 3.3 Expressing VASP, Fascin, and Cdc42 also lead to massive increases in dorsal filopodia.

(A-C) Transfecting known inducers of filopodia such as GFP-VASP, GFP-fascin, and constitutively active GFP-Cdc42(61L) in COS-7 cells all lead to massive increases in dorsal filopodia. Note that in addition to filopodia, the VASP and Cdc42 constructs sometimes also induced small ruffle-like structures. The SEM images illustrated here and in all subsequent figures were obtained using correlative fluorescence-SEM.

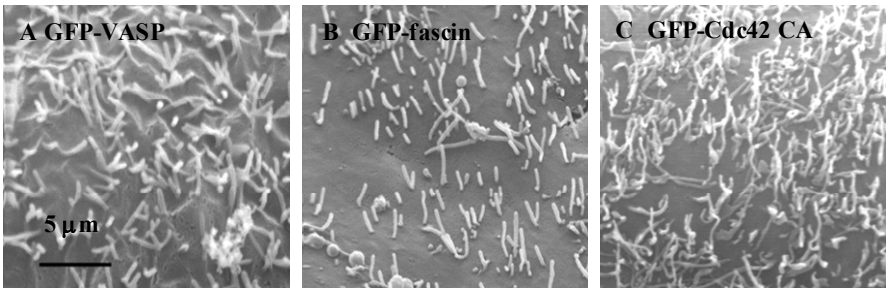
A GFP-VASP
5 µm
B GFP-fascin
C GFP-Cdc42 CA

Figure 3.4 Expressing a Myo10 construct lacking the integrin binding domain also leads to massive increases in dorsal filopodia and localization of Myo10 deletion constructs at the tips of substrate-attached filopodia.

(A-C) Domain mapping experiments show that GFP-Myo10 lacking the integrin binding, FERM domain retains the ability to induce dorsal filopodia when expressed in COS-7 cells, whereas GFP-Myo10 lacking the MyTH4 and FERM domains fails to induce filopodia. The GFP-Myo10-HMM construct, which lacks the PH, MyTH4, and FERM domains, also fails to induce filopodia. The SEM images illustrated here and in all subsequent figures were obtained using correlative fluorescence-SEM. *(D)* The GFP-Myo10 ΔFERM deletion construct localizes at the tips of substrate-attached filopodia as well as the numerous dorsal filopodia induced by this construct. *(E)* Although the GFP-Myo10 ΔMyTH4-FERM construct is unable to induce dorsal filopodia, it retains the ability to localize to the tips of the substrate-attached filopodia present in these cells. *(F)* The ΔMyTH4-FERM-PH construct (GFP-Myo10-HMM) also fails to induce dorsal filopodia while retaining the ability to localize to the tips of substrate-attached filopodia. COS-7 cells were transfected overnight with the indicated constructs, replated on coverslips for ~12 hours, stained for F-actin (red) and imaged for GFP (green) or prepared for correlative SEM.

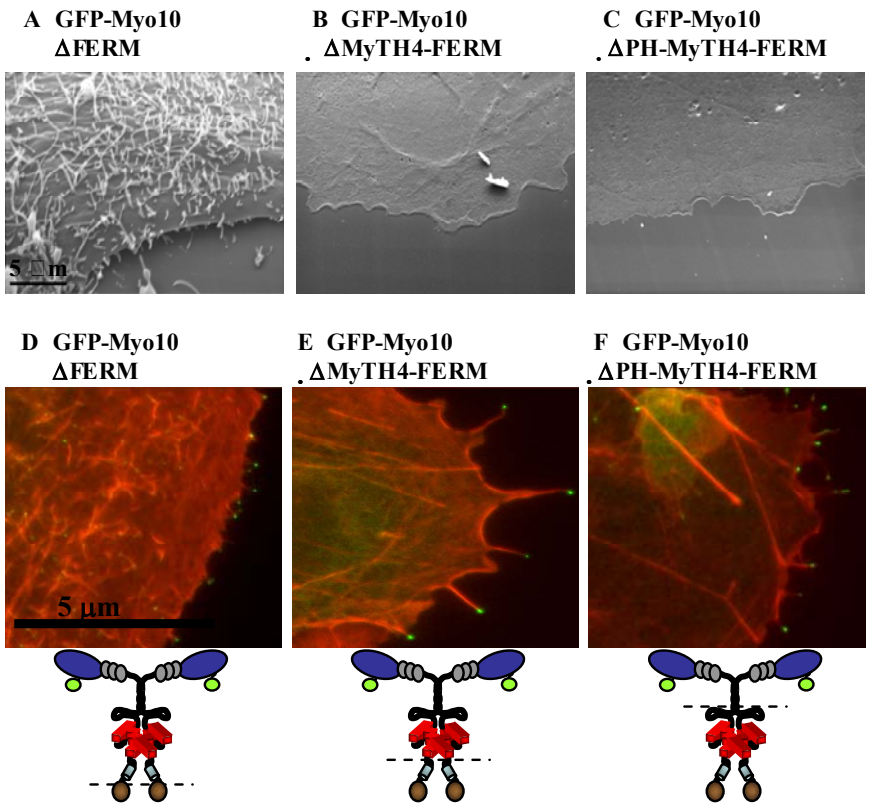
A GFP-Myo10 ΔFERM
B GFP-Myo10 ΔMyTH4-FERM
C GFP-Myo10 ΔPH-MyTH4-FERM
5 □m
D GFP-Myo10 ΔFERM
E GFP-Myo10 ΔMyTH4-FERM
F GFP-Myo10 ΔPH-MyTH4-FERM
5 µm

FERM and the ΔPH-MyTH4-FERM constructs to induce filopodia is not due to an inability to localize to filopodia, but is instead due to deletion of regions in the Myo10 tail required for filopodia formation.

Knock-down of Myo10 leads to loss of dorsal filopodia.

We next asked if endogenous Myo10 is necessary for filopodia formation. We thus used siRNA to knock-down Myo10 in HeLa cells, a cell type that elaborates numerous dorsal filopodia under our standard culture conditions. Densitometry of immunoblots demonstrated that the Myo10 siRNA specifically knocked down ~90% of Myo10 protein by 60-72 hours (Figure 3.5A). SEM revealed that HeLa cells treated with control siRNA have numerous dorsal filopodia per cell (861 +/-37), whereas cells treated with the Myo10 siRNA exhibit decreased dorsal filopodia (207 +/-23)(Figure 3.5B-C). These data demonstrate that Myo10 is required for formation of normal numbers of dorsal filopodia. It is important to note, however, that the loss of dorsal filopodia was not complete and that live cell imaging showed that knock-down cells were still able to extend occasional filopodia (Movies 3.1-3.2). This may reflect incomplete knock-down of Myo10, but it could also indicate that there are Myo10 independent pathways for filopodia formation.

Expressing a dominant negative GFP-Myo10 coiled coil construct also leads to loss of dorsal filopodia.

As an independent strategy to confirm that Myo10 functions in filopodia formation, we also developed a dominant negative approach to inhibit Myo10. Since we had previously found that a head-neck construct fails to localize to filopodial tips while a longer construct

that includes the coiled coil does localize to filopodial tips (Berg and Cheney, 2002), we reasoned that Myo10 is likely to function as a dimer and that overexpression of the coiled coil region might therefore act as a dominant negative. We thus generated a GFP-tagged construct from the putative coiled coil region of human Myo10. Like Myo10 knock-down cells, HeLa cells transfected with the GFP-Myo10 coiled coil exhibit decreased dorsal filopodia (Figure 3.5D). Quantitative experiments revealed that HeLa cells transfected with GFP had 851 +/-51 dorsal filopodia per cell while cells transfected with GFP-Myo10 coiled coil had only 331 +/-62 (Figure 3.6A,B). It should be noted that the GFP-Myo10 coiled coil did not localize to filopodial tips and that expressing a "control" coiled coil from chicken Myo5a did not reduce dorsal filopodia (not shown). The dominant negative experiments thus provide independent confirmation that Myo10 is required for formation of normal numbers of dorsal filopodia.

Inhibiting Myo10 increases cell spreading.

In addition to decreased dorsal filopodia, the most obvious phenotype of HeLa cells treated with siRNA to Myo10 and replated overnight was an approximately 4-fold increase in cell spreading (Figure 3.7). A similar increase in spread area was observed in HeLa cells transfected with GFP coiled-coil and replated overnight. Since these results raised the possibility that decreases in dorsal filopodia are associated with increases in cell spreading, we tested whether increases in dorsal filopodia are associated with decreases in cell spreading. We thus transfected COS-7 cells with GFP-Myo10 to induce dorsal filopodia and replated them ~12 hours. These cells exhibited a ~3-fold decrease in their spread area. We also tested the effect of several constructs of Myo10, which were previously tested for their

ability to induce filopodia in COS-7 cells, on cell spread area. Data from these experiments demonstrate that that only Myo10 constructs capable of inducing filopodia in COS-7 cells were able to decrease the calculated cell spread area (Figure 3.8). Although the precise basis of this effect is not yet clear, it is not due to changes in cell volume and expressing GFP-VASP or GFP-fascin led to similar decreases (Figure 3.7C-3.8D). It is thus likely that the decreased cell spreading is a consequence of the massive increase in dorsal filopodia induced by all three constructs rather than a specific effect of Myo10 expression.

Figure 3.5 Inhibiting Myo10 suppresses dorsal filopodia.

(A) Immunoblot of HeLa cells treated with control or Myo10 siRNA showing specific knock-down of Myo10. Samples were run a 4-20% SDS-PAGE gel, transferred to nitrocellulose, and stained with Ponceau to reveal total protein and then blotted with anti-Myo10 to confirm knock-down. *(B)* SEM of a HeLa cell from the same experiment treated with control siRNA showing the numerous dorsal filopodia normally present on these cells. *(C)* SEM of a HeLa cell from the same experiment treated with Myo10 siRNA showing the loss of dorsal filopodia induced by Myo10 siRNA. *(D)* SEM of a HeLa cell illustrating the loss of dorsal filopodia observed in HeLa cells expressing the dominant negative GFP-Myo10 coiled-coil construct.

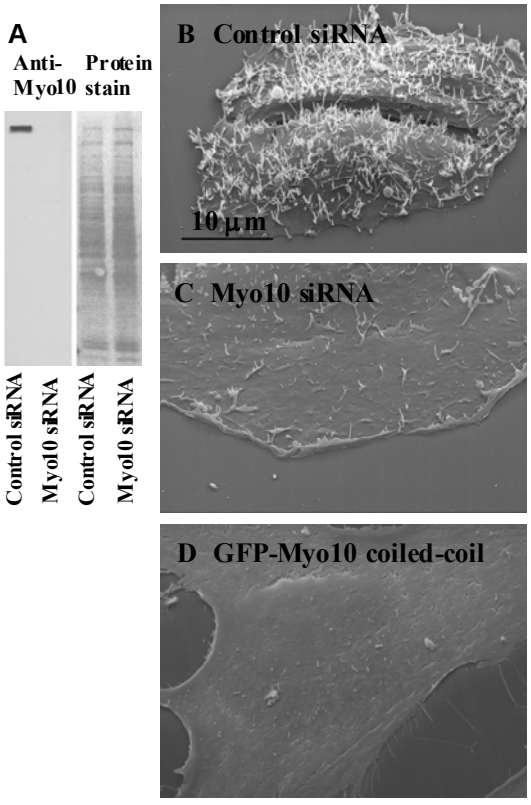
A
Anti-Myo10
Protein stain
Control siRNA
Myo10 siRNA
Control siRNA
Myo10 siRNA
B Control siRNA
10 µm
C Myo10 siRNA
D GFP-Myo10 coiled-coil

Figure 3.6 Quantification of Myo10's effects on filopodia number and cell volume.

(A) COS-7 cells were transfected with GFP or GFP-Myo10 and the number of dorsal filopodia per cell was counted from SEM images. GFP-Myo10 led to a ~500-fold increase in dorsal filopodia per cell. *(B)* A similar experiment demonstrated that treating HeLa cells with Myo10 siRNA led to a ~4-fold decrease in dorsal filopodia per cell. *(C)* Expressing the dominant negative GFP-Myo10 coiled coil construct in HeLa cells also decreased dorsal filopodia. *(D)* None of these treatments led to large changes in cell volume, as calculated from DIC measurement of the diameters of cells that had been trypsinized and fixed. Slender cylindrical structures on the dorsal surface were counted as dorsal filopodia if they had a diameter of ~0.1 um and were greater than ~0.1 um in length. Data are represented as means +/- SEM. N=10 cells per condition for *A*-*C* and 25 cells per condition for *D*. Asterisks indicate means that are significantly different from controls with $P<0.001$ using a Tukey test.

A Myo10 siRNA (HeLa)

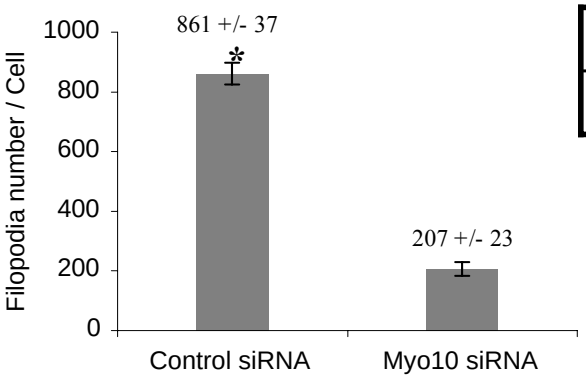

D Cell volume in cubic micron (HeLa)

Control siRNA	**2653 +/- 193**
Myo10 siRNA	**2507 +/- 270**

B Myo10 dominant negative (HeLa)

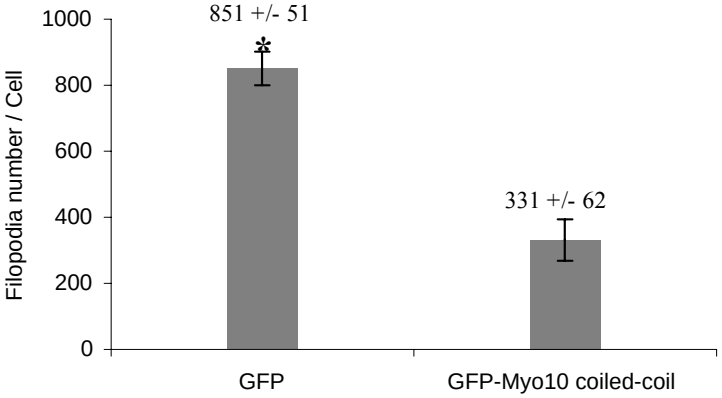

C GFP-Myo10 over-expression (COS-7)

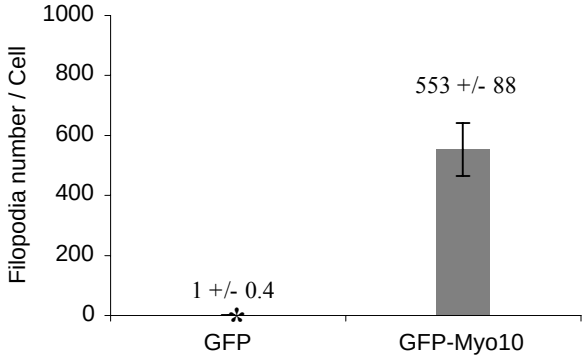

Figure 3.7 Quantification of Myo10's effects on cell spreading

(A) Transfecting COS-7 cells with GFP-Myo10, GFP-VASP, or GFP-fascin, all of which induced dorsal filopodia, led to 2-3-fold decreases in cell spreading. *(B)* Conversely, transfecting HeLa cells with Myo10 siRNA led to large increases in cell spreading. *(C)* Transfecting HeLa cells with the dominant negative GFP-Myo10 coiled coil construct also led to large increases in cell spreading. Note that dominant negative GFP-Cdc42 (15A) also increased cell spreading. The area covered per cell was measured for 25 cells from each condition using light microscopy and the outline tool in Metamorph (Universal Imaging, West Chester, PA). Data are represented as means +/- SEM. Asterisks indicate spread areas that are significantly different from controls with $P<0.001$ using a Tukey test.

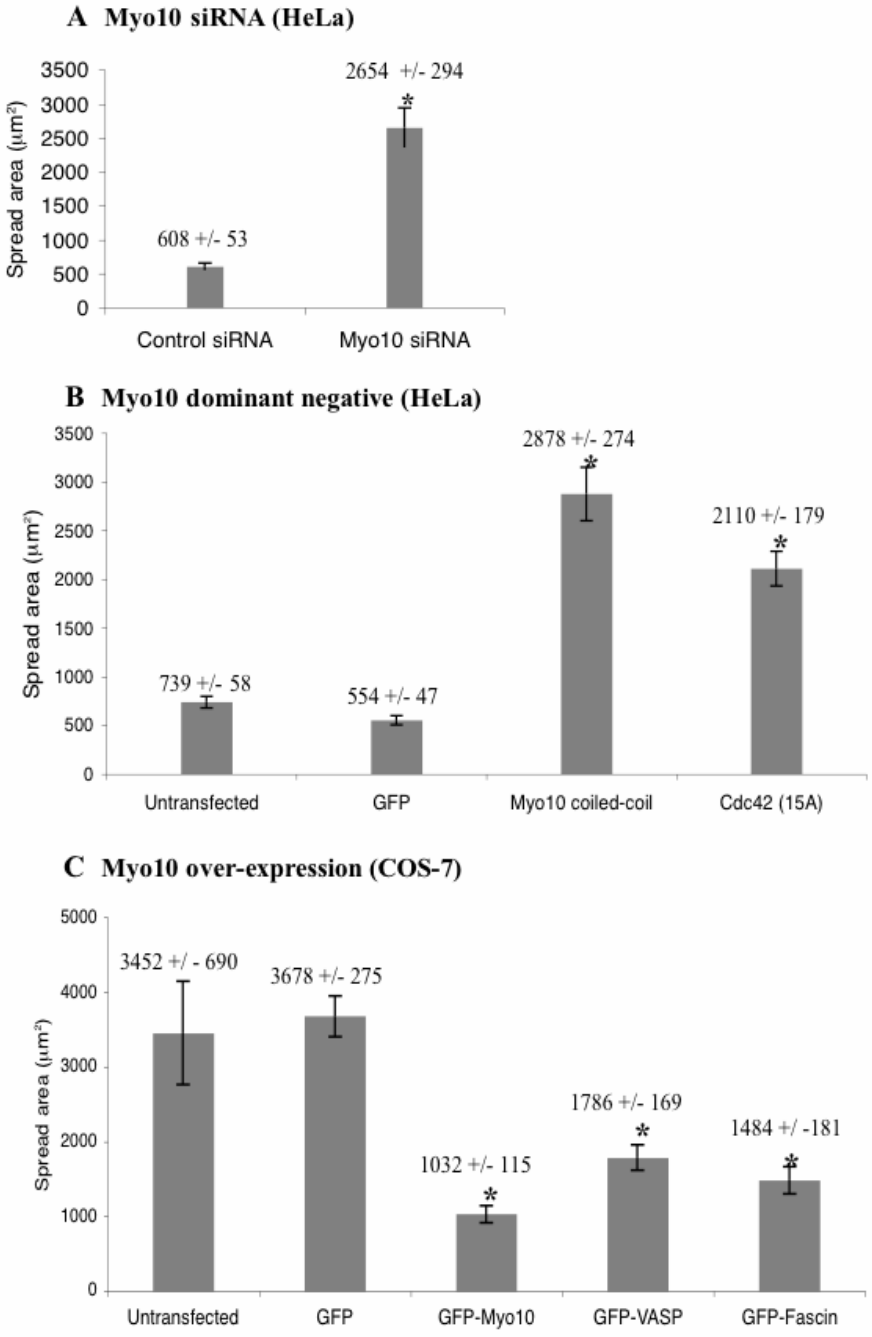
A Myo10 siRNA (HeLa)
Spread area (μm²)
3500
3000
2500
2000
1500
1000
500
0
608 +/- 53
2654 +/- 294
*
Control siRNA
Myo10 siRNA
B Myo10 dominant negative (HeLa)
Spread area (μm²)
739 +/- 58
554 +/- 47
2878 +/- 274
2110 +/- 179
Untransfected
GFP
Myo10 coiled-coil
Cdc42 (15A)
C Myo10 over-expression (COS-7)
Spread area (μm²)
5000
4000
3000
2000
1000
0
3452 +/ - 690
3678 +/- 275
1032 +/- 115
1786 +/- 169
1484 +/ -181
Untransfected
GFP
GFP-Myo10
GFP-VASP
GFP-Fascin

Figure 3.8 Quantification of the effects of constructs of Myo10's on cell spreading.

(A) Transfecting COS-7 cells with GFP-Myo10, GFP-Myo10 ΔFERM, GFP-Cdc42 (CA), and GFP-mDia2 ΔGBD all of which induced dorsal filopodia, led to 2-3-fold decreases in cell spreading. The area covered per cell was measured for 25 cells from each condition using light microscopy and the outline tool in Metamorph (Universal Imaging, West Chester, PA). Data are represented as means +/- SEM. Asterisks indicate spread areas that are significantly different from controls with $P<0.001$ using a Tukey test.

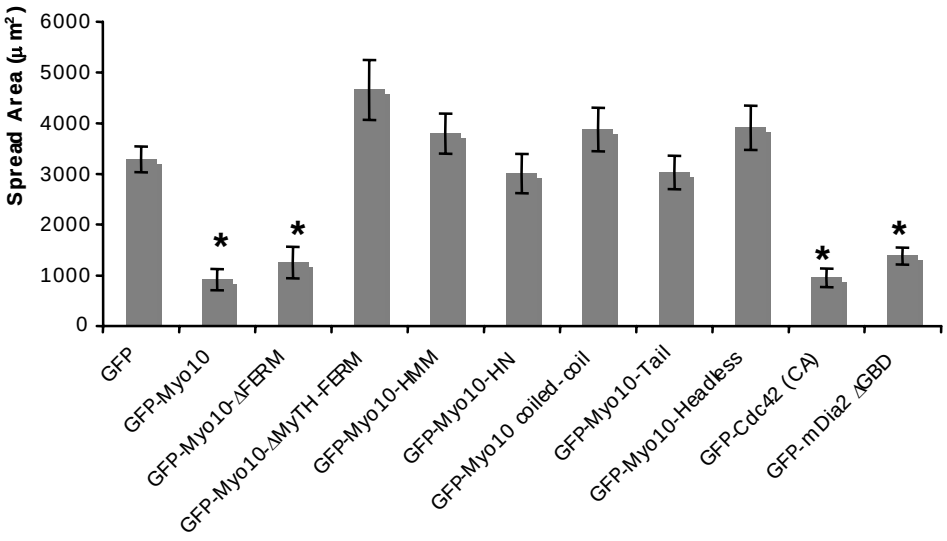
Spread Area (μm²)
6000
5000
4000
3000
2000
1000
0
*
*
*
*
GFP
GFP-Myo10
GFP-Myo10-ΔFERM
GFP-Myo10-ΔMyTH-FERM
GFP-Myo10-HMM
GFP-Myo10-HN
GFP-Myo10 coiled-coil
GFP-Myo10-Tail
GFP-Myo10-Headless
GFP-Cdc42 (CA)
GFP-mDia2 ΔGBD

Myo10 acts downstream of Cdc42

To dissect the molecular mechanisms by which Myo10 induces filopodia, we next investigated the relationship between Myo10 and Cdc42, a master regulator of filopodia formation. We first verified that constitutively active Cdc42 induces dorsal filopodia and that dominant negative Cdc42 suppresses dorsal filopodia (Figure 3.3C and not shown). To determine if Myo10 function requires Cdc42, COS-7 cells were co-transfected with CFP-Myo10 to induce dorsal filopodia and dominant negative GFP-Cdc42 to inhibit Cdc42. These cells elaborated numerous dorsal filopodia, indicating that Myo10 acts either independently or downstream of Cdc42 (Figure 3.9). To test if Myo10 acts downstream of Cdc42, HeLa cells were treated with siRNA to deplete Myo10 and then transfected with constitutively active Cdc42. Constitutively active Cdc42 was unable to induce filopodia in the absence of Myo10 (Figure 3.10A,B), suggesting that Myo10 functions downstream of Cdc42. Importantly, the loss of dorsal filopodia in HeLa cells treated with siRNA to Myo10 could be rescued by transfection with the bovine GFP-Myo10 construct (Figure 3.10C,D), which also provides additional evidence for the specificity of the Myo10 siRNA. Although GFP-fascin was also able to induce numerous filopodia in Myo10 siRNA cells, results with GFP-VASP were less clear (Figure 3.12)

Myo10 can induce dorsal filopodia independently of VASP proteins

Finally, since VASP is present at the tips of filopodia and can induce dorsal filopodia, we also tested whether Myo10 could induce filopodia in MV^{D7} cells--a cell line engineered to lack all three members of the VASP family (Bear et al., 2000). Like COS-7 cells, control MV^{D7} cells transfected with GFP alone had virtually no dorsal filopodia (Figure 3.11A).

MV^{D7} cells expressing GFP-Myo10, however, elaborated numerous dorsal filopodia (Figure 3.11B). This clearly demonstrates that Myo10 can induce dorsal filopodia in the absence of VASP proteins.

Figure 3.9 Myo10 induces dorsal filopodia even in the presence of dominant negative Cdc42.

(A) Like control COS-7 cells, COS-7 cells transfected with dominant negative GFP-Cdc42 (15A) lacked dorsal filopodia. (B) CFP-Myo10, like GFP-Myo10, induced numerous dorsal filopodia when transfected in COS-7 cells. (C) COS-7 cells co-transfected with dominant negative GFP-Cdc42 and CFP-Myo10 exhibited numerous dorsal filopodia, indicating that Myo10 acts either independently or downstream of Cdc42.

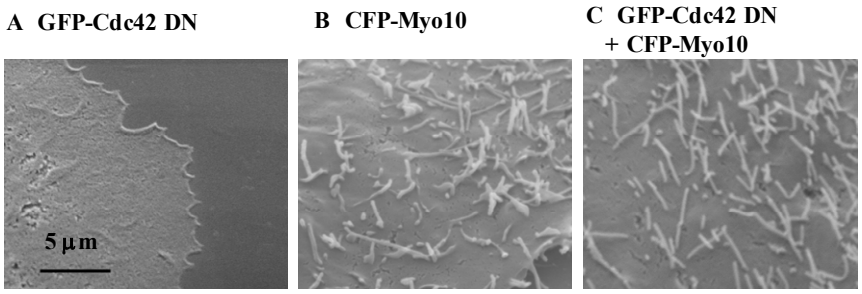
A GFP-Cdc42 DN
B CFP-Myo10
C GFP-Cdc42 DN
+ CFP-Myo10
5 µm

Figure 3.10 Myo10 acts downstream of Cdc42.

(A) Like untreated HeLa cells, HeLa cells treated with a control siRNA and then transfected with constitutively active GFP-Cdc42 exhibit numerous dorsal filopodia. *(B)* Parallel samples treated with the Myo10 siRNA, however, have very few dorsal filopodia even in the presence of constitutively active GFP-Cdc42, indicating that Myo10 functions downstream of Cdc42. *(C,D)* The loss of dorsal filopodia induced by the siRNA to human Myo10 can be rescued by transfection with bovine GFP-Myo10. Note that the constitutively active GFP-Cdc42(61L) construct used here led to a massive induction of filopodia in other situations (Fig. 2C).

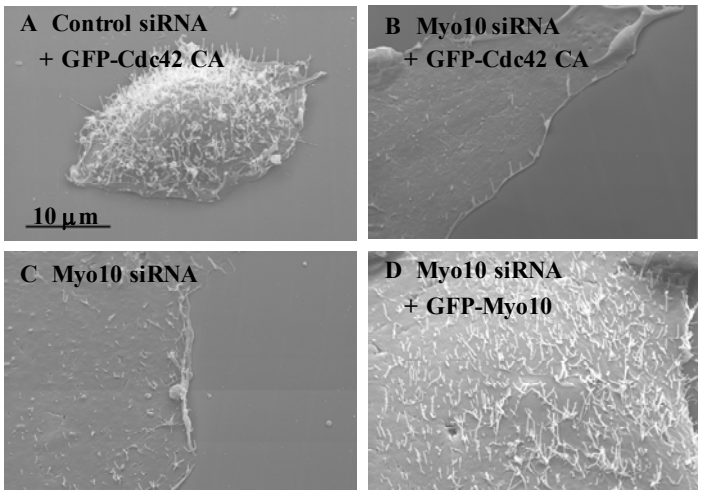
A Control siRNA
+ GFP-Cdc42 CA
10 µm
B Myo10 siRNA
+ GFP-Cdc42 CA
C Myo10 siRNA
D Myo10 siRNA
+ GFP-Myo10

Figure 3.11 Myo10 can induce dorsal filopodia in the absence of VASP family proteins.

(A) Ena/VASP null cells (MV^{D7}) transfected with GFP alone exhibit very few dorsal filopodia. *(B)* Ena/VASP null cells transfected with GFP-Myo10, however, exhibit numerous dorsal filopodia, thus demonstrating that Myo10 does not require VASP proteins for its filopodia promoting activity.

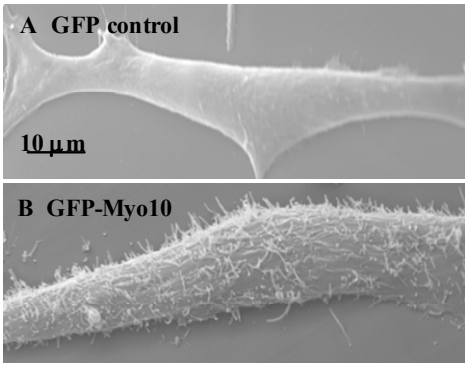
A GFP control
10 µm
B GFP-Myo10

Figure 3.12 GFP-fascin and GFP-Myo10 ΔFERM can induce dorsal filopodia in Myo10 knock-down cells.

(A) HeLa cells treated with control siRNA exhibited numerous dorsal filopodia. *(B)* HeLa cells treated with Myo10 siRNA again showed a dramatic reduction of dorsal filopodia. *(C)* When GFP-VASP was expressed in HeLa cells treated with Myo10 siRNA, a partial and variable induction of dorsal filopodia was observed. *(D)* When GFP-fascin was expressed in HeLa cells treated with Myo10 siRNA, a robust induction of dorsal filopodia was observed. *(E)* Similar experiments showed that the GFP-Myo10 ΔFERM construct induced dorsal filopodia in Myo10 siRNA treated HeLa cells. *(F-H)* The GFP-Myo10 ΔMyTH4-FERM and GFP-Myo10 ΔPH-MyTH4-FERM deletion constructs, as well as GFP alone, all failed to induce filopodia in HeLa cells treated with Myo10 siRNA.

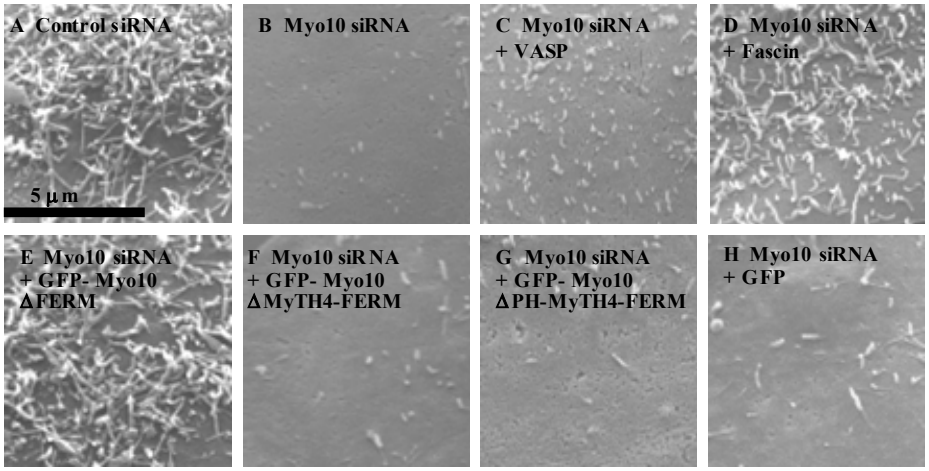
A Control siRNA
5 μm
B Myo10 siRNA
C Myo10 siRNA
+ VASP
D Myo10 siRNA
+ Fascin
E Myo10 siRNA
+ GFP- Myo10
ΔFERM
F Myo10 siRNA
+ GFP- Myo10
ΔMyTH4-FERM
G Myo10 siRNA
+ GFP- Myo10
ΔPH-MyTH4-FERM
H Myo10 siRNA
+ GFP

DISCUSSION

The SEM data presented here demonstrate that Myo10 is a remarkably potent promoter of dorsal filopodia. These data also demonstrate that Myo10 can promote filopodia via mechanisms that do not involve stabilization of substrate-attached filopodia. Consistent with this, deletion of Myo10's FERM domain (the region that binds to integrins) did not impair Myo10's ability to induce filopodia. Thus, although the FERM domain and integrin binding may facilitate the formation of substrate-attached filopodia (Zhang et al., 2004), Myo10 can also induce dorsal filopodia independently of substrate attachment. Deletion of both the MyTH4 domain and the FERM domain of Myo10, however, led to a complete loss of Myo10's ability to induce dorsal filopodia, even though this construct was able to localize to the tips of substrate-attached filopodia. This suggests that the MyTH4 domain, one of the defining features of the MyTH4-FERM myosins, plays an important role in filopodia formation. Since deletion constructs that lack the Myo10 motor domain fail to localize to filopodial tips and do not induce filopodia (Berg and Cheney, 2002), our results support a model for Myo10 function where the motor domain is required to properly localize the tail domain, and a properly localized tail is required for filopodia formation.

We also show here that endogenous Myo10 is necessary for formation of normal numbers of dorsal filopodia using two independent strategies, Myo10 siRNA and a dominant negative construct. This, together with the data showing that Myo10 is a potent inducer of filopodia, demonstrates that Myo10 functions as a molecular motor for filopodia formation. Our work also raises the question of how Myo10 acts to promote filopodia. Our data indicate that Myo10 acts downstream of Cdc42, a regulator of filopodia that acts upstream of actin

nucleators such Arp2/3 (Higgs and Pollard, 2000b) and formins (Peng et al., 2003) and also stimulates actin bundling (Faix and Rottner, 2005). Since Myo10 is an actin-based motor and its motor is necessary for filopodia induction, Myo10 may act on actin generated downstream of Cdc42 action. In the convergent elongation model of filopodia formation, branched actin filaments nucleated by Arp2/3 associate via their tips to form "Λ-precursors" proposed to initiate filopodia (Svitkina et al., 2003). Although VASP is present at the tips of Λ-precursors (Svitkina et al., 2003), the protein(s) that lead the tips of actin filaments to associate with one another in Λ-precursors remain unknown. Like VASP, Myo10 is present at the tips of nascent filopodia as soon as they can be detected (Berg and Cheney, 2002). As expected for a component of Λ-precursors, puncta of GFP-Myo10 have recently been observed to move laterally along the leading edge, where they collide and fuse (Sousa et al., 2006). Since our data show that Myo10 can induce dorsal filopodia in the absence of VASP proteins, Myo10 may be a component of Λ-precursors and thus function in filopodial initiation. If Myo10 promotes filopodia by "focusing" the barbed ends of actin filaments into Λ-precursors, our results show that Myo10's heads are not sufficient for this activity since the HMM-like construct consisting only of the head, neck, and coiled coil is unable to induce dorsal filopodia (Figure 3.3C). It should also be noted that although convergent elongation provides a useful conceptual model for filopodia formation, the nature of the actin network underlying dorsal filopodia is not yet clear and it may differ from the dendritic array observed at the leading edge. It will thus be important to consider other mechanisms by which Myo10 could promote filopodia, such as by delivering/localizing materials required for polymerization to the filopodial tip, interacting with formins, or by pushing the plasma membrane away from the ends of growing actin filaments to facilitate monomer insertion.

Conserved functions of MyTH4-FERM myosins in filopodia and related structures. Like Myo10, other MyTH4-FERM myosins may have similar functions in the formation of filopodia and related structures such as microvilli and stereocilia. Experiments with human Myo15, a MyTH4-FERM myosin that is expressed in the inner ear, show that it localizes to the tips of stereocilia (Belyantseva et al., 2003; Rzadzinska et al., 2004), is necessary for proper stereociliary elongation, and exhibits movements within filopodia strikingly similar to the intrafilopodial motility of Myo10 (Belyantseva et al., 2005). Loss of a *Drosophila* MyTH4-FERM myosin, myosin-VIIa, is the basis of *crinkled*, a usually lethal mutation where escapers exhibit defects in bristles and other structures derived from actin bundles (Kiehart et al., 2004). Another MyTH4-FERM myosin, myosin-VIIb, localizes to the microvilli of secretory epithelial cells (Chen et al., 2001). Finally, deletion of Dictyostelium myosin-VII leads to a 90% loss of filopodia as well as dramatic defects in adhesion and phagocytosis (Titus, 1999b; Tuxworth et al., 2001). Together with the work on Myo10 presented here, these data provide strong evidence that MyTH4-FERM myosins have ancient and highly conserved functions in membrane-cytoskeleton interactions underlying the formation of filopodia and related structures.

CHAPTER FOUR

CONCLUSIONS AND FUTURE DIRECTIONS

Filopodia are finger-like extensions that play important roles in the cell biology governing angiogenesis, neuronal migration and spine formation, and cancer metastasis. Our lab had previously discovered that a novel unconventional myosin, Myo10 localizes strikingly to tips of filopodia and undergoes a novel form of motility that we termed intrafilopodial motility. For this dissertation, I have subsequently concentrated on understanding the cellular function of Myo10. These studies have led to the discovery that Myo10 binds to and undergoes co-transport with β-integrins, Myo10 is a component of the tip complex, and Myo10 is a potent inducer of dorsal filopodia and can act downstream of Cdc42 and independent of VASP.

SUMMARY

The main conclusions of this dissertation are as follows:

1. The FERM domain of Myo10 can bind to the cytoplasmic tail of β-integrins.
2. The FERM domain of Myo10 can activate β1-integrins in a fashion similar to the FERM domain of talin.
3. Myo10 and β3-integrins can undergo co-transport within filopodia.
4. Over-expression of Myo10 results in a 500-fold induction of dorsal filopodia.
5. The MyTH4-FERM domains of Myo10 are necessary for Myo10's ability to induce filopodia.
6. Knocking-down Myo10 in cells results in a dramatic reduction of dorsal filopodia and an increase in cell spread area.
7. The spread area of cells appears to be inversely correlated to the number of dorsal filopodia.
8. Myo10 can act downstream of small GTPase Cdc42, which is a master regulator of filopodia formation.
9. Myo10 can induce filopodia in Mena/VASP null cells suggesting that Myo10 can induce filopodia independent of Mena/VASP proteins.
10. Myo10 co-precipitates with VASP and VASP co-precipitates with Myo10.

Myo10's ROLE IN VERTEBRATE CELL BIOLOGY

Myo10 binds to and colocalizes with VASP at tips of filopodia

The slender actin-based protrusions known as filopodia play a key role in biological processes ranging from growth cone guidance to angiogenesis (Gerhardt et al., 2003; O'Connor et al., 1990). Filopodia are composed of a core of parallel-bundled actin filaments that are rather similar to the microvilli of the gut and the stereocilia of the inner ear. The tips of these actin-rich structures are characterized by the presence of an amorphous dense material when visualized by electron microscopy (Mooseker and Tilney, 1975).

VASP, which localizes to the tips of filopodia, as well as focal adhesions and the leading edge of lamellipodia (Krause et al., 2003) is also a component of the filopodial tip complex. Since VASP family proteins (Ena/VASP/Evl) act as anti-capping proteins and promote polymerization of actin filaments (Krause et al., 2003), the presence of VASP at filopodial tips is expected to stimulate filopodia formation. Consistent with this, VASP has been shown to be important for filopodia formation in *Dictyostelium* (Han et al., 2002) and neuronal growth cones (Lebrand et al., 2004).

Since Myo10 is a core component of the filopodial tip complex and it localizes predominantly to filopodial tips and not to focal adhesions unlike VASP, we hypothesized that Myo10 could serve as a molecular tool to identify other components of the filopodial tip complex. For these experiments I first immunoprecipitated endogenous Myo10 from HeLa cells and then silver stained the gel to identify proteins that specifically coprecipitated with Myo10. Data from these experiments revealed that four proteins of approximate molecular weights 210, 110, 90, and 45 KDa coprecipitated with Myo10, but not with a non-immune

control (Figure 4.1). These experiments demonstrate that consistent with our hypothesis, Myo10 can be used as a molecular tool to help identify proteins of the filopodial tip complex.

Since VASP is a protein that has been previously shown to localize to filopodial tips, focal adhesions and lamellipodia, we next tested if one of these unidentified bands was VASP. Immunoblotting of the Myo10 immunoprecipitate with antibody against VASP showed that a small portion of total endogenous VASP coprecipitates with endogenous Myo10. On the other hand, Arp2/3, which is normally not present in filopodia, does not coprecipitate with Myo10 (Figure 4.2). Conversely, endogenous Myo10 coprecipitates with endogenous VASP (Figure 4.3). We next stained cells with antibodies against Myo10 and VASP to test whether the endogenous proteins co-localizes at tips of filopodia. While VASP was mostly detected at focal adhesions and the edges of lamellipodia, a small portion of VASP co-localized with Myo10 at filopodial tips. Note that Myo10 is not detected at focal adhesions (Figure 4.4). It remains to be established whether the binding between Myo10 and VASP is direct or indirect and also whether VASP undergoes intrafilopodial motility with Myo10. In this regard, I have recently designed a yeast-two-hybrid bait construct of Myo10 and have obtained a VASP prey construct to test if Myo10 binds directly to VASP. Omar Quintero, a postdoc in our lab has recently demonstrated that VASP undergoes cotransport with Myo10 in HeLa cells coexpressing CFP-VASP and GFP-Myo10.

Figure 4.1 Can Myo10 serve as a molecular tool to identify components of the filopodial tip complex?

Figure shows a silver stained gel loaded with samples from a Myo10 immunoprecipitation. Note four unidentified protein bands that coprecipitate with Myo10 and not with non-immune controls. For these experiments, gels were washed twice with 50% methanol, 10% acetic acid (Fixer 1) for 15 min each. Next, gels were agitated in 10% ethanol, 5% glacial acetic acid (Fixer 2) for 6 min and rinsed in distilled water (DW). The gels were then washed twice (9 min each) with 500 ml DW. After washing, gels were agitated in freshly made (in DW) 500 ml of 20mg/L hydrosulfite dithionite for 9 min. Next, 200 ml, 0.1% Silver nitrate (200 mg) in DDW and150µl 37% formaldehyde was added to the gel container and incubated on a shaker for 9 min. Gels were then rinsed 30 sec with DDW to remove excess AgNO3 and 200 ml image developer (1ml 37% formaldehyde per liter of 3% sodium carbonate) mixed with 200 µl 10g/L sodium thiosulfate was added to the gel container and incubate on a shaker to desired staining intensity (3 to 6min). Once desired intensity was observed, the developer was poured off and 80 ml of stop solution containing 50g tris, 25ml glacial acetic per liter of distilled water was added to the gel container. Gels were scanned and processed using Adobe Photoshop.

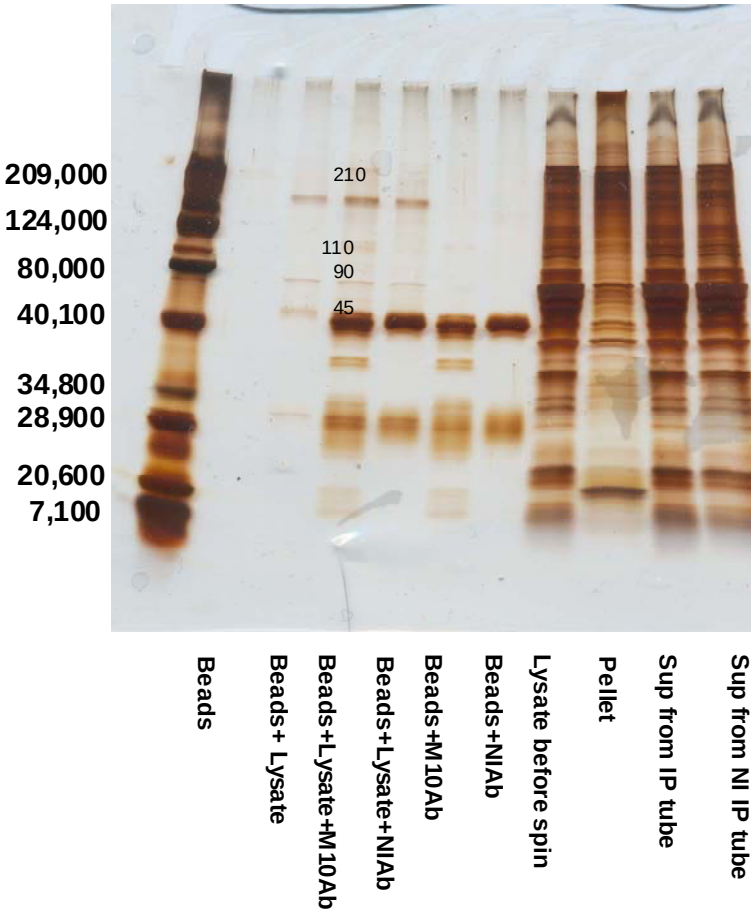
209,000
124,000
80,000
40,100
34,800
28,900
20,600
7,100
210
110
90
45
Beads
Beads+ Lysate
Beads+Lysate+M10Ab
Beads+Lysate+NIAb
Beads+M10Ab
Beads+NIAb
Lysate before spin
Pellet
Sup from IP tube
Sup from NI IP tube

Figure 4.2 VASP co-precipitates with Myo10.

Myo10 or VASP was immunoprecipitated from HeLa cell lysates and then immunoblotted with the indicated antibodies. (A) Immunoblot showing immunoprecipitation of endogenous Myo10 with rabbit anti-Myo10. This blot was stained using the same rabbit antibody to Myo10 and shows that Myo10 is present in the crude lysate and in the immunoprecipitation sample containing beads, lysate, and Myo10 antibody (M10 Ab), but not in control samples such as those containing beads, lysate, and non-immune antibody (NI Ab). (B) Immunoblot of the same samples showing that VASP co-precipitates with Myo10. This blot was stained with mouse anti-VASP and shows that a fraction of VASP coprecipitates with Myo10, consistent with the localization of a small fraction of VASP to filopodial tips. (C) Immunoblot of the same samples showing that pArc3, a component of the Arp2/3 complex, does not co-precipitate with Myo10.

For each immunoprecipitation experiment, the HeLa cells from two 100 mm dishes at ~50% confluence were rinsed briefly with PBS, scraped into 1 ml of ice cold lysis buffer (40 mM HEPES, 75 mM KCl, 2.5 mM $MgCl_2$, 1% Triton-X-100, 2 mM EDTA, 2 mM DTT, 1 mM Pefablock, 5 mM ATP, 5 µg/ml pepstatin A, 5 µM latB, pH 7.4), and lysed by ~10 passages through a tuberculin syringe with a 26 gauge needle. Lysates were centrifuged for 15 minutes at 100,000 g using a tabletop ultracentrifuge and 500 µl aliquots of the supernatant or lysis buffer were placed in a microfuge tube containing 25 µl of packed (and prewashed) Gamma-bind Sepharose beads (Amersham Biosciences) and 2.5 µg of the indicated affinity purified antibody or a non-immune IgG. The beads were incubated for 2 hours at 4˚C, collected by centrifugation for 3 minutes at 14,000 g, washed thrice with lysis buffer, and then resuspended and boiled in 100 µl of SDS sample buffer. 10 µl samples from

the resuspended pellets and the crude lysate were separated on 4-20% SDS-PAGE gels and transferred to nitrocellulose. Nitrocellulose membranes were incubated with 1 µg/ml of anti-VASP, anti-pArc3, or anti-Myo10 for 1 hour, washed 3x with TBST for 10 minutes each, and incubated with donkey secondary antibodies conjugated to HRP (Jackson Laboratories) at 1:40,000 for 45 minutes. Blots were developed using Super Signal West Pico chemiluminescent reagent and X-OMAT Blue films. Images were acquired using an Epson 1640 scanner and Abode Photoshop.

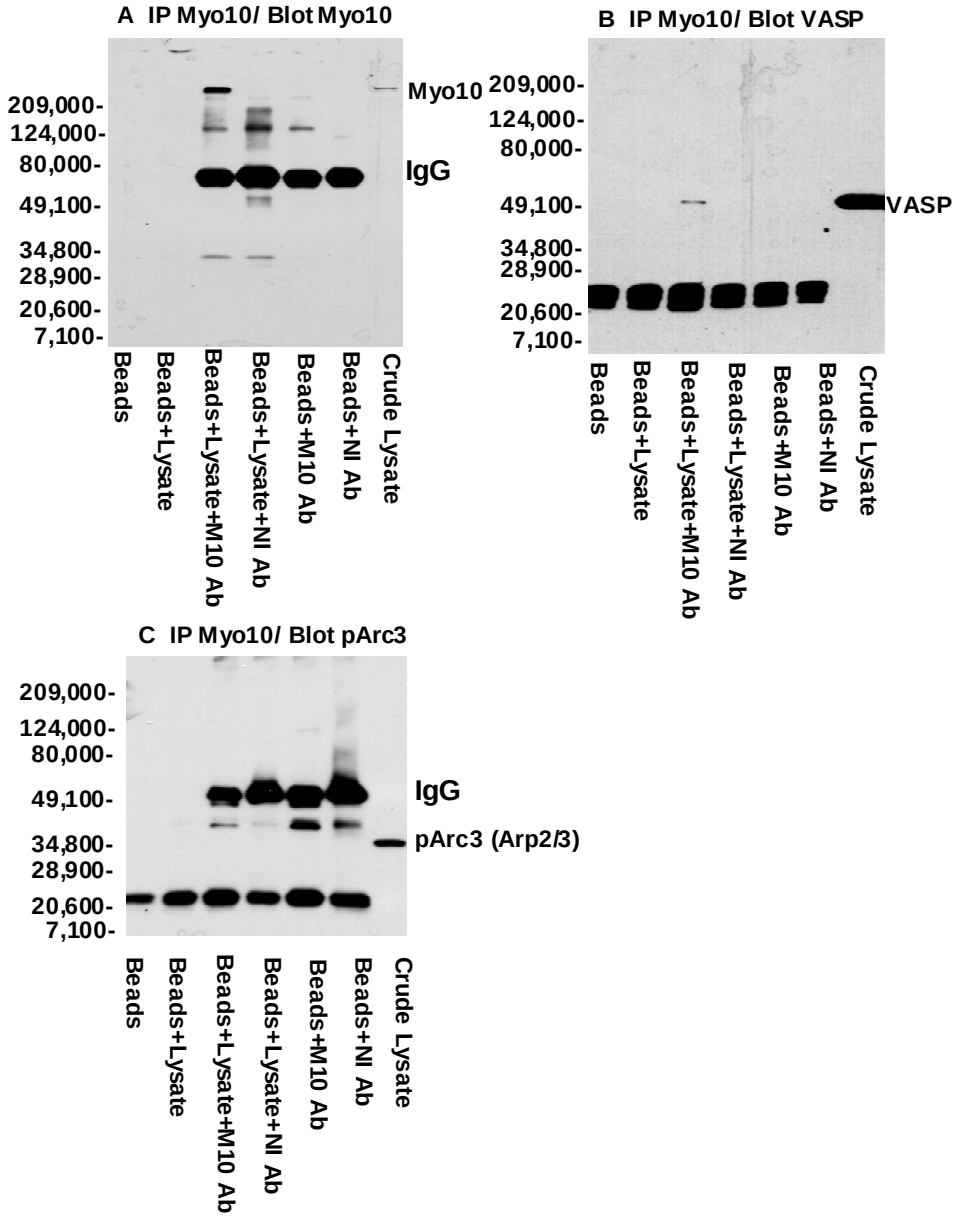
A IP Myo10/ Blot Myo10
209,000-
124,000-
80,000-
49,100-
34,800-
28,900-
20,600-
7,100-
Myo10
IgG
Beads
Beads+Lysate
Beads+Lysate+M10 Ab
Beads+Lysate+NI Ab
Beads+M10 Ab
Beads+NI Ab
Crude Lysate
B IP Myo10/ Blot VASP
209,000-
124,000-
80,000-
49,100-
34,800-
28,900-
20,600-
7,100-
VASP
Beads
Beads+Lysate
Beads+Lysate+M10 Ab
Beads+Lysate+NI Ab
Beads+M10 Ab
Beads+NI Ab
Crude Lysate
C IP Myo10/ Blot pArc3
209,000-
124,000-
80,000-
49,100-
34,800-
28,900-
20,600-
7,100-
IgG
pArc3 (Arp2/3)
Beads
Beads+Lysate
Beads+Lysate+M10 Ab
Beads+Lysate+NI Ab
Beads+M10 Ab
Beads+NI Ab
Crude Lysate

Figure 4.3 Myo10 co-precipitates with VASP.

VASP was immunoprecipitated from HeLa cell lysates. (A) Immunoblot showing immunoprecipitation of endogenous VASP by mouse anti-VASP. VASP was immunoprecipitated with mouse anti-VASP and then immunoblotted with rabbit anti-VASP. (B) Immunoblot showing that Myo10 coprecipitates with VASP. Samples from the same VASP immunoprecipitation were immunoblotted with anti-Myo10. The positions of molecular mass standards are indicated on the left of each immunoblot and the identities of major stained bands are indicated on the right. Note that in some cases the secondary antibodies used for immunoblotting reacted with bands associated with the IgG or beads required for the immunoprecipitations.

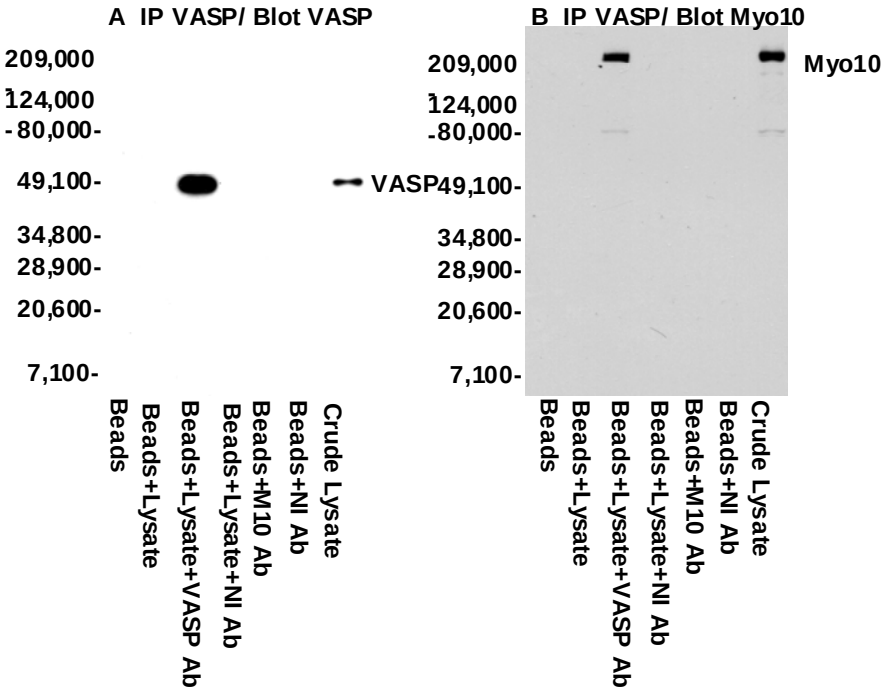
A IP VASP/ Blot VASP
209,000
124,000
80,000
49,100
34,800
28,900
20,600
7,100
VASP
Beads
Beads+Lysate
Beads+Lysate+VASP Ab
Beads+Lysate+M10 Ab
Beads+Lysate+NI Ab
Beads+NI Ab
Crude Lysate
B IP VASP/ Blot Myo10
209,000
124,000
80,000
49,100
34,800
28,900
20,600
7,100
Myo10
Beads
Beads+Lysate
Beads+Lysate+VASP Ab
Beads+Lysate+NI Ab
Beads+M10 Ab
Beads+NI Ab
Crude Lysate

Figure 4.4 Myo10 and VASP co-localize at tips of filopodia.

HeLa cells fixed and stained for endogenous Myo10 (green) and VASP (red) showing that the two proteins colocalize at tips of filopodia. Scale bar is 10 μm. Arrows point to filopodial tips.

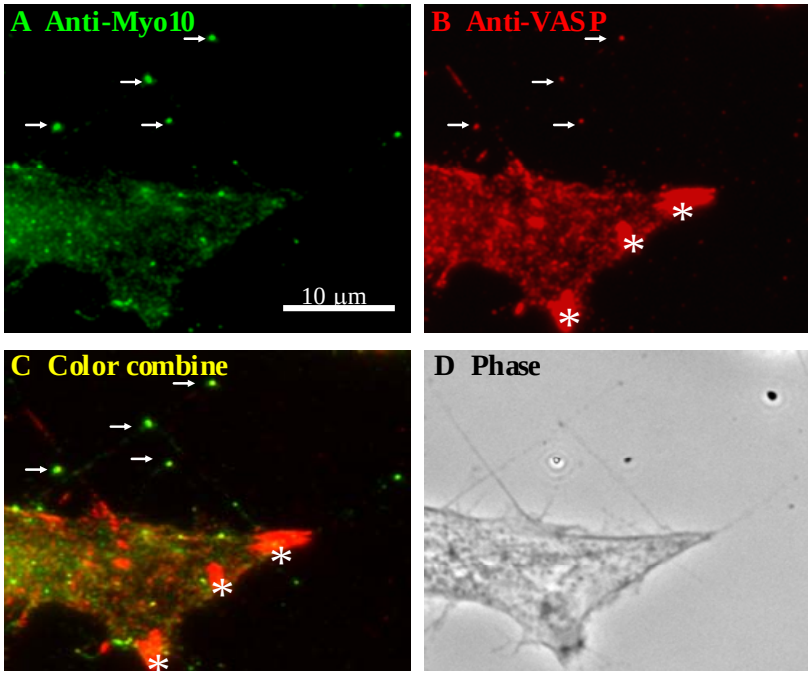
A Anti-Myo10
10 μm
B Anti-VASP
C Color combine
D Phase

Myosin-X appears to function as a dimer

Myosin-X (Myo10) is an unconventional myosin of the MyTH4-FERM family that localizes to the tips of filopodia and has been hypothesized to act as part of a filopodial tip complex important for filopodia formation (Berg and Cheney, 2002; Sousa et al., 2006; Sousa and Cheney, 2005). Myo10 contains a motor domain that can bind actin, hydrolyze ATP, and produce force (Homma and Ikebe, 2005; Kovacs et al., 2005). The neck of Myo10 consists of three IQ motifs, each of which can bind calmodulin (Homma et al., 2001). The Myo10 tail contains a segment of ~130 amino acids that was initially predicted to form a coiled coil and function as a dimerization domain (Berg et al., 2000). The coiled-coil has been hypothesized to mediate dimerization of Myo10. Although, these studies indicate that Myo10 might function as a monomer as 90% of the purified Myo10 HMM molecules, which contain the head neck and coiled-coil regions of Myo10, were monomers, the fact that 10% of purified Myo10- HMM molecules formed dimers raises the interesting possibility that Myo10 might undergo regulated dimerization (Knight et al., 2005). Consistent with this hypothesis our lab has recently generated data that demonstrates that a forced dimer construct of Myo10 is sufficient for localization to the filopodial tip. This forced dimer construct that localized to filopodial tips consists of the head, neck, first 34 amino acids of the coiled-coil and a GCN4 leucine zipper, which was used to mediate forced dimerization. Interestingly, a construct containing the head, neck, and GCN4 leucine zipper and a construct containing head, neck, and first 34 amino acids of the coiled-coil showed little or no localization to filopodial tips indicating that the first 34 amino acids and GCN4 mediated dimerization of Myo10 were both necessary for Myo10 head neck construct's localization to filopodial tips. In preliminary experiments, constructs of Myo10 that were previously reported to lack the

ability to localize to filopodial tips when expressed alone (Table 4.1), localized to filopodial tips when coexpressed with full length GFP-Myo10. Interestingly, the localization of these constructs to filopodial tips when co-expressed with Myo10 was specific to Myo10 since coexpression of these constructs with a filopodial tip protein CFP-VASP did not result in filopodial tip localization of these constructs. These data indicate that Myo10 functions either as a dimer or oligomer at the filopodial tip. Since Myo10 head neck construct (lacks the coiled-coil dimerization domain) and the CFP-Myo10 full length construct both localize to filopodial tips when coexpressed and also since the GFP-Myo10 tail construct (lacks coiled-coil dimerization domain) and CFP-Myo10 HMM construct localizes to filopodial tips when coexpressed raise the possibility that in one hypothetical model of Myo10 function, the Myo10 head might bind to the tail of Myo10 and thus localize to filopodial tips. One future direction is to further validate these preliminary set of experiments to determine if Myo10 functions as a regulated dimer at tips of filopodia.

Table 4.1 Does Myo10 function as a dimer at filopodial tips?

Table shows results of over-expression or coexpression of contructs of Myo10 in HeLa cells. + denotes localization to filopodial tips and – denotes that construct was not detected at filopodial tips. +/- denotes localization of first but not the second construct to filopodial tips. For example, CFP-Myo10/GFP +/- denotes that CFP-Myo10 localized to filopodial tips, but not GFP. +/+ denotes that both expressed contructs localized to filopodial tips**.** SH denotes slow hydrolysis mutant and WB denotes weak binding mutant of Myo10. GFP-Myo10 HMM resembles the Heavy Mero Myosin construct, which contains the Head, neck and coiled-coil domains of Myo10 fused to GFP at the N-terminus.

Construct	Filopodial tips	Construct	Filopodial tips
GFP	-	CFP-Myo10+GFP	+/-
GFP-Myo10	+	CFP-Myo10+GFP-Myo10	+/+
GFP-Myo10 SH	+	CFP-Myo10+GFP-Myo10 SH	+/+
GFP-Myo10 WB	-	CFP-Myo10+GFP-Myo10 WB	+/+
GFP-Myo10 headless	-	CFP-Myo10+GFP-Myo10 Headless	+/+
GFP-Myo10 Headneck	-	CFP-Myo10+GFP-Myo10 Head neck	+/+
GFP-Myo10 Coiled coil	-	CFP-Myo10+GFP-coiled-coil	+/-
GFP-Myo10 Tail	-	CFP-Myo10+GFP-tail	+/+
GFP-Myo10 HMM	+	CFP-Myo10+GFP-Myo10 HMM	+/+
CFP-VASP+ GFP	+/-	CFP-Myo10HMM +GFP	+/-
CFP-VASP+ GFP-Myo10	+/+	CFP-Myo10HMM +GFP-Myo10	+/+
CFP-VASP+ GFP-Myo10 SH	+/-	CFP-Myo10HMM +GFP-Myo10 SH	+/+
CFP-VASP+ GFP-Myo10 WB	+/-	CFP-Myo10HMM +GFP-Myo10 WB	+/+
CFP-VASP+ GFP-Myo10 Headless	+/-	CFP-Myo10HMM +GFP-Myo10 headless	+/+
CFP-VASP+ GFP-Myo10 Headneck	+/-	CFP-Myo10HMM +GFP-Myo10 headneck	+/-
CFP-VASP+ GFP-Myo10 Tail	+/-	CFP-Myo10HMM +GFP-Myo10 tail	+/+

Dimerization of Myosin-X might serve to cluster barbed ends of lamellipodial actin filaments predestined to form filopodia

One of the unanswered questions regarding filopodia formation by convergent elongation is how lamellipodial actin filaments, which are pre-destined to form filopodia, associate to initiate filopodia formation. In this regard, the persistent elongation of filaments by itself would not result in their local accumulation unless they were able to associate with each other. Privileged barbed ends seem to combine the ability for continuous elongation with potential to associate with one another. The cross-linking molecules mediating formation of the initiation complex by association of barbed ends remain unclear are likely to be components of the filopodial tip complex. Given our data that Myo10 is stable at filopodial tips even after overnight incubation in lysis buffer containing phalloidin and the hypothesis that Myo10 might function as a dimer that contains two actin binding sites raises the interesting possibility that Myo10 might serve to cross-link filament barbed ends together during filopodia initiation. This result suggests that bundling and barbed-end interaction might be mediated by different molecules-Myo10 and fascin. The molecular compositions of the filopodial tip complex remains to be established. However, proteins previously found to localize specifically to filopodial tips, including Ena/VASP proteins, are predicted to be members of this complex. One possibility is that Ena/VASP proteins, which mediate protection of barbed ends from capping, may also work as barbed end "glue" because of their ability to oligomerize (Bachmann et al., 1999). In support of this idea, a domain mediating oligomerization of Mena has been shown to be required for full function of Mena in cell motility (Loureiro et al., 2002). Another possibility is that additional (yet unidentified) molecules within the filopodial tip complex mediate interaction between barbed ends. These

possibilities are not mutually exclusive, and the hypothetical barbed end linking molecules may act indirectly through Ena/VASP proteins, which would have the benefit of rendering the anti-capping and clustering capabilities to the same subset of filaments.

The combination of continuous elongation and self-association properties of privileged barbed ends allows one to explain how filaments in the dendritic network become gradually associated during filopodia initiation. During elongation, the barbed ends of diagonally oriented filaments drift laterally along the edge, which increases chances of their collision. Such lateral movements of lamellipodial filaments were proposed to mediate formation of filopodia due to activity of bundling proteins (Small et al., 1982). Myo10 has recently been shown to undergo such lateral movements at the leading edge of CAD (a mouse neuronal cell line) cells prior to fusion along with other GFP-Myo10 puncta and elongation of filopodia (Sousa et al., 2006). These results put together raise the interesting possibility and provide additional clues that Myo10 might function to cross-link lamellipodial actin filaments destined to form filopodia during filopodia formation by convergent elongation.

Myo10's ROLE IN CELL PHYSIOLOGY

Myo10 plays a key role in BMP6 induced endothelial cell migration

Endothelial cell migration is a key step during angiogenesis. During angiogenesis, endothelial path finder cells are known to extend long filopodia that are hypothesized to act as cellular sensors, which guide migrating cells in the right direction (Gerhardt et al., 2003). Abnormalities of this process are thought to lead to cardiovascular disease. The bone

morphogenetic proteins (BMP) are known to be potent stimulators of cell migration and angiogenesis (He and Chen, 2005). However, the signaling pathways necessary for migration induced by BMPs are still incompletely understood. To search for novel genes contributing to BMP-induced endothelial migration, our collaborators from Cam Patterson's laboratory (University of North Carolina at Chapel Hill, NC) performed gene expression profiling experiments using microarray analysis technology and found that Myo10, which is known to localize to and induce filopodia, is potently upregulated by BMP2 or BMP6. RT-PCR and western blotting analysis demonstrated more than 10-fold increase of Myo10 mRNA and protein levels. This upregulation of Myo10 appears to be regulated through the Smad pathway since Smad inhibitors Smad6 and Smad7 significantly inhibited Myo10 upregulation induced by BMP6. The functional significance of the data obtained from microarray analysis was next tested using a cell culture system. Data from these experiments have shown that in mouse primary endothelial cells, BMP6-induced Myo10 localizes at tips of filopodia and BMP6 treated endothelial cells showed an increase in filopodia number as determined by scanning electron microscopy method to study dorsal filopodia that I helped develop in our laboratory. This finding is consistent with my observation that overexpression of Myo10 induces filopodia number (Chapter 3). Interestingly, biochemical experiments reveal that endogenous Myo10 and BMP6 type I receptor ALK6 coprecipitate and in cells treated with BMP6, ALK6 translocates into filopodia, co-localizes with Myo10 and undergoes intrafilopodial motility raising the possibility that ALK6 might serve as a candidate cargo for Myo10. To test if Myo10 is necessary for endothelial cell migration, Boyden chamber assays to study cell migration were performed and data from these experiments indicate that the knockdown of Myo10 with specific small hairpin- (sh-) RNA’s

inhibits BMP6-induced endothelial migration indicating that Myo10 might function downstream of BMP6 signaling. In summary, these findings along with our data on Myo10 strongly suggests that filopodia formation and transport of cargoes such as the signaling molecule ALK6 to filopodial tips by Myo10 might be central to BMP6 induced endothelial cell migration and signaling.

Myo10's ROLE IN INFECTION AND DISEASE

Myo10 plays an important role in actin-based motility of Shigella in infected host cells

Shigella flexneri are Gram-negative, non-motile, non-spore forming rod-shaped bacteria that are highly infectious agents. *Shigella flexneri* infects humans by invading the epithelium of the colon and is responsible, worldwide, for an estimated 165 million episodes of shigellosis and 1.5 million deaths per year. The bacterium is commonly found in water polluted with human feces. It is transmitted in contaminated food or water and through contact between people. Upon infection, humans develop severe abdominal cramps, fever, and frequent passage of bloody stools. Shigellosis is not only a significant cause of infant mortality in developing nations but maintains endemic levels of infection worldwide. New treatments are needed for this highly infectious microbe because antibiotics are often inadequate and drug-resistant strains are on the rise. A deeper understanding of the infection cycle of *Shigella* might help develop new drugs that target this infectious organism and prevent the spread of infection.

Recent advances in this area have shown that *Shigella* enters the cytoplasm of gastrointestinal epithelial cells, and subsequently move to the cell periphery to form finger-

like filopodia. Filopodia are thought to play and important role in the spread of infection to neighboring cells. Intracellular motility of *Shigella* from the cytoplasm to the cell periphery into finger-like filopodia is thus a vital step in *S. flexneri's* pathogenesis and requires that the bacterium hijack the host cell's actin machinery. Previous studies have successfully reconstituted actin-based motility of *S. flexneri and Listeria monocytogenes* (another bacteria that undergoes intra- and intercellular actin-based motility) in vitro by providing a small number of actin-binding proteins (Cameron et al., 2000). These studies have indicated that myosin motors are not necessary for intracellular motility of *Listeria* (Carlsson and Brown, 2006). Collaboration with the Southwick laboratory has resulted in new data that raises important questions regarding this previous observation. The Southwick laboratory (University of Florida, FL) has found that in living HeLa cells, while GFP-Myo10 concentrates in the actin tails of motile *Shigella*, as well as along the sides of filopodia containing *Shigella*, it fails to localize to *Listeria*-induced actin structures. Furthermore, using the siRNA knock-down strategy that I have previously demonstrated to result in ~90% knock-down of endogenous Myo10 (Chapter 3) resulted in a significant reduction in *S. flexneri* speeds by one third, as compared to infected cells transfected with control siRNA. Importantly, knock-down of Myo10 had no effect on *L. monocytogenes* intracellular speeds. These data suggest that *Shigella*, but not *Listeria*, utilizes Myo10 for efficient intracellular movement in living host cells. These studies also show that in tissue culture cells, Myo10 localizes primarily to the tips of filopodia and occasionally along the leading edge. However, in cells infected with *Shigella*, Myo10 is recruited to the actin-comet tail of *Shigella* raising important questions as to whether normal function of Myo10 is inhibited in cells infected with *Shigella*.

Myo10 plays a central role in viral budding and spread of viral infection

Like bacteria, viruses are also known to exploit the host cell cytoskeleton to establish and spread infection. Recent reports have implicated that filopodia play a central role in viral infection. For example, viruses have been shown to surf along filopodia to establish infection and spread from cell to cell. In this regard, African swine fever has been recently shown to serve as examples that exploit filopodia during its infection cycle (Jouvenet et al., 2006).

Our collaborators from Dr. Stephan Becker's laboratory (Marburg Institute, Germany) have recently published data showing that the actin cytoskeleton is involved in the release of Marburg virus particles (MARV). They found that peripherally located nucleoplasmids and envelope precursors of MARV are located either at the tips or along the sides of filopodial actin bundles. Importantly, they have also demonstrated that viral budding occurs almost exclusively in filopodia. Inhibiting actin polymerization in MARV infected cells significantly diminished the amount of viral particles released into the medium. This data suggested that dynamic polymerization of actin in filopodia is essential for efficient release of MARV. The viral matrix protein VP40 plays a key role in the release of MARV (Bamberg et al., 2005) and our collaborators further found that the intracellular localization of recombinant VP40 and it's release in the form of virus-like particles was strongly influenced by over-expression or inhibition of Myo10 and Cdc42, proteins important in filopodia formation and function. It is interesting to note here that I have recently demonstrated that Myo10 acts downstream of Cdc42. Since my data also shows that GFP-Myo10 HMM and GFP-Myo10-coiled-coil act as dominant negatives with respect to filopodia formation, we suggested the use of these constructs to test the hypothesis that release of virus-like particles is inhibited in cells expressing a dominant negative construct of Myo10. Consistent with this hypothesis our

collaborators showed that coexpression of Myo10 HMM or Myo10 coiled-coil significantly reduced release of VP40 virus-like particles and coexpression of VP40 and dominant negative Cdc42 showed similar results. These data strongly suggest that Myo10 plays an important role in the release of Marburg virus particles by a mechanism that involves Myo10's ability to form filopodia. The data from our lab taken together with the data from our collaborators show that Myo10 might induce filopodia by binding to VASP, which is important for anti-capping and actin polymerization of filament barbed ends, that Myo10 might play the role of a sensor in endothelial cell migration, and that Myo10 might play an important role in spread of infection by viruses and bacteria.

In conclusion, Myo10 plays important roles in vertebrate cell biology, endothelial cell physiology, and in the pathology of infection and disease by microorganisms such as *Shigella* and *Marburg*. These studies pave a path for future discoveries yet to be made on this novel unconventional myosin, Myo10 that might not only elucidate how filopodia form, but might also translate to the function of other MyTH4-FERM class of myosins, which are central to inner ear stereocilia function.

APPENDIX

MOVIE LEGENDS

Movie 2.1. HeLa cells expressing GFP-β3 integrins and showing that GFP-β3 integrins undergo intrafilopodial motility.

Movie 2.2. HeLa cells expressing GFP-β3 integrins and CFP-Myo10 showing that both proteins undergo cotransport in filopodia.

Movie 2.3. HeLa cells expressing GFP and CFP-Myo10 showing that GFP does not exhibit intrafilopodial motility.

Movie 2.4. Control siRNA treated HeLa cell expressing GFP-β3 integrin showing that GFP-β3 integrin undergoes intrafilopodial motility and localizes to filopodial tips in control siRNA treated HeLa cells.

Movie 2.5. HeLa cells treated with siRNA against Myo10 and expressing GFP-β3 integrins showing that GFP-β3 integrins does not undergoes intrafilopodial motility in Myo10 knockdown cells.

Movie 2.6. HeLa cells expressing YFP-dSH2 and CFP-Myo10 showing that both tyrosine-phosphorylated proteins and Myo10 undergo cotransport in filopodia.

Movie 3.1. HeLa cells treated with control siRNA exhibit numerous long, dynamic filopodia. This video illustrates the typical behavior of control HeLa cells, which extend numerous long and dynamic dorsal filopodia. HeLa cells were transfected with control siRNA and replated at 48 hours onto glass coverslips in the presence of serum. 12 hours after replating cells were imaged using phase contrast microscopy and a frame interval of 5 seconds. Scale bar equals 10 microns.

Movie 3.2. HeLa cells treated with Myo10 siRNA exhibit decreased filopodia. This video illustrates the typical behavior of HeLa cells treated with Myo10 siRNA. These cells have relatively few dorsal filopodia, although some short filopodia can still be observed, especially along the edge of the cell. Note also that cells treated with Myo10 siRNA retain the ability generate retraction fibers, several of which are visible in this cell. HeLa cells were

transfected with Myo10 siRNA and replated at 48 hours onto glass coverslips in the presence of serum. 12 hours after replating cells were imaged using phase contrast microscopy and a frame interval of 5 seconds. Scale bar equals 10 microns.

REFERENCES

Adams, J. C. and Schwartz, M. A. (2000). Stimulation of fascin spikes by thrombospondin-1 is mediated by the GTPases Rac and Cdc42. *J Cell Biol* **150**, 807-22.

Anderson, A. O. and Anderson, N. D. (1976). Lymphocyte emigration from high endothelial venules in rat lymph nodes. *Immunology* **31**, 731-48.

Bamberg, S., Kolesnikova, L., Moller, P., Klenk, H. D. and Becker, S. (2005). VP24 of Marburg virus influences formation of infectious particles. *J Virol* 79, 13421-33.

Bartles, J. R. (2000). Parallel actin bundles and their multiple actin-bundling proteins. *Curr Opin Cell Biol* **12**, 72-8.

Barzik, M., Kotova, T. I., Higgs, H. N., Hazelwood, L., Hanein, D., Gertler, F. B. and Schafer, D. A. (2005). Ena/VASP proteins enhance actin polymerization in the presence of barbed end capping proteins. *J Biol Chem* **280**, 28653-62.

Bear, J. E., Loureiro, J. J., Libova, I., Fassler, R., Wehland, J. and Gertler, F. B. (2000). Negative regulation of fibroblast motility by Ena/VASP proteins. *Cell* **101**, 717-28.

Bear, J. E., Svitkina, T. M., Krause, M., Schafer, D. A., Loureiro, J. J., Strasser, G. A., Maly, I. V., Chaga, O. Y., Cooper, J. A., Borisy, G. G. et al. (2002). Antagonism between Ena/VASP proteins and actin filament capping regulates fibroblast motility. *Cell* **109**, 509-21.

Belyantseva, I. A., Boger, E. T. and Friedman, T. B. (2003). Myosin XVa localizes to the tips of inner ear sensory cell stereocilia and is essential for staircase formation of the hair bundle. *Proc Natl Acad Sci U S A* **100**, 13958-63.

Belyantseva, I. A., Boger, E. T., Naz, S., Frolenkov, G. I., Sellers, J. R., Ahmed, Z. M., Griffith, A. J. and Friedman, T. B. (2005). Myosin-XVa is required for tip localization of whirlin and differential elongation of hair-cell stereocilia. *Nat Cell Biol* **7**, 148-56.

Berg, J. S. and Cheney, R. E. (2002). Myosin-X is an unconventional myosin that undergoes intrafilopodial motility. *Nat Cell Biol* **4**, 246-50.

Berg, J. S., Derfler, B. H., Pennisi, C. M., Corey, D. P. and Cheney, R. E. (2000). Myosin-X, a novel myosin with pleckstrin homology domains, associates with regions of dynamic actin. *J Cell Sci* **113 Pt 19**, 3439-51.

Berg, J. S., Powell, B. C. and Cheney, R. E. (2001). A millennial myosin census. *Mol Biol Cell* **12**, 780-94.

Bloor J. W. and Keihart D.P. (2001). zipper Nonmuscle myosin-II functions downstream of PS2 integrin in Drosophila myogenesis and is necessary for myofibril formation. Dev Biol. **239 (2)**, 215-28.

Bohil, A. B., Robertson, B. W. and Cheney, R. E. (2006). Myosin-X is a molecular motor that functions in filopodia formation. *Proc Natl Acad Sci U S A* **103**, 12411-6.

Bokel, C. and Brown, N. H. (2002). Integrins in development: moving on, responding to, and sticking to the extracellular matrix. *Dev Cell* **3**, 311-21.

Bretscher, A. and Weber, K. (1979). Villin: the major microfilament-associated protein of the intestinal microvillus. *Proc Natl Acad Sci U S A* **76**, 2321-5.

Calderwood, D. A., Yan, B., de Pereda, J. M., Alvarez, B. G., Fujioka, Y., Liddington, R. C. and Ginsberg, M. H. (2002). The phosphotyrosine binding-like domain of talin activates integrins. *J Biol Chem* **277**, 21749-58.

Cameron, L. A., Giardini, P. A., Soo, F. S. and Theriot, J. A. (2000). Secrets of actin-based motility revealed by a bacterial pathogen. *Nat Rev Mol Cell Biol* **1**, 110-9.

Carlsson, F. and Brown, E. J. (2006). Actin-based motility of intracellular bacteria, and polarized surface distribution of the bacterial effector molecules. *J Cell Physiol* **209**, 288-96.

Chen, Z.-Y., Hasson, T., Zhang, D.-S., Schwender, B. J., Derfler, B. H., Mooseker, M. S. and Corey, D. P. (2001a). Myosin VIIb, a novel unconventional myosin, is a

constituent of microvilli in transporting epithelia. *Genomics* **72**, 285-296.

Chen, Z. Y., Hasson, T., Zhang, D. S., Schwender, B. J., Derfler, B. H., Mooseker, M. S. and Corey, D. P. (2001b). Myosin-VIIb, a novel unconventional myosin, is a constituent of microvilli in transporting epithelia. *Genomics* **72**, 285-96.

Czuchra, A., Wu, X., Meyer, H., van Hengel, J., Schroeder, T., Geffers, R., Rottner, K. and Brakebusch, C. (2005). Cdc42 is not essential for filopodium formation, directed migration, cell polarization, and mitosis in fibroblastoid cells. *Mol Biol Cell* **16**, 4473-84.

Dent, E. W. and Gertler, F. B. (2003). Cytoskeletal dynamics and transport in growth cone motility and axon guidance. *Neuron* **40**, 209-27.

Drenckhahn, D., Engel, K., Hofer, D., Merte, C., Tilney, L. and Tilney, M. (1991). Three different actin filament assemblies occur in every hair cell: each contains a specific actin crosslinking protein. *J Cell Biol* **112**, 641-51.

Ellis, S. and Mellor, H. (2000). The novel Rho-family GTPase rif regulates coordinated actin-based membrane rearrangements. *Curr Biol* **10**, 1387-90.

Faix, J. and Rottner, K. (2005). The making of filopodia. *Curr Opin Cell Biol*.**18(1)**,18-25.

Falet, H., Hoffmeister, K. M., Neujahr, R. and Hartwig, J. H. (2002). Normal Arp2/3 complex activation in platelets lacking WASp. *Blood* **100**, 2113-22.

Forscher, P. and Smith, S. J. (1988). Actions of cytochalasins on the organization of actin filaments and microtubules in a neuronal growth cone. *J Cell Biol* **107**, 1505-16.

Gerhardt, H., Golding, M., Fruttiger, M., Ruhrberg, C., Lundkvist, A., Abramsson, A., Jeltsch, M., Mitchell, C., Alitalo, K., Shima, D. et al. (2003). VEGF guides angiogenic sprouting utilizing endothelial tip cell filopodia. *J Cell Biol* **161**, 1163-77.

Grabham, P. W., Foley, M., Umeojiako, A. and Goldberg, D. J. (2000). Nerve growth factor stimulates coupling of beta1 integrin to distinct transport mechanisms in the filopodia of growth cones. *J Cell Sci* **113 (Pt 17)**, 3003-12.

Grabham, P. W. and Goldberg, D. J. (1997). Nerve growth factor stimulates the accumulation of beta1 integrin at the tips of filopodia in the growth cones of sympathetic neurons. *J Neurosci* **17**, 5455-65.

Han, Y. H., Chung, C. Y., Wessels, D., Stephens, S., Titus, M. A., Soll, D. R. and Firtel, R. A. (2002). Requirement of a vasodilator-stimulated phosphoprotein family member for cell adhesion, the formation of filopodia, and chemotaxis in dictyostelium. *J Biol Chem* **277**, 49877-87.

He, C. and Chen, X. (2005). Transcription regulation of the vegf gene by the BMP/Smad pathway in the angioblast of zebrafish embryos. *Biochem Biophys Res Commun* 329, 324-30.

Heintzelman, M. B. and Mooseker, M. S. (1992). Assembly of the intestinal brush border cytoskeleton. *Curr Top Dev Biol* **26**, 93-122.

Higashida, C., Miyoshi, T., Fujita, A., Oceguera-Yanez, F., Monypenny, J., Andou, Y., Narumiya, S. and Watanabe, N. (2004). Actin polymerization-driven molecular movement of mDia1 in living cells. *Science* **303**, 2007-10.

Higgs, H. N. and Pollard, T. D. (2000). Activation by Cdc42 and PIP(2) of Wiskott-Aldrich syndrome protein (WASp) stimulates actin nucleation by Arp2/3 complex. *J Cell Biol* **150**, 1311-20.

Hirokawa, N., Tilney, L. G., Fujiwara, K. and Heuser, J. E. (1982). Organization of actin, myosin, and intermediate filaments in the brush border of intestinal epithelial cells. *J Cell Biol* **94**, 425-43.

Homma, K. and Ikebe, M. (2005). Myosin X is a high duty ratio motor. *J Biol Chem* **280**, 29381-91.

Homma, K., Saito, J., Ikebe, R. and Ikebe, M. (2001). Motor function and regulation of myosin X. *J Biol Chem* **276**, 34348-54.

Hufner, K., Higgs, H. N., Pollard, T. D., Jacobi, C., Aepfelbacher, M. and Linder, S. (2001). The verprolin-like central (vc) region of Wiskott-Aldrich syndrome protein induces Arp2/3 complex-dependent actin nucleation. *J Biol Chem* **276**, 35761-7.

Hufner, K., Schell, B., Aepfelbacher, M. and Linder, S. (2002). The acidic regions of WASp and N-WASP can synergize with CDC42Hs and Rac1 to induce filopodia and lamellipodia. *FEBS Lett* **514**, 168-74.

Isakoff, S. J., Cardozo, T., Andreev, J., Li, Z., Ferguson, K. M., Abagyan, R., Lemmon, M. A., Aronheim, A. and Skolnik, E. Y. (1998). Identification and analysis of PH domain-containing targets of phosphatidylinositol 3-kinase using a novel in vivo assay in yeast. *Embo J* **17**, 5374-87.

Jouvenet, N., Windsor, M., Rietdorf, J., Hawes, P., Monaghan, P., Way, M. and Wileman, T. (2006). African swine fever virus induces filopodia-like projections at the plasma membrane. *Cell Microbiol* 8, 1803-1811.

Kiehart, D. P., Franke, J. D., Chee, M. K., Montague, R. A., Chen, T. L., Roote, J. and Ashburner, M. (2004). Drosophila crinkled, mutations of which disrupt morphogenesis and cause lethality, encodes fly myosin VIIA. *Genetics* **168**, 1337-52.

Knight, P. J., Thirumurugan, K., Yu, Y., Wang, F., Kalverda, A. P., Stafford, W. F., 3rd, Sellers, J. R. and Peckham, M. (2005). The predicted coiled-coil domain of myosin 10 forms a novel elongated domain that lengthens the head. *J Biol Chem.* **280(41)**, 34702-8.

Kovacs, M., Wang, F. and Sellers, J. R. (2005). Mechanism of action of myosin X, a membrane-associated molecular motor. *J Biol Chem*. **280(15)**, 15071-83.

Krause, M., Dent, E. W., Bear, J. E., Loureiro, J. J. and Gertler, F. B. (2003). Ena/VASP proteins: regulators of the actin cytoskeleton and cell migration. *Annu Rev Cell Dev Biol* **19**, 541-64.

Krause, M., Leslie, J. D., Stewart, M., Lafuente, E. M., Valderrama, F., Jagannathan, R., Strasser, G. A., Rubinson, D. A., Liu, H., Way, M. et al. (2004). Lamellipodin, an Ena/VASP Ligand, Is Implicated in the Regulation of Lamellipodial Dynamics. *Dev Cell* **7**, 571-83.

Kussel-Andermann, P., El-Amraoui, A., Safieddine, S., Nouaille, S., Perfettini, I., Lecuit, M., Cossart, P., Wolfrum, U. and Petit, C. (2000). Vezatin, a novel transmembrane protein, bridges myosin VIIA to the cadherin-catenins complex. *Embo J* **19**, 6020-9.

Lebrand, C., Dent, E. W., Strasser, G. A., Lanier, L. M., Krause, M., Svitkina, T. M., Borisy, G. G. and Gertler, F. B. (2004). Critical role of Ena/VASP proteins for filopodia formation in neurons and in function downstream of netrin-1. *Neuron* **42**, 37-49.

Lehmann, M. J., Sherer, N. M., Marks, C. B., Pypaert, M. and Mothes, W. (2005). Actin- and myosin-driven movement of viruses along filopodia precedes their entry into cells. *J Cell Biol* **170**, 317-25.

Les Erickson, F., Corsa, A. C., Dose, A. C. and Burnside, B. (2003). Localization of a class III myosin to filopodia tips in transfected HeLa cells requires an actin-binding site in its tail domain. *Mol Biol Cell* **14**, 4173-80.

Liddington, R. C. and Ginsberg, M. H. (2002). Integrin activation takes shape. *J Cell Biol* **158**, 833-9.

Lidke, D. S., Lidke, K. A., Rieger, B., Jovin, T. M. and Arndt-Jovin, D. J. (2005). Reaching out for signals: filopodia sense EGF and respond by directed retrograde transport of activated receptors. *J Cell Biol* **170**, 619-26.

Lidke, D. S., Nagy, P., Heintzmann, R., Arndt-Jovin, D. J., Post, J. N., Grecco, H. E., Jares-Erijman, E. A. and Jovin, T. M. (2004). Quantum dot ligands provide new insights into erbB/HER receptor-mediated signal transduction. *Nat Biotechnol* **22**, 198-203.

Lin, H. W., Schneider, M. E. and Kachar, B. (2005). When size matters: the dynamic regulation of stereocilia lengths. *Curr Opin Cell Biol* **17**, 55-61.

Lloyd, R. V., Vidal, S., Jin, L., Zhang, S., Kovacs, K., Horvath, E., Scheithauer, B. W., Boger, E. T., Fridell, R. A. and Friedman, T. B. (2001). Myosin XVA expression in the pituitary and in other neuroendocrine tissues and tumors. *Am J Pathol* **159**, 1375-82.

Loomis, P. A., Zheng, L., Sekerkova, G., Changyaleket, B., Mugnaini, E. and Bartles, J. R. (2003). Espin cross-links cause the elongation of microvillus-type parallel actin bundles in vivo. *J Cell Biol* **163**, 1045-55.

Mallavarapu, A. and Mitchison, T. (1999). Regulated actin cytoskeleton assembly at filopodium tips controls their extension and retraction. *J Cell Biol* **146**, 1097-106.

Martel, V., Racaud-Sultan, C., Dupe, S., Marie, C., Paulhe, F., Galmiche, A., Block, M. R. and Albiges-Rizo, C. (2001). Conformation, localization, and integrin binding of talin depend on its interaction with phosphoinositides. *J Biol Chem* **276**, 21217-27.

Martin, K. H., Slack, J. K., Boerner, S. A., Martin, C. C. and Parsons, J. T. (2002). Integrin connections map: to infinity and beyond. *Science* **296**, 1652-3.

Miller, J., Fraser, S. E. and McClay, D. (1995). Dynamics of thin filopodia during sea urchin gastrulation. *Development* **121**, 2501-11.

Mitchison, T. and Kirschner, M. (1988). Cytoskeletal dynamics and nerve growth. *Neuron* **1**, 761-72.

Mooseker, M. S. and Tilney, L. G. (1975). Organization of an actin filament-membrane complex. Filament polarity and membrane attachment in the microvilli of intestinal epithelial cells. *J Cell Biol* **67**, 725-43.

Mullins, R. D., Heuser, J. A. and Pollard, T. D. (1998). The interaction of Arp2/3 complex with actin: nucleation, high affinity pointed end capping, and formation of branching networks of filaments. *Proc Natl Acad Sci U S A* **95**, 6181-6.

Murphy, G. A., Solski, P. A., Jillian, S. A., Perez de la Ossa, P., D'Eustachio, P., Der, C. J. and Rush, M. G. (1999). Cellular functions of TC10, a Rho family GTPase: regulation of morphology, signal transduction and cell growth. *Oncogene* **18**, 3831-45.

Nobes, C. D. and Hall, A. (1995). Rho, rac, and cdc42 GTPases regulate the assembly of multimolecular focal complexes associated with actin stress fibers, lamellipodia, and filopodia. *Cell* **81**, 53-62.

O'Connor, T. P., Duerr, J. S. and Bentley, D. (1990). Pioneer growth cone steering decisions mediated by single filopodial contacts in situ. *J Neurosci* **10**, 3935-46.

Onfelt, B., Nedvetzki, S., Yanagi, K. and Davis, D. M. (2004). Cutting edge:

Membrane nanotubes connect immune cells. *J Immunol* **173**, 1511-3.

Otto, J. J., Kane, R. E. and Bryan, J. (1979). Formation of filopodia in coelomocytes: localization of fascin, a 58,000 dalton actin cross-linking protein. *Cell* **17**, 285-93.

Partridge, M. A. and Marcantonio, E. E. (2006). Initiation of Attachment and Generation of Mature Focal Adhesions by Integrin-containing Filopodia in Cell Spreading. *Mol Biol Cell* **17(10)**, 4237-48.

Pellegrin, S. and Mellor, H. (2005). The Rho family GTPase Rif induces filopodia through mDia2. *Curr Biol* **15**, 129-33.

Penas, P. F., Garcia-Diez, A., Sanchez-Madrid, F. and Yanez-Mo, M. (2000). Tetraspanins are localized at motility-related structures and involved in normal human keratinocyte wound healing migration. *J Invest Dermatol* **114**, 1126-35.

Peng, J., Wallar, B. J., Flanders, A., Swiatek, P. J. and Alberts, A. S. (2003). Disruption of the Diaphanous-related formin Drf1 gene encoding mDia1 reveals a role for Drf3 as an effector for Cdc42. *Curr Biol* **13**, 534-45.

Pollard, T. D. and Borisy, G. G. (2003). Cellular motility driven by assembly and disassembly of actin filaments. *Cell* **112**, 453-65.

Ramirez-Weber, F. A. and Kornberg, T. B. (2000). Signaling reaches to new dimensions in Drosophila imaginal discs. *Cell* **103**, 189-92.

Reinhard, M., Halbrugge, M., Scheer, U., Wiegand, C., Jockusch, B. M. and Walter, U. (1992). The 46/50 kDa phosphoprotein VASP purified from human platelets is a novel protein associated with actin filaments and focal contacts. *Embo J* **11**, 2063-70.

Reuther, G. W., Lambert, Q. T., Booden, M. A., Wennerberg, K., Becknell, B., Marcucci, G., Sondek, J., Caligiuri, M. A. and Der, C. J. (2001). Leukemia-associated Rho guanine nucleotide exchange factor, a Dbl family protein found mutated in leukemia, causes transformation by activation of RhoA. *J Biol Chem* **276**, 27145-51.

Robles, E., Woo, S. and Gomez, T. M. (2005). Src-dependent tyrosine phosphorylation

at the tips of growth cone filopodia promotes extension. *J Neurosci* **25**, 7669-81.

Rogers, M. S. and Strehler, E. E. (2001). The tumor-sensitive calmodulin-like protein is a specific light chain of human unconventional myosin x. *J Biol Chem* **276**, 12182-9.

Rosenbaum, J. L. and Witman, G. B. (2002). Intraflagellar transport. *Nat Rev Mol Cell Biol* **3**, 813-25.

Rzadzinska, A., Schneider, M., Noben-Trauth, K., Bartles, J. R. and Kachar, B. (2005). Balanced levels of Espin are critical for stereociliary growth and length maintenance. *Cell Motil Cytoskeleton* **62**, 157-65.

Rzadzinska, A. K., Schneider, M. E., Davies, C., Riordan, G. P. and Kachar, B. (2004). An actin molecular treadmill and myosins maintain stereocilia functional architecture and self-renewal. *J Cell Biol* **164**, 887-97.

Sanger, J. M., Chang, R., Ashton, F., Kaper, J. B. and Sanger, J. W. (1996). Novel form of actin-based motility transports bacteria on the surfaces of infected cells. *Cell Motil Cytoskeleton* **34**, 279-87.

Schirenbeck, A., Arasada, R., Bretschneider, T., Stradal, T. E., Schleicher, M. and Faix, J. (2006). The bundling activity of vasodilator-stimulated phosphoprotein is required for filopodium formation. *Proc Natl Acad Sci U S A* **103**, 7694-9.

Sheetz, M. P., Baumrind, N. L., Wayne, D. B. and Pearlman, A. L. (1990). Concentration of membrane antigens by forward transport and trapping in neuronal growth cones. *Cell* **61**, 231-41.

Sousa, A. D., Berg, J. S., Robertson, B. W., Meeker, R. B. and Cheney, R. E. (2006). Myo10 in brain: developmental regulation, identification of a headless isoform and dynamics in neurons. *J Cell Sci* **119**, 184-94.

Sousa, A. D. and Cheney, R. E. (2005). Myosin-X: a molecular motor at the cell's fingertips. *Trends Cell Biol* **15**, 533-9.

Steffen, A., Faix, J., Resch, G. P., Linkner, J., Wehland, J., Small, J. V., Rottner, K.

and Stradal, T. E. (2006). Filopodia formation in the absence of functional WAVE- and Arp2/3-complexes. *Mol Biol Cell* **17**, 2581-91.

Stoffler, H. E., Honnert, U., Bauer, C. A., Hofer, D., Schwarz, H., Muller, R. T., Drenckhahn, D. and Bahler, M. (1998). Targeting of the myosin-I myr 3 to intercellular adherens type junctions induced by dominant active Cdc42 in HeLa cells. *J Cell Sci* **111 (Pt 18)**, 2779-88.

Stoffler, H. E., Ruppert, C., Reinhard, J. and Bahler, M. (1995). A novel mammalian myosin I from rat with an SH3 domain localizes to Con A-inducible, F-actin-rich structures at cell-cell contacts. *J Cell Biol* **129**, 819-30.

Stradal, T., Courtney, K. D., Rottner, K., Hahne, P., Small, J. V. and Pendergast, A. M. (2001). The Abl interactor proteins localize to sites of actin polymerization at the tips of lamellipodia and filopodia. *Curr Biol* **11**, 891-5.

Svitkina, T. M. and Borisy, G. G. (1998). Correlative light and electron microscopy of the cytoskeleton of cultured cells. *Methods Enzymol* **298**, 570-92.

Svitkina, T. M. and Borisy, G. G. (1999). Arp2/3 complex and actin depolymerizing factor/cofilin in dendritic organization and treadmilling of actin filament array in lamellipodia. *J Cell Biol* **145**, 1009-26.

Svitkina, T. M., Bulanova, E. A., Chaga, O. Y., Vignjevic, D. M., Kojima, S., Vasiliev, J. M. and Borisy, G. G. (2003). Mechanism of filopodia initiation by reorganization of a dendritic network. *J Cell Biol* **160**, 409-21.

Thomas, G. J., Lewis, M. P., Whawell, S. A., Russell, A., Sheppard, D., Hart, I. R., Speight, P. M. and Marshall, J. F. (2001). Expression of the alphavbeta6 integrin promotes migration and invasion in squamous carcinoma cells. *J Invest Dermatol* **117**, 67-73.

Tilney, L. G., Derosier, D. J. and Mulroy, M. J. (1980). The organization of actin filaments in the stereocilia of cochlear hair cells. *J Cell Biol* **86**, 244-59.

Titus, M. A. (1999). A class VII unconventional myosin is required for phagocytosis. *Curr Biol* **9**, 1297-303.

Tsuruta, D., Gonzales, M., Hopkinson, S. B., Otey, C., Khuon, S., Goldman, R. D. and Jones, J. C. (2002). Microfilament-dependent movement of the beta3 integrin subunit within focal contacts of endothelial cells. *Faseb J* **16**, 866-8.

Tuxworth, R. I., Weber, I., Wessels, D., Addicks, G. C., Soll, D. R., Gerisch, G. and Titus, M. A. (2001). A role for myosin VII in dynamic cell adhesion. *Current Biology* **11**, 318-329.

Tzima, E., Del Pozo, M. A., Kiosses, W. B., Mohamed, S. A., Li, S., Chien, S. and Schwartz, M. A. (2002). Activation of Rac1 by shear stress in endothelial cells mediates both cytoskeletal reorganization and effects on gene expression. *Embo J* **21**, 6791-800.

Vasioukhin, V., Bauer, C., Yin, M. and Fuchs, E. (2000). Directed actin polymerization is the driving force for epithelial cell-cell adhesion. *Cell* **100**, 209-19.

Vignjevic, D., Yarar, D., Welch, M. D., Peloquin, J., Svitkina, T. and Borisy, G. G. (2003). Formation of filopodia-like bundles in vitro from a dendritic network. *J Cell Biol* **160**, 951-62.

Weber, K. L., Sokac, A. M., Berg, J. S., Cheney, R. E. and Bement, W. M. (2004). A microtubule-binding myosin required for nuclear anchoring and spindle assembly. *Nature* **431**, 325-9.

Weil, D., Blanchard, S., Kaplan, J., Guilford, P., Gibson, F., Walsh, J., Mburu, P., Varela, A., Levilliers, J. and Weston, M. D. (1995). Defective myosin VIIA gene responsible for Usher syndrome type 1B. *Nature* **374**, 60-1.

Wood, W., Jacinto, A., Grose, R., Woolner, S., Gale, J., Wilson, C. and Martin, P. (2002). Wound healing recapitulates morphogenesis in Drosophila embryos. *Nat Cell Biol* **4**, 907-12.

Wood, W. and Martin, P. (2002). Structures in focus--filopodia. *Int J Biochem Cell Biol* **34**, 726-30.

Wu, D. Y., Wang, L. C., Mason, C. A. and Goldberg, D. J. (1996). Association of beta 1 integrin with phosphotyrosine in growth cone filopodia. *J Neurosci* **16**, 1470-8.

Yang, L., Wang, L. and Zheng, Y. (2006). Gene Targeting of Cdc42 and Cdc42GAP Affirms the Critical Involvement of Cdc42 in Filopodia Induction, Directed Migration, and Proliferation in Primary Mouse Embryonic Fibroblasts. *Mol Biol Cell* **17(11)**, 4675-85.

Zhang, H., Berg, J. S., Li, Z., Wang, Y., Lang, P., Sousa, A. D., Bhaskar, A., Cheney, R. E. and Stromblad, S. (2004). Myosin-X provides a motor-based link between integrins and the cytoskeleton. *Nat Cell Biol* **6**, 523-31.

Zheng, L., Sekerkova, G., Vranich, K., Tilney, L. G., Mugnaini, E. and Bartles, J. R. (2000). The deaf jerker mouse has a mutation in the gene encoding the espin actin-bundling proteins of hair cell stereocilia and lacks espins. *Cell* **102**, 377-85.